UNIVERSITY OF CALIFORNIA SAN DIEGO

Precision Functional Mapping in Child Development and Tourette Syndrome

A Dissertation submitted in partial satisfaction of the requirements
for the degree Doctor of Philosophy

in

Cognitive Science

by

Matthew Feigelis

Committee in charge:

Professor Deanna Greene, Chair
Professor Mikio Aoi
Professor Gedeon Deák
Professor Anastasia Kiyonaga

2024

The Dissertation of Matthew Feigelis is approved, and it is acceptable in quality and form for publication on microfilm and electronically.

University of California San Diego

2024

DEDICATION

This thesis is dedicated to my parents, brother, and nearest friends. Without their support, the work presented here would not have been possible.

TABLE OF CONTENTS

DISSERTATION APPROVAL PAGE iii

DEDICATION iv

TABLE OF CONTENTS v

LIST OF FIGURES vii

LIST OF TABLES viii

ACKNOWLEDGEMENTS ix

VITA x

ABSTRACT OF THE DISSERTATION xi

Chapter 1 Functional connectivity in the Gilles de la Tourette syndrome 1

1.1 Abstract 1

1.2 Introduction 1

1.3 Functional connectivity 2

1.4 Applications of functional connectivity to TS 7

1.5 Limitations and future directions 16

1.6 References 21

Chapter 2 Precision functional mapping reveals less inter-individual variability in the child vs. adult brain 33

2.1 Abstract 33

2.2 Introduction 34

2.3 Methods 37

2.4 Results 44

2.5 Discussion 57

2.6 References 61

Chapter 3 Precision functional mapping of motor tics in individual children with Tourette syndrome 73

3.1 Abstract 73
3.2 Introduction 74
3.3 Methods 77
3.4 Results 81
3.5 Discussion 88
3.6 References 92

LIST OF FIGURES

Figure 2.1 cPFM dataset summary and reliability 47

Figure 2.2: Childhood cortical functional networks 49

Figure 2.3: cPFM network density maps 50

Figure 2.4: Cortical variants in childhood 52

Figure 2.5: Functional network similarity across the child and adult PFM participants 54

Figure 2.6: Within age-group similarity maps for children and adults. (A-B) 55

Figure 2.7: Between age-group similarity 56

Figure 3.1: Urge activation maps 83

Figure 3.2: PT102, PT105, PT108 individual-specific functional networks 84

Figure 3.3: Network overlap with urge activation maps 86

Figure 3.4: Urge, onset, offset, progression 87

Supplementary Figure 2.1: ABCD 7,316 RSFC network template 69

Supplementary Figure 2.2: cPFM cortical functional networks, medial view 70

Supplementary Figure 2.3: cPFM functional network similarity controlling across age groups . 71

Supplementary Figure 3.1: Unthresholded activation maps for urge, onset, and offset windows ..... .98

LIST OF TABLES

Table 2.1: cPFM participant demographic information 46

Table 3.2: Participant demographic, clinical, and MRI information 82

Supplementary Table 2.1: RSFC comparison group demographics 72

ACKNOWLEDGEMENTS

Firstly, I would like to thank Deanna Greene for her consistent support across all aspects of my PhD. I would also like to thank my committee members Gedeon Deák, Mikio Aoi, and Anastasia Kiyonaga for providing consistent and helpful feedback throughout my thesis work. I would like to thank the professors I had the pleasure of working with and learning from during my time at UCSD including but not limited to Angela Yu, Federico Rossano, Gedeon Deák, Andrea Chiba, and Marta Kutas. I am grateful to the Halıcıoğlu Data Science Institute for the generous funding provided through their Data science PhD Fellowship. I would like to thank everyone in the Greene Lab including Sana Ali, Abigail Baim, Damion Demeter, Emily Koithan, and Salma Zreik. Their consistent support across all aspects of research including data collection, processing, analysis, and writing have been invaluable.

Chapter 1, in part, is a reprint of the material as it appears in International Review of Movement Disorders 2022. Feigelis M, Greene DJ. The dissertation author was the primary investigator and author of this material.

Chapter 2, in part, is currently being prepared for submission for publication of the material. Feigelis M, Demeter DV, Ali SA, Baim AR, Koithan E, Zreik S, Greene DJ. The dissertation author was the joint primary researcher and author of this material.

Chapter 3, in part, is currently being prepared for submission for publication of the material. Feigelis M, Baim AR, Zreik S, Demeter DV, Ali SA, Koithan E, Greene DJ. The dissertation author was the primary researcher and author of this material.

VITA

2016 Associate of Science in Mathematics, Middlesex County College

2018 Bachelor of Arts in Mathematics, Statistics Rutgers University

2023 Master of Science in Cognitive Science, University of California San Diego

2024 Doctor of Philosophy in Cognitive Science, University of California San Diego

ABSTRACT OF THE DISSERTATION

Precision Functional Mapping in Child Development and Tourette Syndrome

by

Matthew Feigelis

Doctor of Philosophy in Cognitive Science

University of California San Diego, 2024

Professor Deanna Greene, Chair

Our understanding of human neurodevelopment relies on group/population averages, but we know that individual differences in brain function are related to many life outcomes and the development of neuropsychiatric disorders. Precision functional mapping (PFM) is the precise and reliable characterization of functional brain organization at the individual level, made possible through the collection of large amounts of resting-state fMRI data from each individual.

PFM shifts the focus from studying the group to studying the individual, characterizing individual differences in functional organization that have previously been blurred by heavy reliance on group-average techniques. In this thesis, I use a PFM approach to characterize individual brain function in children, adults, and people with Tourette syndrome. First, I introduce the method of functional connectivity to study brain organization in individuals with Tourette syndrome (Chapter 1). Second, I present a study characterizing individual-specific brain organization in childhood, finding a core organization shared by all children, with inter-individual variability occurring in the bilateral frontal cortex and the temporo-occipito-parietal junction (Chapter 2). Compared with PFM data from adults, children had less inter-individual variability in functional organization within their age group, suggesting a refinement in functional organization with age. Third, I present a study characterizing tic symptoms in Tourette syndrome at the individual participant level (Chapter 3). By simultaneously collecting densely sampled resting-state fMRI data and naturally occurring tics in the scanner, activation maps corresponding to motor tics were referenced to each individual's functional brain networks. During the time period prior to the tic, which is associated with urge/discomfort building up to a tic, brain activation localized within the boundaries of each individual's cingulo-opercular and somato-cognitive action networks. Other regions and network involvement during tic symptoms differed across individuals, possibly related to different types of tics. By studying individuals, I identify previously blurred individual differences in brain function in development and in a neuropsychiatric disorder, which may ultimately increase the clinical utility of neuroimaging methods.

Chapter 1 Functional connectivity in the Gilles de la Tourette syndrome

1.1 Abstract

Functional connectivity is an analytic approach that examines the functional relationships between brain regions using neuroimaging data. It provides a window into the systems level of the brain and allows for the interrogation of information exchange between distributed areas. Functional connectivity has been increasingly applied in Tourette syndrome (TS) research in order to investigate functional connections between specific brain regions and networks. In the following chapter, we review the literature and highlight the utility of functional connectivity as a method to understand the pathophysiology associated with TS. Through comparisons to control groups, alongside correlations between symptoms and clinical, behavioral, and cognitive measures, growing evidence suggests that TS is associated with widespread alterations in functional connectivity across numerous brain regions and networks. The limitations of current studies and promising future directions are discussed.

1.2 Introduction

Methodological advancements surrounding the study of brain function has propelled forward research on the neurobiological mechanisms underlying Tourette syndrome (TS). In particular, the method of functional connectivity has begun to offer insights into the neural underpinnings of tic disorders. This chapter will focus on the method of functional connectivity with respect to TS research. We will first introduce functional connectivity and how it is used, then survey recent applications of functional connectivity in TS research, and then conclude with a discussion of the limitations of the existing studies and promising future directions.

1.3 Functional connectivity

Functional connectivity is an analytic approach that examines the functional relationships between brain regions. The method has been increasingly applied to non-invasive brain imaging techniques, such as functional magnetic resonance imaging (fMRI) and electroencephalography (EEG), which allow for an accessible way to investigate the function of the brain in humans in vivo. Implemented in this way, functional connectivity provides a window into the systems level of the brain. Functional activity within regions of the brain can be organized into systems (or "networks," the term most commonly used in literature), providing an avenue to interrogate information exchange between distributed areas. The complex interactions among regions and networks reflect motor, sensory, cognitive, and affective processes. Moreover, disruptions in these interactions can relate to disordered processes seen in various clinical populations.

Functional connectivity is defined as the statistical dependence of the time series of activity between different parts of the brain (Friston, 2011; Sporns, 2013). Regions that show high statistical dependence with each other are said to be functionally connected. In practice, Pearson's correlation is often used as the measure of statistical dependence, but other methods may be used as well, such as coherence or mutual information (see Mohanty et al., 2020). Thus, the correlation value (or coherence value, etc.) between the time series signal measured from different brain regions is referred to as the functional connectivity between those regions. With fMRI, correlations are calculated between the blood oxygenation level-dependent (BOLD) signal measured over time across voxels or specified regions of the brain. With EEG, correlations are calculated between the electrical signal measured over time across electrodes placed on the scalp. Although there is often correspondence between functional connectivity and physical anatomical

connections, there is clear, strong functional connectivity between regions that do not have monosynaptic anatomical connections (Honey et al., 2009; Tyszka et al., 2011; Sporns, 2013).

In this chapter, most of the studies reviewed used "resting state" fMRI to investigate functional connectivity in TS. That is, fMRI data are acquired while participants are in a "resting state" in which they are instructed to lay in the MRI scanner in the absence of an explicit task to perform. This approach contrasts the more traditional task fMRI design, in which participants perform an experimental task during fMRI data acquisition. In fact, the low frequency, spontaneous fluctuations in fMRI activity that are measured with resting state functional connectivity were traditionally thought to reflect noise that was filtered from the data. Rather, it was discovered that these low frequency, spontaneous fluctuations show structured correlational relationships among regions corresponding to brain systems that have been previously well characterized (Biswal et al., 1995; Greicius et al., 2003; Dosenbach et al., 2008). This discovery has led to the popularity of resting state fMRI as a way to map and interrogate the functional network organization of the human brain, and investigate its relationship to cognition and disease.

Functional networks measured during resting state were first identified using seed-based methods. When selecting a seed region in the brain (i.e., a region of interest, typically defined as a single voxel or collection of voxels), correlations are calculated between that seed region's BOLD activity and the activity of all other regions of the brain. One of the earliest studies of resting state functional connectivity placed a seed in the left primary motor cortex and revealed structured correlations in the homotopic motor cortex, supplementary motor area, and motor nuclei of the cerebellum, thalamus, and striatum, hence comprising the large-scale motor system (Biswal et al., 1995). This study further demonstrated exceptional overlap between this

collection of correlated brain regions and regions activated during a finger tapping task using traditional task fMRI. Other early seed-based studies revealed strong resting state correlations among distributed sets of brain regions resembling collections of regions co-activated during cognitive tasks, revealing "control" networks, as well as regions that show task-related decreases in activity, revealing the default mode network (Greicius et al., 2003; Dosenbach et al., 2007; Seeley et al., 2007; Dosenbach et al., 2008). Tools from graph theory and network science, including clustering methods, were then used to identify functional networks at a whole-brain level (e.g., Power et al., 2011). These methods consider all pairwise correlations between numerous brain regions, and identify multiple large-scale functional networks at once, expanding on the earlier seed-based studies. Descriptions of whole brain functional organization comprising approximately 7-25 functional networks derived from resting state functional connectivity are consistent across varying methods and research teams (Power et al., 2011; Yeo et al., 2011; Gordon et al., 2016). The functional networks identified using these new methods replicated those that were found in earlier seed-based investigations and have elucidated our understanding of how these networks are organized and interact.

The nature of functional connectivity (as well as structural connectivity) data, with measurable relationships between elements, lends itself to the use of graph theory and network-based analyses. These methods represent the brain as a graph, a mathematical object formally defined as a set of nodes and edges, providing a rigorous framework for measuring the relationships between brain regions (see Rubinov & Sporns, 2010 for review). In the functional context, the nodes of the graph are often functionally homogenous regions of the brain, and the edges are the pairwise correlational relationships between the nodes (Wig et al., 2011). The aggregation of nodes (e.g., regions) and edges (e.g., correlations) form a network (the brain).

Using this framework, there are various network analyses or graph metrics that can be computed to formally describe properties of the network. For example, module (or community, subnetwork, cluster) detection involves identifying modules within a network, in which modules are densely interconnected sets of nodes (Sporns & Betzel, 2016). With respect to functional connectivity, modules are sets of brain regions that are strongly correlated with each other, but weakly correlated with regions in other modules. As mentioned above, brain networks have a modular structure, consisting of approximately 7-25 functional networks with specialized functions (Power et al., 2011; Yeo et al., 2011; Gordon et al. 2016). Additional metrics from graph theory offer the ability to characterize other aspects of integration, segregation, and influence of individual nodes or modules of the network (Sporns, 2013). For example, a node's "degree" is the number of functional connections to that node from other nodes in the network, and the shortest "path length" between two nodes is the minimum number of steps needed to traverse between them (Rubinov & Sporns, 2010). The average of the shortest path lengths between all pairs of nodes in a network can be related to the ability of a network to rapidly integrate specialized information between distributed nodes (Rubinov & Sporns, 2010). However, some graph metrics, such as those based on path length, must be interpreted with caution in networks constructed from weighted functional correlations due to ambiguity in the interpretations (Rubinov & Sporns et al., 2010; Wig et al., 2011; Power et al. 2013).

Several properties of resting state functional networks make them well suited for investigations of human cognition, development, and disease. First, they have been found to be largely consistent between individuals, showing a strong group average structure of core anatomical regions that consistently correspond to the same functional network across different individuals (Gordon et al., 2017). Interestingly, regions of individual variation surround these

core regions, with certain networks showing larger cross-subject variability than others (Dworetsky et al., 2021). As stated above, the group averaged network structure has been shown to be reproducible, with numerous research groups and varying methods converging on similar brain-wide network spatial topography (Power et al., 2011, Yeo et al., 2011; Gordon et al., 2016). Second, functional connectivity and the derived functional networks have been shown to reflect largely stable, trait-like attributes of individual people, such as those associated with disease, rather than state-like attributes, such as variations associated with thought patterns over time (Gratton et al., 2018). Individual variability in network organization has also been shown to be stable within participants across scanning sessions and days (Seitzman et al., 2019). Patterns of variations that are reliably measured from individuals may be used to identify subgroups of participants sharing similar neural features. Subgroup membership could then be investigated, linking common variations in functional network organization to differences in behavior, demographics, or disease. For example, symptom heterogeneity in particular disorders may be a function of the specific variation in the individual or subgroup. Third, resting state fMRI data can be collected from participants of many levels of cognitive ability, as long as they can lay in the scanner and hold still. The absence of complex experimental tasks also reduces the likelihood of confounds related to task performance (Church et al., 2010).

Differences in functional connectivity within networks known to support sensory, motor, and cognitive functions have been shown to underlie phenotypic variation in factors such as cognitive performance, demographics, and disease states. For example, functional connectivity has been shown to reflect individual differences in performance on a sustained attention task (Rosenberg et al., 2016), measures of IQ (Santarnecchi et al., 2014) and fluid intelligence (Hearne et al., 2016), and to act as a ‘fingerprint’ for individual identification (Finn et al., 2015).

Furthermore, functional connectivity has been shown to be predictive of demographic traits, including sex (Weis et al., 2020) and age (Dosenbach et al., 2010; Nielsen et al., 2019). The ability to use resting state functional connectivity to predict an individual's age suggests it may be a useful clinical marker for atypical development, where predictions of low or high age relative to true age may suggest immature or overmature brain circuitry. The success and predictive power of functional connectivity in relation to behavior and demographic traits further suggests functional networks may be used to measure differences between clinical populations and control populations. Studies directly comparing clinical patients to control subjects have begun revealing widespread differences in functional connectivity in numerous disorders, including autism, ADHD, and schizophrenia (Fan et al., 2011; Uddin et al., 2013; Fair et al., 2013; Chen et al., 2016; Sheffield & Barch, 2016).

Considering the complex array of symptoms associated with TS, involving motor, sensory, and cognitive processes, in addition to the high rates of comorbid symptoms and diagnoses – most commonly attention-deficit/hyperactivity disorder (ADHD) and obsessive-compulsive disorder (OCD) (Freeman et al., 2000; Cavanna et al., 2009) – it is unlikely TS involves isolated dysfunction within a single brain structure, region, or network. Thus, functional connectivity offers a way to examine the large-scale brain systems underlying cognitive and sensorimotor functions and how they interact, which may be disrupted in TS patients.

1.4 Applications of functional connectivity to TS

Given its usefulness for interrogating interacting functional networks in the brain, functional connectivity has gained traction as a method to better understand the pathophysiology of TS. Most of the studies we discuss here used resting state fMRI and computed temporal

correlations between brain regions to assess functional connectivity, though we note when other imaging methods (e.g., task fMRI connectivity, EEG) or analytic approaches (e.g., regional homogeneity) were applied.

Research investigating functional connectivity in TS has taken two broad approaches. The first approach is testing for differences in functional connectivity metrics between a group of patients with TS and a group of control subjects. Using such group comparisons, researchers have identified brain regional connections and networks with altered functional connectivity in TS. The second approach is testing for relationships between functional connectivity estimates and continuous clinical, behavioral, or cognitive measures. Using this correlational approach, researchers have identified brain regional connections and networks that relate to symptom severity, tic suppression ability, and impulsivity. This section will thus focus on applications of functional connectivity to study the pathophysiology of TS, surveying first the literature on group differences in TS patients compared to controls, and then the associations between functional connectivity and clinical, behavioral, and cognitive measures, whilst considering similarities and differences in the methods and findings.

1.4.1 Differences in functional connectivity between TS patients and controls

Subcortical structures are common targets of investigation in TS research, given their known roles in motor control. One leading theory of TS pathophysiology posits disruption in cortico-striato-thalamo-cortical (CSTC) circuitry, in which there is aberrant activity in particular sets of striatal neurons, leading to the productions of tics (Mink, 2001; Mink, 2003). Thus, several studies have examined functional connectivity in the basal ganglia and thalamus, key nodes in this circuitry. The most consistent finding has been stronger functional connectivity

within subcortical regions and between subcortical and cortical regions in patients with TS compared to controls. Specifically, patients with TS showed stronger functional connectivity compared to controls within striatal and thalamic nodes (Zito et al., 2021; Tikoo et al., 2020). Consistent with these findings, differences in graph theory metrics (e.g., global efficiency, degree) between patients with TS and controls suggest increased functional integration in subcortical regions in TS (Tinaz et al., 2015; Ramkiran et al., 2019). When investigating cortico-subcortical circuitry, stronger functional connectivity has been reported in cortico-striatal and cortico-thalamic connections (Ramkiran et al., 2019) as well as within *a priori* defined cortico-subcortical networks (Worbe et al., 2012). Thus, there is consistency in the literature demonstrating stronger functional connectivity involving the subcortex in TS compared to controls, which may reflect aberrant activity within CSTC circuitry. Of course, future work is needed to clarify how altered connectivity within and between subcortical regions relates directly to the theory of CSTC dysfunction.

The cerebellum is also involved in motor control (as well as cognitive processes) and has known anatomical connections to and from the cortex and thalamus. A few studies have found altered cortico-cerebellar connectivity in TS patients, specifically decreased functional connectivity between the cerebellum and frontal regions, as well as between the cerebellum and the thalamus and sensorimotor cortex (Ramkiran et al., 2019; Tikoo et al., 2021). Consistently, decreased regional homogeneity (ReHo), a measure of neural synchronization that looks at a region's connectivity with its nearest neighbors, has been reported in the cerebellum of TS patients (Liu et al. 2017). While research on the cerebellum in TS has been relatively sparse, cerebellar volume has been shown to be associated with tic severity in both children and adults (Tobe et al., 2010), and has been theorized to play a role in the production of motor tics

(Caligiore et al., 2017). Therefore, the reports of altered cerebellar functional connectivity in TS lend support to this hypothesis.

Beyond the subcortex and cerebellum, numerous studies have examined functional connectivity within and between well characterized cortical functional networks. The default mode network, which comprises the medial prefrontal cortex, posterior cingulate, precuneus, and lateral parietal cortex, has received a lot of attention in the functional connectivity literature (Raichle, 2015). It has been referred to as the "task-negative network" due to consistent deactivations observed during task performance, and has been shown to be involved in mentalizing, social reasoning, and autobiographical memory (Schacter et al., 2007; Andrews-Hanna et al., 2010; Uddin et al., 2019). Studies of TS have found increased functional connectivity within the default mode network as well as between the default mode network and the frontoparietal network compared to controls (Fan et al., 2018; Tikoo et al., 2020). Conversely, graph theory metrics demonstrated decreased path length, local efficiency, and clustering coefficient within the default mode network in TS (Ramkiran et al. 2019; Openneer et al., 2020). Lower local efficiency and clustering coefficient metrics suggest reduced and less efficient short-range connectivity of the default mode network in TS patients. One hypothesis is that the default mode network is involved in tic suppression through the monitoring of premonitory urge sensations, given its role in internally focused tasks (Morand-Beaulieu et al., 2021). Whether increased or decreased functional connectivity within the default mode network in TS would support this hypothesis is not yet clear.

It has also been proposed that the impaired inhibition of movements and vocalizations that results in tics may generalize to brain networks underlying cognitive and inhibitory control more broadly. There are multiple "control" networks in the brain that have been well described,

including the frontoparietal and cingulo-opercular networks. The frontoparietal network has key nodes in dorsal and lateral frontal cortex and the inferior parietal lobe, and is involved in adaptive cognitive control during top down, goal-directed tasks; the cingulo-opercular network has key nodes in the dorsal anterior cingulate, supplementary motor area, anterior insula, and parietal operculum, and is involved in maintenance of task sets (Dosenbach et al., 2007; Dosenbach et al. 2008). When comparing TS patients to controls, there is evidence for altered functional connectivity within these control networks. Specifically, adults and children with TS showed reduced functional connectivity within the frontoparietal network (Fan et al., 2018; Tikoo et al., 2020). Adults with TS also showed altered graph theory metrics in regions that are part of the cingulo-opercular network, including reduced node degree in the left mid-cingulate cortex, reduced path length in the insula, reduced betweenness centrality in the right mid-insula, and increased betweenness centrality in the right dorsal anterior insula (Tinaz et al. 2015; Ramkiran et al. 2019). Previously, studies showing that control networks followed "younger" functional connectivity patterns suggested that these networks are immature in TS (Church et al., 2009; Worbe et al. 2012). However, it is likely that such results were largely affected by motion artifact (see Limitations and Future Directions). Thus, there are several possible interpretations for the differences observed in control networks in TS. These differences may relate to faulty inhibitory control mechanisms which are causally responsible for the production of tics. Alternatively or in addition, these differences may reflect compensatory mechanisms that come online in order to control, or attempt to control, tics.

The studies discussed thus far used univariate statistical approaches to compare patients with TS to controls. Yet, functional connectivity data can be quite complex, including thousands of region-to-region connections. Multivariate statistical approaches, on the other hand, can take

advantage of high dimensional data and identify patterns amongst many variables (features). Multivariate machine learning classification and prediction methods have been used to discriminate individuals based on whole-brain functional connectivity data, in which each functional connection is a single feature. Details about these methods can be found elsewhere (Nielsen et al., 2020b), but briefly, a classifier is trained on multivariate data to discriminate two groups (e.g., patients vs. controls). Then, the classifier is tested using new samples (e.g., new or left-out participants) that were not used for training. This testing phase of classification can then generate an accuracy rate, measuring how often the classifier categorizes the new sample accurately (e.g., is this new participant a patient or a control?). This classification approach can be extended to continuous variables as well (e.g., age, tic severity) to predict the value of that continuous variable for the test samples. Using these classification and prediction methods, functional connectivity has been leveraged for successful prediction of age across development (Nielsen et al., 2019) and classification of patient groups vs. controls, including ADHD (Fair et al., 2013), schizophrenia (Fan et al., 2011), and autism (Uddin et al., 2013). Several groups have shown successful classification of patients with TS vs. controls using multivariate machine learning, with accuracy rates ranging 65-89% (Greene et al., 2016; Wen et al., 2018; Nielsen et al., 2020; Zito et al., 2021). The power of these multivariate methods was highlighted when support vector machine learning algorithms classified children as TS or control with 70% accuracy based on ~30,000 functional connections across the whole brain, while univariate group comparisons of those ~30,000 functional connections did not yield any significant differences between groups after multiple comparisons correction (Greene et al., 2016). Additionally, these methods have demonstrated differences between children and adults in the functional connectivity patterns that best distinguished TS vs. controls (Nielsen et al., 2020). Namely,

diagnostic classifiers trained on one age group (children or adults) did not generalize to the other age group, lending support for the idea that there are differences in brain connectivity between childhood and adulthood TS.

One challenge with multivariate machine learning approaches is uncovering the neurobiological mechanisms that contribute to successful classification or prediction. The algorithms that have been used in TS research, namely support vector machine classification, generate a weight value for each feature (i.e., functional connection), which can be interpreted as a measure of importance of that feature for diagnostic classification. The most heavily weighted functional connections in the TS diagnostic classification models span many different brain regions and networks (Greene et al., 2016; Wen et al., 2018; Zito et al., 2021), consistent with the univariate group comparisons showing differences across the subcortex, cerebellum, and multiple cortical networks. However, it is important to note that the interpretability of functional connectivity feature weights has been questioned, and hence, may not provide reliable insight into neurobiological mechanism (Tian & Zalesky, 2021; Nielsen et al., 2020b).

1.4.2 Associations between functional connectivity and clinical, behavioral, and cognitive measures in TS

In order to assess tic symptom severity in patients with TS, the Yale Global Tic Severity Scale (YGTSS) is commonly administered. The YGTSS is a clinical rating scale measuring the number, frequency, intensity, and complexity of motor and phonic tics during the past week through a semi-structured clinical interview (Leckman et al., 1989). While multiple studies found significant negative correlations between functional connectivity and YGTSS scores, the regions

and networks showing these relationships were not systematic, which may be due to differing methodology and small sample sizes.

The significant negative associations between YGTSS scores and functional connectivity have been found in the cerebellum and in regions belonging to the default mode network and several control networks. Specifically, functional connections within the frontoparietal network and the cerebellum, and between the cerebellum and prefrontal cortex were weaker in patients with more severe symptoms (Tikoo et al., 2020; Tikoo et al., 2021). In addition, interhemispheric functional connectivity in the anterior cingulate cortex, which is part of the cingulo-opercular network, was weaker with increasing symptom severity (Liao et al., 2017). Using graph theory metrics, reduced local efficiency and clustering coefficient in the default mode and frontoparietal networks was also associated with increased symptom severity (Openneer et al., 2020). There is one report of a positive relationship between striato-cortical connectivity and YGTSS scores. In particular, connectivity between the putamen and sensorimotor cortex and between the caudate and superior occipital gyrus increased with worsening symptom severity (Bhikram et al., 2020). All of these studies, however, were limited by small sample sizes, which reduces the reliability and replicability of brain-behavior relationships (Marek et al., 2022), thus warranting caution. Indeed, multivariate methods may be more powerful at detecting these relationships. Yet, studies using multivariate methods, such as support vector regression, have not demonstrated successful prediction of YGTSS based on whole-brain functional connectivity data (Greene et al., 2016; Zito et al., 2021).

As patients with TS typically have the ability to voluntarily suppress tics for a short period of time, there have been some investigations of the association between functional connectivity and tic suppression ability. Tic suppression paradigms implemented during fMRI

data acquisition compare a free ticcing state, in which subjects are instructed that they can tic freely when needed, to a tic suppression state, in which subjects are instructed to inhibit their tics. Increased functional connectivity has been reported within the inferior frontal gyrus during tic suppression compared to free ticcing, and was further associated with tic suppression ability inside and outside the scanner (Ganos et al., 2014). Using EEG, tic suppression was shown to be associated with large scale increases of functional connectivity across numerous cortical areas, including frontal and sensorimotor regions, in the alpha frequency band (Serrien et al., 2005; Morand-Beaulieu et al., 2021). The regions falling within the default mode and frontoparietal networks in these studies further support a key role for these networks in TS pathophysiology.

TS has often been characterized as a disorder of inhibitory control, leading to the inability to suppress movements/vocalization in response to a premonitory urge, but also generalizing to executive functions. Investigations of executive functions in TS patients have been quite mixed, but a meta-analysis found evidence for inhibitory control deficits with small effect sizes (Morand-Beaulieu et al., 2017). A pair of recent studies investigated functional connectivity correlates of different domains of impulsivity in TS patients. Behaviorally, inhibitory deficits in an emotional stop signal task were found only in medicated patients, and inhibitory deficits in a four-choice serial reaction time task were found only in unmedicated patients (Atkinson et al., 2020; Atkinson et al., 2021). In both studies, associations with functional connectivity in numerous cortical and subcortical regions were reported in the subgroup demonstrating the behavioral deficits. Worse performance on the emotional stop signal task, meaning greater impulsivity, was associated with increased functional connectivity between the inferior frontal gyrus and bilateral superior temporal gyri, along with reduced functional connectivity between the cerebellum and the subthalamic nucleus. Greater impulsivity in the four-choice serial

reaction time task was associated with increased functional connectivity between the right orbitofrontal gyrus and bilateral caudate nucleus, along with reduced functional connectivity between the cerebellum and cortical regions. Differences in functional connectivity amongst the medicated and unmedicated TS subgroups, compared to control subjects, suggest a contribution of medications to behavior via functional connections.

1.5 Limitations and future directions

Investigations into TS pathophysiology using functional connectivity methods have largely examined heterogeneous cohorts, varying by factors such as medication usage, comorbid conditions, symptom severity, age, and sex. These factors can have their own independent effects on functional connectivity, and hence, make it difficult to disentangle effects due to TS pathophysiology and those due to other variables. For example, conditions highly comorbid with TS, such as ADHD and OCD, are each independently associated with widespread alterations in functional connectivity when compared to control groups (Stern et al., 2012; Fair et al., 2013; Posner et al., 2014; Mostert et al., 2016; Vaghi et al., 2017). Stimulants often used to treat ADHD, and prescribed to TS patients with comorbid ADHD, such as methylphenidate, have been also shown to systematically impact functional connectivity (Rubia et al., 2009; Sripada et al., 2013). Antipsychotic medications, which are commonly prescribed to TS patients to treat tics, such as aripiprazole and risperidone, have been shown to induce widespread changes in cortico-subcortical connectivity during the treatment of psychosis (Sarpal et al., 2015). Moreover, functional connectivity has also been shown to change with age over development (Dosenbach et al., 2010; Meier et al., 2012; Fair et al., 2013; Satterthwaite et al., 2013; Nielsen et

al., 2019). Thus, the heterogeneity in the samples present in functional connectivity studies of TS can complicate interpretation of results.

While excluding for or limiting these variables could reduce confounding effects, the high rates of comorbidities and medication use in TS complicates the issue. For one, recruiting "TS-only" or "drug-naïve" populations is difficult, given a more limited participant pool. Furthermore, and potentially even more importantly, targeting recruitment to a more restrictive sample reduces the generalizability of the study to the majority of patients, particularly those who most often seek clinical care and treatment (Gilbert & Buncher, 2005; Greene et al., 2016b). In our own research, we argue for inclusive sampling in order to capture more representative samples, and recommend accounting for these variables in the analyses. For example, subgroup analyses can test for differences that may be attributable to other factors. Such an approach has demonstrated that multivariate machine learning classification results were not driven by comorbidities, medication status, or sex (Nielsen et al., 2020), and has revealed differences in functional connectivity between medicated and unmedicated TS patients (Zito et al., 2021).

Many, if not all investigations of functional connectivity in TS thus far were limited by small sample sizes resulting in low statistical power, which is a common problem across the literature (Button et al., 2013). Subgroup analyses, such as those to account for heterogeneity in comorbid conditions or medication status suggested above, may be difficult to conduct with small sample sizes. Moving forward, large n studies, through working consortia such as the Adolescent Brain Cognitive Development (ABCD) study (supported by NIH; Casey et al., 2018), or the aggregation of data across labs, is a necessary next step for the field. There are large consortia for genetics data in TS, including the Psychiatric Genomics Consortium - Tourette Syndrome Working Group (Mufford et al. 2019, Yu et al., 2019) and the ENIGMA Consortium

(Bearden & Thompson, 2017), which has a Tourette syndrome working group that is currently gathering neuroimaging data in TS. There has been one consortium focused on neuroimaging data in TS supported by the Tourette Association of America, leading to larger samples for structural MRI analyses (Greene et al., 2017). Extending these consortia to functional data will help the field move forward to improve our understanding of the functional brain differences associated with TS.

One major hurdle in MRI, and in functional connectivity studies in particular, is head motion in the scanner. It turns out that even after standard motion correction procedures for fMRI, functional connectivity results can be systematically biased by motion artifact (Power et al., 2012; Power et al., 2014; Satterthwaite et al., 2012; Van Djik et al., 2012). Specifically, sub-millimeter head movements can lead to artificial increases in functional connectivity between brain regions that are spatially proximal and decreases in functional connectivity between brain regions that spatially distal. This apparent increased short-range and decreased long-range functional connectivity can be particularly problematic in group comparison studies. Children and patient groups tend to move more in the MRI scanner compared to adults and control populations (Dosenbach et al., 2017), leading to a systematic difference in head motion when comparing groups. These differences can generate the appearance of increased short-range functional connectivity in children compared to adults or in patients compared to controls, for example. Thus, this issue is particularly pertinent to consider when investigating a neurodevelopmental disorder such as TS. Recent progress in data processing strategies has shown that removing fMRI volumes that exceed strict motion estimate thresholds, in addition to regressing out the global brain signal, minimizes distance dependent motion artifact (Ciric et al., 2017). Thus, these processing strategies have been proposed as optimal for studies investigating

group or individual differences (Satterthwaite et al., 2019). The majority of TS functional connectivity studies surveyed above, however, did not implement these methods, potentially confounding the effects of true biological differences with differences in in-scanner head motion. Looking to the future, the widespread implementation, and advancement of processing strategies should disentangle these effects, minimizing the effects of motion on functional connectivity results.

An exciting avenue for future research consists of studies that densely sample resting state fMRI data in individual patients. In contrast to standard large n studies with low amounts of data per subject that rely on group averaging, a dense sampling (or "precision fMRI") approach collects large amounts of data from each individual, resulting in reliable estimates of functional connectivity on the individual level (Laumann et al., 2015). Recent work using densely sampled individual subjects has revealed stable and reliable individual differences in functional network organization across the cerebral cortex, subcortex, and cerebellum in healthy young adult subjects (Gordon et al., 2017; Gratton et al., 2018; Marek et al., 2018; Greene et al., 2020; Sylvester et al., 2020; Zheng et al., 2021). At least 45 total minutes of low-motion data was needed to obtain these reliable estimates of functional connectivity in the cerebral cortex (Gordon et al., 2017), with more data being needed for other structures, such as the cerebellum (requiring at least 90 minutes; Marek et al., 2018) and the basal ganglia and thalamus (requiring at least 100 minutes; Greene et al., 2020). There is promise, however, that with advancements in multi-echo fMRI sequences, reliable estimates could be obtained with less data per individual (Lynch et al., 2020). The individual differences that can be measured with precision fMRI, but are often blurred through group averaging, have the potential to increase the clinical and translational utility of functional connectivity, such as through subgroup identification and

individualized treatment strategies. For example, individual variation in functional network organization may be used to identify candidate target regions for treatment of TS with transcranial magnetic stimulation (TMS), deep brain stimulation (DBS), or neurofeedback (Martinez-Ramirez et al., 2018; Sukhodolsky et al., 2020). As the same anatomical location may correspond to different functional networks between individuals, the underlying cognitive and sensorimotor functions of that location may dictate the response to treatment on the individual level. Since TS patients vary clinically in the type of tics, diagnosed comorbidities, experience of sensory of cognitive deficits, and response to treatment, relating this symptom level heterogeneity to reliable estimates of functional connectivity on the individual level may be the path towards application of neuroimaging to clinical utility.

Another important direction for future studies is consideration of the developmental trajectory of TS. Symptom severity and the types of symptoms themselves change over development within individual patients. A typical trajectory of tic symptoms is often described, with the average age of tic onset at 6-7 years old, followed by worsening until severity peaks in late childhood/early adolescence, and then improvement into adolescence and early adulthood (Leckman et al., 1998; Leckman et al., 2006). Further, there is individual variation in this trajectory, with individual differences in worsening or improvement of symptoms with age. Thus, it will be important to investigate the developmental changes that occur and that vary across individuals with TS in the context of typical developmental changes in functional connectivity. Longitudinal designs will be particularly important for uncovering these developmental changes. While cross sectional designs are and will continue to be useful, it is difficult to disambiguate effects that are causes or consequences of the disorder. Thus, the field

would benefit from studies that longitudinally track the developmental course of the disorder along with associated changes in brain functional connectivity.

The method of functional connectivity has begun to, and will continue to, contribute to a more thorough, mechanistic account of TS. In addition, functional connectivity has the potential to offer true clinical and translational utility through the advancement of diagnosis and personalized treatment strategies. The future is bright, as TS researchers work toward using larger sample sizes, accounting for heterogeneity, controlling for confounds, improving data quality and increasing quantity, and implementing longitudinal designs to further our understanding of the functional brain network organization of TS.

Acknowledgment

Chapter 1, in part, is a reprint of the material as it appears in International Review of Movement Disorders 2022. Feigelis M, Greene DJ. The dissertation author was the primary investigator and author of this material.

1.6 References

Andrews-Hanna, J.R., Reidler, J.S., Sepulcre, J., Poulin, R., Buckner, R.L., 2010. Functional-Anatomic Fractionation of the Brain's Default Network. Neuron 65, 550–562. https://doi.org/10.1016/j.neuron.2010.02.005

Atkinson-Clement, C., Porte, C.-A., de Liege, A., Klein, Y., Delorme, C., Beranger, B., Valabregue, R., Gallea, C., Robbins, T.W., Hartmann, A., Worbe, Y., 2021. Impulsive prepotent actions and tics in Tourette disorder underpinned by a common neural network. Mol Psychiatry 26, 3548–3557. https://doi.org/10.1038/s41380-020-00890-5

Atkinson-Clement, C., Porte, C.-A., de Liege, A., Wattiez, N., Klein, Y., Beranger, B., Valabregue, R., Sofia, F., Hartmann, A., Pouget, P., Worbe, Y., 2020. Neural correlates and role of medication in reactive motor impulsivity in Tourette disorder. Cortex 125, 60–72. https://doi.org/10.1016/j.cortex.2019.12.007

Bearden, C.E., Thompson, P.M., 2017. Emerging Global Initiatives in Neurogenetics: The Enhancing Neuroimaging Genetics through Meta-analysis (ENIGMA) Consortium. Neuron 94, 232–236. https://doi.org/10.1016/j.neuron.2017.03.033

Bhikram, T., Arnold, P., Crawley, A., Abi-Jaoude, E., Sandor, P., 2020. The functional connectivity profile of tics and obsessive-compulsive symptoms in Tourette Syndrome. Journal of Psychiatric Research 123, 128–135. https://doi.org/10.1016/j.jpsychires.2020.01.019

Biswal, B., Zerrin Yetkin, F., Haughton, V.M., Hyde, J.S., 1995. Functional connectivity in the motor cortex of resting human brain using echo-planar mri. Magn. Reson. Med. 34, 537–541. https://doi.org/10.1002/mrm.1910340409

Button, K.S., Ioannidis, J.P.A., Mokrysz, C., Nosek, B.A., Flint, J., Robinson, E.S.J., Munafò, M.R., 2013. Power failure: why small sample size undermines the reliability of neuroscience. Nat Rev Neurosci 14, 365–376. https://doi.org/10.1038/nrn3475

Caligiore, D., Mannella, F., Arbib, M.A., Baldassarre, G., 2017. Dysfunctions of the basal ganglia-cerebellar-thalamo-cortical system produce motor tics in Tourette syndrome. PLoS Comput Biol 13, e1005395. https://doi.org/10.1371/journal.pcbi.1005395

Casey, B.J., Cannonier, T., Conley, M.I., Cohen, A.O., Barch, D.M., Heitzeg, M.M., Soules, M.E., Teslovich, T., Dellarco, D.V., Garavan, H., Orr, C.A., Wager, T.D., Banich, M.T., Speer, N.K., Sutherland, M.T., Riedel, M.C., Dick, A.S., Bjork, J.M., Thomas, K.M., Chaarani, B., Mejia, M.H., Hagler, D.J., Daniela Cornejo, M., Sicat, C.S., Harms, M.P., Dosenbach, N.U.F., Rosenberg, M., Earl, E., Bartsch, H., Watts, R., Polimeni, J.R., Kuperman, J.M., Fair, D.A., Dale, A.M., 2018. The Adolescent Brain Cognitive Development (ABCD) study: Imaging acquisition across 21 sites. Developmental Cognitive Neuroscience 32, 43–54. https://doi.org/10.1016/j.dcn.2018.03.001

Cavanna, A.E., Servo, S., Monaco, F., Robertson, M.M., 2009. The Behavioral Spectrum of Gilles de la Tourette Syndrome. JNP 21, 13–23. https://doi.org/10.1176/jnp.2009.21.1.13

Chen, Heng, Duan, X., Liu, F., Lu, F., Ma, X., Zhang, Y., Uddin, L.Q., Chen, Huafu, 2016. Multivariate classification of autism spectrum disorder using frequency-specific resting-state functional connectivity—A multi-center study. Progress in Neuro-Psychopharmacology and Biological Psychiatry 64, 1–9. https://doi.org/10.1016/j.pnpbp.2015.06.014

Church, J.A., Fair, D.A., Dosenbach, N.U.F., Cohen, A.L., Miezin, F.M., Petersen, S.E., Schlaggar, B.L., 2009. Control networks in paediatric Tourette syndrome show immature and anomalous patterns of functional connectivity. Brain 132, 225–238. https://doi.org/10.1093/brain/awn223

Church, J.A., Petersen, S.E., Schlaggar, B.L., 2010. The “Task B problem” and other considerations in developmental functional neuroimaging. Hum. Brain Mapp. 31, 852–862. https://doi.org/10.1002/hbm.21036

Ciric, R., Wolf, D.H., Power, J.D., Roalf, D.R., Baum, G.L., Ruparel, K., Shinohara, R.T., Elliott, M.A., Eickhoff, S.B., Davatzikos, C., Gur, R.C., Gur, R.E., Bassett, D.S., Satterthwaite, T.D., 2017. Benchmarking of participant-level confound regression strategies for the control of motion artifact in studies of functional connectivity. NeuroImage 154, 174–187. https://doi.org/10.1016/j.neuroimage.2017.03.020

Dosenbach, N.U.F., Fair, D.A., Cohen, A.L., Schlaggar, B.L., Petersen, S.E., 2008. A dual-networks architecture of top-down control. Trends in Cognitive Sciences 12, 99–105. https://doi.org/10.1016/j.tics.2008.01.001

Dosenbach, N.U.F., Fair, D.A., Miezin, F.M., Cohen, A.L., Wenger, K.K., Dosenbach, R.A.T., Fox, M.D., Snyder, A.Z., Vincent, J.L., Raichle, M.E., Schlaggar, B.L., Petersen, S.E., 2007. Distinct brain networks for adaptive and stable task control in humans. Proc. Natl. Acad. Sci. U.S.A. 104, 11073–11078. https://doi.org/10.1073/pnas.0704320104

Dosenbach, N.U.F., Koller, J.M., Earl, E.A., Miranda-Dominguez, O., Klein, R.L., Van, A.N., Snyder, A.Z., Nagel, B.J., Nigg, J.T., Nguyen, A.L., Wesevich, V., Greene, D.J., Fair, D.A., 2017. Real-time motion analytics during brain MRI improve data quality and reduce costs. NeuroImage 161, 80–93. https://doi.org/10.1016/j.neuroimage.2017.08.025

Dosenbach, N.U.F., Nardos, B., Cohen, A.L., Fair, D.A., Power, J.D., Church, J.A., Nelson, S.M., Wig, G.S., Vogel, A.C., Lessov-Schlaggar, C.N., Barnes, K.A., Dubis, J.W., Feczko, E., Coalson, R.S., Pruett, J.R., Barch, D.M., Petersen, S.E., Schlaggar, B.L., 2010. Prediction of Individual Brain Maturity Using fMRI. Science 329, 1358–1361. https://doi.org/10.1126/science.1194144

Dworetsky, A., Seitzman, B.A., Adeyemo, B., Neta, M., Coalson, R.S., Petersen, S.E., Gratton, C., 2021. Probabilistic mapping of human functional brain networks identifies regions of high group consensus. NeuroImage 237, 118164. https://doi.org/10.1016/j.neuroimage.2021.118164

Fair, D.A., Nigg, J.T., Iyer, S., Bathula, D., Mills, K.L., Dosenbach, N.U.F., Schlaggar, B.L., Mennes, M., Gutman, D., Bangaru, S., Buitelaar, J.K., Dickstein, D.P., Di Martino, A., Kennedy, D.N., Kelly, C., Luna, B., Schweitzer, J.B., Velanova, K., Wang, Y.-F., Mostofsky, S., Castellanos, F.X., Milham, M.P., 2013. Distinct neural signatures detected for ADHD subtypes after controlling for micro-movements in resting state functional connectivity MRI data. Front. Syst. Neurosci. 6. https://doi.org/10.3389/fnsys.2012.00080

Fan, S., van den Heuvel, O.A., Cath, D.C., de Wit, S.J., Vriend, C., Veltman, D.J., van der Werf, Y.D., 2018. Altered Functional Connectivity in Resting State Networks in Tourette's Disorder. Front. Hum. Neurosci. 12, 363. https://doi.org/10.3389/fnhum.2018.00363

Fan, Y., Liu, Y., Wu, H., Hao, Y., Liu, H., Liu, Z., Jiang, T., 2011. Discriminant analysis of functional connectivity patterns on Grassmann manifold. NeuroImage 56, 2058–2067. https://doi.org/10.1016/j.neuroimage.2011.03.051

Finn, E.S., Shen, X., Scheinost, D., Rosenberg, M.D., Huang, J., Chun, M.M., Papademetris, X., Constable, R.T., 2015. Functional connectome fingerprinting: identifying individuals using patterns of brain connectivity. Nat Neurosci 18, 1664–1671. https://doi.org/10.1038/nn.4135

Freeman, R.D., Fast, D.K., Burd, L., Kerbeshian, J., Robertson, M.M., Sandor, P., 2000. An international perspective on Tourette syndrome: selected findings from 3500 individuals in 22 countries. Dev Med Child Neurol 42, 436–447. https://doi.org/10.1017/S0012162200000839

Friston, K.J., 2011. Functional and Effective Connectivity: A Review. Brain Connectivity 1, 13–36. https://doi.org/10.1089/brain.2011.0008

Ganos, C., Kahl, U., Brandt, V., Schunke, O., Bäumer, T., Thomalla, G., Roessner, V., Haggard, P., Münchau, A., Kühn, S., 2014. The neural correlates of tic inhibition in Gilles de la Tourette syndrome. Neuropsychologia 65, 297–301. https://doi.org/10.1016/j.neuropsychologia.2014.08.007

Gilbert, D.L., Buncher, C.R., 2005. Assessment of Scientific and Ethical Issues in Two Randomized Clinical Trial Designs for Patients With Tourette's Syndrome: A Model for Studies of Multiple Neuropsychiatric Diagnoses. JNP 17, 324–332. https://doi.org/10.1176/jnp.17.3.324

Gordon, E.M., Laumann, T.O., Adeyemo, B., Huckins, J.F., Kelley, W.M., Petersen, S.E., 2016. Generation and Evaluation of a Cortical Area Parcellation from Resting-State Correlations. Cereb. Cortex 26, 288–303. https://doi.org/10.1093/cercor/bhu239

Gordon, E.M., Laumann, T.O., Gilmore, A.W., Newbold, D.J., Greene, D.J., Berg, J.J., Ortega, M., Hoyt-Drazen, C., Gratton, C., Sun, H., Hampton, J.M., Coalson, R.S., Nguyen, A.L., McDermott, K.B., Shimony, J.S., Snyder, A.Z., Schlaggar, B.L., Petersen, S.E., Nelson, S.M., Dosenbach, N.U.F., 2017. Precision Functional Mapping of Individual Human Brains. Neuron 95, 791-807.e7. https://doi.org/10.1016/j.neuron.2017.07.011

Gratton, C., Laumann, T.O., Nielsen, A.N., Greene, D.J., Gordon, E.M., Gilmore, A.W., Nelson, S.M., Coalson, R.S., Snyder, A.Z., Schlaggar, B.L., Dosenbach, N.U.F., Petersen, S.E., 2018. Functional Brain Networks Are Dominated by Stable Group and Individual Factors, Not Cognitive or Daily Variation. Neuron 98, 439-452.e5. https://doi.org/10.1016/j.neuron.2018.03.035

Greene, D.J., Black, K.J., Schlaggar, B.L., 2016a. Considerations for MRI study design and implementation in pediatric and clinical populations. Developmental Cognitive Neuroscience 18, 101–112. https://doi.org/10.1016/j.dcn.2015.12.005

Greene, D.J., Church, J.A., Dosenbach, N.U.F., Nielsen, A.N., Adeyemo, B., Nardos, B., Petersen, S.E., Black, K.J., Schlaggar, B.L., 2016b. Multivariate pattern classification of pediatric Tourette syndrome using functional connectivity MRI. Dev Sci 19, 581–598. https://doi.org/10.1111/desc.12407

Greene, D.J., Marek, S., Gordon, E.M., Siegel, J.S., Gratton, C., Laumann, T.O., Gilmore, A.W., Berg, J.J., Nguyen, A.L., Dierker, D., Van, A.N., Ortega, M., Newbold, D.J., Hampton, J.M., Nielsen, A.N., McDermott, K.B., Roland, J.L., Norris, S.A., Nelson, S.M., Snyder, A.Z., Schlaggar, B.L., Petersen, S.E., Dosenbach, N.U.F., 2020. Integrative and Network-Specific Connectivity of the Basal Ganglia and Thalamus Defined in Individuals. Neuron 105, 742-758.e6. https://doi.org/10.1016/j.neuron.2019.11.012

Greene, D.J., Williams III, A.C., Koller, J.M., Schlaggar, B.L., Black, K.J., The Tourette Association of America Neuroimaging Consortium, 2017. Brain structure in pediatric Tourette syndrome. Mol Psychiatry 22, 972–980. https://doi.org/10.1038/mp.2016.194

Greicius, M.D., Krasnow, B., Reiss, A.L., Menon, V., 2003. Functional connectivity in the resting brain: A network analysis of the default mode hypothesis. Proc. Natl. Acad. Sci. U.S.A. 100, 253–258. https://doi.org/10.1073/pnas.0135058100

Hearne, L.J., Mattingley, J.B., Cocchi, L., 2016. Functional brain networks related to individual differences in human intelligence at rest. Sci Rep 6, 32328. https://doi.org/10.1038/srep32328

Honey, C.J., Sporns, O., Cammoun, L., Gigandet, X., Thiran, J.P., Meuli, R., Hagmann, P., 2009. Predicting human resting-state functional connectivity from structural connectivity. Proc. Natl. Acad. Sci. U.S.A. 106, 2035–2040. https://doi.org/10.1073/pnas.0811168106

Laumann, T.O., Gordon, E.M., Adeyemo, B., Snyder, A.Z., Joo, S.J., Chen, M.-Y., Gilmore, A.W., McDermott, K.B., Nelson, S.M., Dosenbach, N.U.F., Schlaggar, B.L., Mumford, J.A., Poldrack, R.A., Petersen, S.E., 2015. Functional System and Areal Organization of a Highly Sampled Individual Human Brain. Neuron 87, 657–670. https://doi.org/10.1016/j.neuron.2015.06.037

Leckman, J.F., Bloch, M.H., Scahill, L., King, R.A., 2006. Tourette Syndrome: The Self Under Siege. J Child Neurol 21, 642–649. https://doi.org/10.1177/08830738060210081001

Leckman, J.F., Riddle, M.A., Hardin, M.T., Ort, S.I., Swartz, K.L., Stevenson, J., Cohen, D.J., 1989. The Yale Global Tic Severity Scale: Initial Testing of a Clinician-Rated Scale of Tic Severity. Journal of the American Academy of Child & Adolescent Psychiatry 28, 566–573. https://doi.org/10.1097/00004583-198907000-00015

Leckman, J.F., Zhang, H., Vitale, A., Lahnin, F., Lynch, K., Bondi, C., Kim, Y.-S., Peterson, B.S., n.d. Course of Tic Severity in Tourette Syndrome: The First Two Decades 6.

Liao, W., Yu, Y., Miao, H.-H., Feng, Y.-X., Ji, G.-J., Feng, J.-H., 2017. Inter-hemispheric Intrinsic Connectivity as a Neuromarker for the Diagnosis of Boys with Tourette Syndrome. Mol Neurobiol 54, 2781–2789. https://doi.org/10.1007/s12035-016-9863-9

Liu, Y., Wang, J., Zhang, J., Wen, H., Zhang, Y., Kang, H., Wang, X., Li, W., He, H., Peng, Y., 2017. Altered Spontaneous Brain Activity in Children with Early Tourette Syndrome: a Resting-state fMRI Study. Sci Rep 7, 4808. https://doi.org/10.1038/s41598-017-04148-z

Lynch, C.J., Power, J.D., Scult, M.A., Dubin, M., Gunning, F.M., Liston, C., 2020. Rapid Precision Functional Mapping of Individuals Using Multi-Echo fMRI. Cell Reports 33, 108540. https://doi.org/10.1016/j.celrep.2020.108540

Marek, S., Siegel, J.S., Gordon, E.M., Raut, R.V., Gratton, C., Newbold, D.J., Ortega, M., Laumann, T.O., Adeyemo, B., Miller, D.B., Zheng, A., Lopez, K.C., Berg, J.J., Coalson, R.S., Nguyen, A.L., Dierker, D., Van, A.N., Hoyt, C.R., McDermott, K.B., Norris, S.A., Shimony, J.S., Snyder, A.Z., Nelson, S.M., Barch, D.M., Schlaggar, B.L., Raichle, M.E., Petersen, S.E., Greene, D.J., Dosenbach, N.U.F., 2018. Spatial and Temporal Organization of the Individual Human Cerebellum. Neuron 100, 977-993.e7. https://doi.org/10.1016/j.neuron.2018.10.010

Marek, S., Tervo-Clemmens, B., Calabro, F.J., Montez, D.F., Kay, B.P., Hatoum, A.S., Donohue, M.R., Foran, W., Miller, R.L., Hendrickson, T.J., Malone, S.M., Kandala, S., Feczko, E., Miranda-Dominguez, O., Graham, A.M., Earl, E.A., Perrone, A.J., Cordova, M., Doyle, O., Moore, L.A., Conan, G.M., Uriarte, J., Snider, K., Lynch, B.J., Wilgenbusch, J.C., Pengo, T., Tam, A., Chen, J., Newbold, D.J., Zheng, A., Seider, N.A., Van, A.N., Metoki, A., Chauvin, R.J., Laumann, T.O., Greene, D.J., Petersen, S.E., Garavan, H., Thompson, W.K., Nichols, T.E., Yeo, B.T.T., Barch, D.M., Luna, B., Fair, D.A., Dosenbach, N.U.F., 2022. Reproducible brain-wide association studies require thousands of individuals. Nature 603, 654–660. https://doi.org/10.1038/s41586-022-04492-9

Martinez-Ramirez, D., Jimenez-Shahed, J., Leckman, J.F., Porta, M., Servello, D., Meng, F.-G., Kuhn, J., Huys, D., Baldermann, J.C., Foltynie, T., Hariz, M.I., Joyce, E.M., Zrinzo, L., Kefalopoulou, Z., Silburn, P., Coyne, T., Mogilner, A.Y., Pourfar, M.H., Khandhar, S.M., Auyeung, M., Ostrem, J.L., Visser-Vandewalle, V., Welter, M.-L., Mallet, L., Karachi, C., Houeto, J.L., Klassen, B.T., Ackermans, L., Kaido, T., Temel, Y., Gross, R.E., Walker, H.C., Lozano, A.M., Walter, B.L., Mari, Z., Anderson, W.S., Changizi, B.K., Moro, E., Zauber, S.E., Schrock, L.E., Zhang, J.-G., Hu, W., Rizer, K., Monari, E.H., Foote, K.D., Malaty, I.A., Deeb, W., Gunduz, A., Okun, M.S., 2018. Efficacy and Safety of Deep Brain Stimulation in Tourette Syndrome: The International Tourette Syndrome Deep Brain Stimulation Public Database and Registry. JAMA Neurol 75, 353. https://doi.org/10.1001/jamaneurol.2017.4317

Meier, T.B., Desphande, A.S., Vergun, S., Nair, V.A., Song, J., Biswal, B.B., Meyerand, M.E., Birn, R.M., Prabhakaran, V., 2012. Support vector machine classification and characterization of age-related reorganization of functional brain networks. NeuroImage 60, 601–613. https://doi.org/10.1016/j.neuroimage.2011.12.052

Mink, J.W., 2003. The Basal Ganglia and Involuntary Movements: Impaired Inhibition of Competing Motor Patterns. Arch Neurol 60, 1365. https://doi.org/10.1001/archneur.60.10.1365

Mink, J.W., 2001. Basal ganglia dysfunction in Tourette's syndrome: a new hypothesis. Pediatric Neurology 25, 190–198. https://doi.org/10.1016/S0887-8994(01)00262-4

Mohanty, R., Sethares, W.A., Nair, V.A., Prabhakaran, V., 2020. Rethinking Measures of Functional Connectivity via Feature Extraction. Sci Rep 10, 1298. https://doi.org/10.1038/s41598-020-57915-w

Morand-Beaulieu, S., Grot, S., Lavoie, J., Leclerc, J.B., Luck, D., Lavoie, M.E., 2017. The puzzling question of inhibitory control in Tourette syndrome: A meta-analysis. Neuroscience & Biobehavioral Reviews 80, 240–262. https://doi.org/10.1016/j.neubiorev.2017.05.006
Morand-Beaulieu, S., Wu, J., Mayes, L.C., Grantz, H., Leckman, J.F., Crowley, M.J., Sukhodolsky, D.G., 2021. Increased Alpha-Band Connectivity During Tic Suppression in Children With Tourette Syndrome Revealed by Source Electroencephalography Analyses. Biological Psychiatry: Cognitive Neuroscience and Neuroimaging. https://doi.org/10.1016/j.bpsc.2021.05.001

Mostert, J.C., Shumskaya, E., Mennes, M., Onnink, A.M.H., Hoogman, M., Kan, C.C., Arias Vasquez, A., Buitelaar, J., Franke, B., Norris, D.G., 2016. Characterising resting-state functional connectivity in a large sample of adults with ADHD. Progress in Neuro-Psychopharmacology and Biological Psychiatry 67, 82–91. https://doi.org/10.1016/j.pnpbp.2016.01.011

Mufford, M., Cheung, J., Jahanshad, N., van der Merwe, C., Ding, L., Groenewold, N., Koen, N., Chimusa, E.R., Dalvie, S., Ramesar, R., Knowles, J.A., Lochner, C., Hibar, D.P., Paschou, P., van den Heuvel, O.A., Medland, S.E., Scharf, J.M., Mathews, C.A., Thompson, P.M., Stein, D.J., Psychiatric Genomics Consortium - Tourette Syndrome working group, 2019. Concordance of genetic variation that increases risk for Tourette Syndrome and that influences its underlying neurocircuitry. Transl Psychiatry 9, 120. https://doi.org/10.1038/s41398-019-0452-3

Nielsen, A.N., Barch, D.M., Petersen, S.E., Schlaggar, B.L., Greene, D.J., 2020a. Machine Learning With Neuroimaging: Evaluating Its Applications in Psychiatry. Biological Psychiatry: Cognitive Neuroscience and Neuroimaging 5, 791–798. https://doi.org/10.1016/j.bpsc.2019.11.007

Nielsen, A.N., Gratton, C., Church, J.A., Dosenbach, N.U.F., Black, K.J., Petersen, S.E., Schlaggar, B.L., Greene, D.J., 2020b. Atypical Functional Connectivity in Tourette Syndrome Differs Between Children and Adults. Biological Psychiatry 87, 164–173. https://doi.org/10.1016/j.biopsych.2019.06.021

Nielsen, A.N., Greene, D.J., Gratton, C., Dosenbach, N.U.F., Petersen, S.E., Schlaggar, B.L., 2019. Evaluating the Prediction of Brain Maturity From Functional Connectivity After Motion Artifact Denoising. Cerebral Cortex 29, 2455–2469. https://doi.org/10.1093/cercor/bhy117

Openneer, T.J.C., Marsman, J.-B.C., van der Meer, D., Forde, N.J., Akkermans, S.E.A., Naaijen, J., Buitelaar, J.K., Dietrich, A., Hoekstra, P.J., 2020. A graph theory study of resting-state functional connectivity in children with Tourette syndrome. Cortex 126, 63–72. https://doi.org/10.1016/j.cortex.2020.01.006

Posner, J., Marsh, R., Maia, T.V., Peterson, B.S., Gruber, A., Simpson, H.B., 2014. Reduced functional connectivity within the limbic cortico-striato-thalamo-cortical loop in unmedicated adults with obsessive-compulsive disorder: Limbic CSTC Loop Connectivity in OCD. Hum. Brain Mapp. 35, 2852–2860. https://doi.org/10.1002/hbm.22371

Power, J.D., Barnes, K.A., Snyder, A.Z., Schlaggar, B.L., Petersen, S.E., 2012. Spurious but systematic correlations in functional connectivity MRI networks arise from subject motion. NeuroImage 59, 2142–2154. https://doi.org/10.1016/j.neuroimage.2011.10.018

Power, J.D., Cohen, A.L., Nelson, S.M., Wig, G.S., Barnes, K.A., Church, J.A., Vogel, A.C., Laumann, T.O., Miezin, F.M., Schlaggar, B.L., Petersen, S.E., 2011. Functional Network Organization of the Human Brain. Neuron 72, 665–678. https://doi.org/10.1016/j.neuron.2011.09.006

Power, J.D., Mitra, A., Laumann, T.O., Snyder, A.Z., Schlaggar, B.L., Petersen, S.E., 2014. Methods to detect, characterize, and remove motion artifact in resting state fMRI. NeuroImage 84, 320–341. https://doi.org/10.1016/j.neuroimage.2013.08.048

Power, J.D., Schlaggar, B.L., Lessov-Schlaggar, C.N., Petersen, S.E., 2013. Evidence for Hubs in Human Functional Brain Networks. Neuron 79, 798–813. https://doi.org/10.1016/j.neuron.2013.07.035

Raichle, M.E., 2015. The Brain's Default Mode Network. Annu. Rev. Neurosci. 38, 433–447. https://doi.org/10.1146/annurev-neuro-071013-014030

Ramkiran, S., Heidemeyer, L., Gaebler, A., Shah, N.J., Neuner, I., 2019. Alterations in basal ganglia-cerebello-thalamo-cortical connectivity and whole brain functional network topology in Tourette's syndrome. NeuroImage: Clinical 24, 101998. https://doi.org/10.1016/j.nicl.2019.101998

Rosenberg, M.D., Finn, E.S., Scheinost, D., Papademetris, X., Shen, X., Constable, R.T., Chun, M.M., 2016. A neuromarker of sustained attention from whole-brain functional connectivity. Nat Neurosci 19, 165–171. https://doi.org/10.1038/nn.4179

Rubia, K., Halari, R., Cubillo, A., Mohammad, A.-M., Brammer, M., Taylor, E., 2009. Methylphenidate normalises activation and functional connectivity deficits in attention and motivation networks in medication-naïve children with ADHD during a rewarded continuous performance task. Neuropharmacology 57, 640–652. https://doi.org/10.1016/j.neuropharm.2009.08.013

Rubinov, M., Sporns, O., 2010. Complex network measures of brain connectivity: Uses and interpretations. NeuroImage 52, 1059–1069. https://doi.org/10.1016/j.neuroimage.2009.10.003

Santarnecchi, E., Galli, G., Polizzotto, N.R., Rossi, A., Rossi, S., 2014. Efficiency of weak brain connections support general cognitive functioning: Efficiency of Weak and Strong Brain Connections and Intelligence. Hum. Brain Mapp. 35, 4566–4582. https://doi.org/10.1002/hbm.22495

Sarpal, D.K., Robinson, D.G., Lencz, T., Argyelan, M., Ikuta, T., Karlsgodt, K., Gallego, J.A., Kane, J.M., Szeszko, P.R., Malhotra, A.K., 2015. Antipsychotic Treatment and Functional

Connectivity of the Striatum in First-Episode Schizophrenia. JAMA Psychiatry 72, 5. https://doi.org/10.1001/jamapsychiatry.2014.1734

Satterthwaite, T.D., Ciric, R., Roalf, D.R., Davatzikos, C., Bassett, D.S., Wolf, D.H., 2019. Motion artifact in studies of functional connectivity: Characteristics and mitigation strategies. Hum. Brain Mapp. 40, 2033–2051. https://doi.org/10.1002/hbm.23665

Satterthwaite, T.D., Wolf, D.H., Loughead, J., Ruparel, K., Elliott, M.A., Hakonarson, H., Gur, R.C., Gur, R.E., 2012. Impact of in-scanner head motion on multiple measures of functional connectivity: Relevance for studies of neurodevelopment in youth. NeuroImage 60, 623–632. https://doi.org/10.1016/j.neuroimage.2011.12.063

Satterthwaite, T.D., Wolf, D.H., Ruparel, K., Erus, G., Elliott, M.A., Eickhoff, S.B., Gennatas, E.D., Jackson, C., Prabhakaran, K., Smith, A., Hakonarson, H., Verma, R., Davatzikos, C., Gur, R.E., Gur, R.C., 2013. Heterogeneous impact of motion on fundamental patterns of developmental changes in functional connectivity during youth. NeuroImage 83, 45–57. https://doi.org/10.1016/j.neuroimage.2013.06.045

Schacter, D.L., Addis, D.R., Buckner, R.L., 2007. Remembering the past to imagine the future: the prospective brain. Nat Rev Neurosci 8, 657–661. https://doi.org/10.1038/nrn2213
Seeley, W.W., Menon, V., Schatzberg, A.F., Keller, J., Glover, G.H., Kenna, H., Reiss, A.L., Greicius, M.D., 2007. Dissociable Intrinsic Connectivity Networks for Salience Processing and Executive Control. Journal of Neuroscience 27, 2349–2356. https://doi.org/10.1523/JNEUROSCI.5587-06.2007

Seitzman, B.A., Gratton, C., Laumann, T.O., Gordon, E.M., Adeyemo, B., Dworetsky, A., Kraus, B.T., Gilmore, A.W., Berg, J.J., Ortega, M., Nguyen, A., Greene, D.J., McDermott, K.B., Nelson, S.M., Lessov-Schlaggar, C.N., Schlaggar, B.L., Dosenbach, N.U.F., Petersen, S.E., 2019. Trait-like variants in human functional brain networks. Proc. Natl. Acad. Sci. U.S.A. 116, 22851–22861. https://doi.org/10.1073/pnas.1902932116

Serrien, D.J., Orth, M., Evans, A.H., Lees, A.J., Brown, P., 2005. Motor inhibition in patients with Gilles de la Tourette syndrome: functional activation patterns as revealed by EEG coherence. Brain 128, 116–125. https://doi.org/10.1093/brain/awh318

Sheffield, J.M., Barch, D.M., 2016. Cognition and resting-state functional connectivity in schizophrenia. Neuroscience & Biobehavioral Reviews 61, 108–120. https://doi.org/10.1016/j.neubiorev.2015.12.007

Sporns, O., 2013. Structure and function of complex brain networks. Dialogues in Clinical Neuroscience 15, 16.
Sporns, O., Betzel, R.F., 2016. Modular Brain Networks. Annu. Rev. Psychol. 67, 613–640. https://doi.org/10.1146/annurev-psych-122414-033634

Sripada, C.S., Kessler, D., Welsh, R., Angstadt, M., Liberzon, I., Phan, K.L., Scott, C., 2013. Distributed effects of methylphenidate on the network structure of the resting brain: A

connectomic pattern classification analysis. NeuroImage 81, 213–221. https://doi.org/10.1016/j.neuroimage.2013.05.016

Stern, E.R., Fitzgerald, K.D., Welsh, R.C., Abelson, J.L., Taylor, S.F., 2012. Resting-State Functional Connectivity between Fronto-Parietal and Default Mode Networks in Obsessive-Compulsive Disorder. PLoS ONE 7, e36356. https://doi.org/10.1371/journal.pone.0036356

Sukhodolsky, D.G., Walsh, C., Koller, W.N., Eilbott, J., Rance, M., Fulbright, R.K., Zhao, Z., Bloch, M.H., King, R., Leckman, J.F., Scheinost, D., Pittman, B., Hampson, M., 2020. Randomized, Sham-Controlled Trial of Real-Time Functional Magnetic Resonance Imaging Neurofeedback for Tics in Adolescents With Tourette Syndrome. Biological Psychiatry 87, 1063–1070. https://doi.org/10.1016/j.biopsych.2019.07.035

Sylvester, C.M., Yu, Q., Srivastava, A.B., Marek, S., Zheng, A., Alexopoulos, D., Smyser, C.D., Shimony, J.S., Ortega, M., Dierker, D.L., Patel, G.H., Nelson, S.M., Gilmore, A.W., McDermott, K.B., Berg, J.J., Drysdale, A.T., Perino, M.T., Snyder, A.Z., Raut, R.V., Laumann, T.O., Gordon, E.M., Barch, D.M., Rogers, C.E., Greene, D.J., Raichle, M.E., Dosenbach, N.U.F., 2020. Individual-specific functional connectivity of the amygdala: A substrate for precision psychiatry. Proc. Natl. Acad. Sci. U.S.A. 117, 3808–3818. https://doi.org/10.1073/pnas.1910842117

Thomas Yeo, B.T., Krienen, F.M., Sepulcre, J., Sabuncu, M.R., Lashkari, D., Hollinshead, M., Roffman, J.L., Smoller, J.W., Zöllei, L., Polimeni, J.R., Fischl, B., Liu, H., Buckner, R.L., 2011. The organization of the human cerebral cortex estimated by intrinsic functional connectivity. Journal of Neurophysiology 106, 1125–1165. https://doi.org/10.1152/jn.00338.2011

Tian, Y., Zalesky, A., 2021. Machine learning prediction of cognition from functional connectivity: Are feature weights reliable? NeuroImage 245, 118648. https://doi.org/10.1016/j.neuroimage.2021.118648

Tikoo, S., Cardona, F., Tommasin, S., Giannì, C., Conte, G., Upadhyay, N., Mirabella, G., Suppa, A., Pantano, P., 2020. Resting-state functional connectivity in drug-naive pediatric patients with Tourette syndrome and obsessive-compulsive disorder. Journal of Psychiatric Research 129, 129–140. https://doi.org/10.1016/j.jpsychires.2020.06.021

Tikoo, S., Suppa, A., Tommasin, S., Giannì, C., Conte, G., Mirabella, G., Cardona, F., Pantano, P., 2021. The Cerebellum in Drug-naive Children with Tourette Syndrome and Obsessive–Compulsive Disorder. Cerebellum. https://doi.org/10.1007/s12311-021-01327-7

Tinaz, S., Malone, P., Hallett, M., Horovitz, S.G., 2015. Role of the right dorsal anterior insula in the urge to tic in tourette syndrome: Right Dorsal Anterior Insula in Tourette. Mov Disord. 30, 1190–1197. https://doi.org/10.1002/mds.26230

Tobe, R.H., Bansal, R., Xu, D., Hao, X., Liu, J., Sanchez, J., Peterson, B.S., 2010. Cerebellar morphology in Tourette syndrome and obsessive-compulsive disorder. Ann Neurol. 67, 479–487. https://doi.org/10.1002/ana.21918

Tyszka, J.M., Kennedy, D.P., Adolphs, R., Paul, L.K., 2011. Intact Bilateral Resting-State Networks in the Absence of the Corpus Callosum. Journal of Neuroscience 31, 15154–15162. https://doi.org/10.1523/JNEUROSCI.1453-11.2011

Uddin, L.Q., Supekar, K., Lynch, C.J., Khouzam, A., Phillips, J., Feinstein, C., Ryali, S., Menon, V., 2013. Salience Network–Based Classification and Prediction of Symptom Severity in Children With Autism. JAMA Psychiatry 70, 869. https://doi.org/10.1001/jamapsychiatry.2013.104

Uddin, L.Q., Yeo, B.T.T., Spreng, R.N., 2019. Towards a Universal Taxonomy of Macro-scale Functional Human Brain Networks. Brain Topogr 32, 926–942. https://doi.org/10.1007/s10548-019-00744-6

Vaghi, M.M., Vértes, P.E., Kitzbichler, M.G., Apergis-Schoute, A.M., van der Flier, F.E., Fineberg, N.A., Sule, A., Zaman, R., Voon, V., Kundu, P., Bullmore, E.T., Robbins, T.W., 2017. Specific Frontostriatal Circuits for Impaired Cognitive Flexibility and Goal-Directed Planning in Obsessive-Compulsive Disorder: Evidence From Resting-State Functional Connectivity. Biological Psychiatry 81, 708–717. https://doi.org/10.1016/j.biopsych.2016.08.009

Van Dijk, K.R.A., Sabuncu, M.R., Buckner, R.L., 2012. The influence of head motion on intrinsic functional connectivity MRI. NeuroImage 59, 431–438. https://doi.org/10.1016/j.neuroimage.2011.07.044

Weis, S., Patil, K.R., Hoffstaedter, F., Nostro, A., Yeo, B.T.T., Eickhoff, S.B., 2020. Sex Classification by Resting State Brain Connectivity. Cerebral Cortex 30, 824–835. https://doi.org/10.1093/cercor/bhz129

Wen, H., Liu, Y., Rekik, I., Wang, S., Chen, Z., Zhang, J., Zhang, Y., Peng, Y., He, H., 2018. Combining Disrupted and Discriminative Topological Properties of Functional Connectivity Networks as Neuroimaging Biomarkers for Accurate Diagnosis of Early Tourette Syndrome Children. Mol Neurobiol 55, 3251–3269. https://doi.org/10.1007/s12035-017-0519-1

Wig, G.S., Schlaggar, B.L., Petersen, S.E., 2011. Concepts and principles in the analysis of brain networks: Brain networks. Annals of the New York Academy of Sciences 1224, 126–146. https://doi.org/10.1111/j.1749-6632.2010.05947.x

Worbe, Y., Malherbe, C., Hartmann, A., Pélégrini-Issac, M., Messé, A., Vidailhet, M., Lehéricy, S., Benali, H., 2012. Functional immaturity of cortico-basal ganglia networks in Gilles de la Tourette syndrome. Brain 135, 1937–1946. https://doi.org/10.1093/brain/aws056

Yeo, B.T.T., Krienen, F.M., Sepulcre, J., Sabuncu, M.R., Lashkari, D., Hollinshead, M., Roffman, J.L., Smoller, J.W., Zöllei, L., Polimeni, J.R., Fischl, B., Liu, H., Buckner, R.L., 2011. The organization of the human cerebral cortex estimated by intrinsic functional connectivity. J Neurophysiol 106, 1125–1165. https://doi.org/10.1152/jn.00338.2011

Yu, D., Sul, J.H., Tsetsos, F., Nawaz, M.S., Huang, A.Y., Zelaya, I., Illmann, C., Osiecki, L., Darrow, S.M., Hirschtritt, M.E., Greenberg, E., Muller-Vahl, K.R., Stuhrmann, M., Dion, Y., Rouleau, G., Aschauer, H., Stamenkovic, M., Schlögelhofer, M., Sandor, P., Barr, C.L., Grados, M., Singer, H.S., Nöthen, M.M., Hebebrand, J., Hinney, A., King, R.A., Fernandez, T.V., Barta, C., Tarnok, Z., Nagy, P., Depienne, C., Worbe, Y., Hartmann, A., Budman, C.L., Rizzo, R., Lyon, G.J., McMahon, W.M., Batterson, J.R., Cath, D.C., Malaty, I.A., Okun, M.S., Berlin, C., Woods, D.W., Lee, P.C., Jankovic, J., Robertson, M.M., Gilbert, D.L., Brown, L.W., Coffey, B.J., Dietrich, A., Hoekstra, P.J., Kuperman, S., Zinner, S.H., Luðvigsson, P., Sæmundsen, E., Thorarensen, Ó., Atzmon, G., Barzilai, N., Wagner, M., Moessner, R., Ophoff, R., Pato, C.N., Pato, M.T., Knowles, J.A., Roffman, J.L., Smoller, J.W., Buckner, R.L., Willsey, A.J., Tischfield, J.A., Heiman, G.A., Stefansson, H., Stefansson, K., Posthuma, D., Cox, N.J., Pauls, D.L., Freimer, N.B., Neale, B.M., Davis, L.K., Paschou, P., Coppola, G., Mathews, C.A., Scharf, J.M., Tourette Association of America International Consortium for Genetics, Gilles de la Tourette GWAS Replication Initiative, the Tourette International Collaborative Genetics Study, the Psychiatric Genomics Consortium Tourette Syndrome Working Group, 2019. Interrogating the Genetic Determinants of Tourette's Syndrome and Other Tic Disorders Through Genome-Wide Association Studies. AJP 176, 217–227. https://doi.org/10.1176/appi.ajp.2018.18070857

Zheng, A., Montez, D.F., Marek, S., Gilmore, A.W., Newbold, D.J., Laumann, T.O., Kay, B.P., Seider, N.A., Van, A.N., Hampton, J.M., Alexopoulos, D., Schlaggar, B.L., Sylvester, C.M., Greene, D.J., Shimony, J.S., Nelson, S.M., Wig, G.S., Gratton, C., McDermott, K.B., Raichle, M.E., Gordon, E.M., Dosenbach, N.U.F., 2021. Parallel hippocampal-parietal circuits for self- and goal-oriented processing. Proc. Natl. Acad. Sci. U.S.A. 118, e2101743118. https://doi.org/10.1073/pnas.2101743118

Zito, G.A., Hartmann, A., Béranger, B., Weber, S., Aybek, S., Faouzi, J., Roze, E., Vidailhet, M., Worbe, Y., 2021. Multivariate classification provides a neural signature of Tourette disorder. Psychol. Med. 1–9. https://doi.org/10.1017/S0033291721004232

Chapter 2 Precision functional mapping reveals less inter-individual variability in the child vs. adult brain

2.1 Abstract

Characterizing functional brain organization during childhood is important for understanding individual differences in cognitive development and the occurrence of neurodevelopmental disorders. Previous studies using group-average approaches obscure individual differences in brain organization, thereby limiting our understanding of brain development. Precision functional mapping (PFM) is an approach that shifts the focus from group-averaged to individual brain function by obtaining large amounts of fMRI data from each individual. In this study, we demonstrate the feasibility of collecting high-quality PFM resting state fMRI data in children to examine individual-specific features of brain organization during childhood. We successfully obtained an average of ~3 hours of resting state fMRI data from 12 participants aged 8-12 years old. We show that high reliability of functional connectivity estimates are achieved with 45-50 minutes of high quality, low-motion data. Children shared a core functional network topography, with the greatest inter-individual variability at network edges and in association regions across the bilateral frontal cortex and the temporo–occipito–parietal junction. This core functional topography was also shared with adults. Compared with adults, children had less inter-individual variability in functional organization between individuals in their age group, suggesting that functional brain organization undergoes a refinement process with age to achieve greater individual variability in adulthood. This child PFM dataset is being released as a public resource to support future research on brain development and developmental disorders.

2.2 Introduction

During childhood and adolescence, brain systems, along with cognitive and motor abilities, undergo rapid and significant changes (Blakemore, 2012; Giedd et al., 1999; Houston et al., 2014; Mills et al., 2016; Stiles & Jernigan, 2010; Tervo-Clemmens et al., 2023). This critical period of development has been linked to individuals' academic success (Best et al., 2011), liability to neuropsychiatric illness (Paus et al., 2008), and general outcomes of well-being (Robson et al., 2020). The normative developmental trajectory of cognition and motor function has been associated with the selective integration and segregation of various brain regions and large-scale functional brain systems (Grayson & Fair, 2017; Keller et al., 2023; Luna et al., 2015; Luo et al., 2024). Thus, the considerable variability in cognitive function among children (Siegler, 2007; Tervo-Clemmens et al., 2023) may be underpinned by individual differences in functional brain organization (Cui et al., 2020). A deeper understanding of these individual differences may lead to better explanations of variable academic and social success and guide intervention therapies for at-risk children.

Standard group-level neuroimaging studies (i.e., averaging data across a group of individuals) have characterized large-scale functional brain network organization in children (Muetzel et al., 2016; Thomason et al., 2011), providing central tendencies from which to examine changes over development, deviations in psychopathology, and relationships to phenotypic measures. In particular, testing relationships between brain and phenotypic measures, such as cognitive or clinical features, has been a leading approach to study individual differences. Large sample datasets, such as the ABCD study (Casey et al., 2018), provides adequate power to test brain-behavior relationships across thousands of children (Marek et al., 2022). However, central tendencies inherently blur individual variability in network

organization, which has been previously highlighted in adults (Gordon, Laumann, Gilmore, et al., 2017). These individual differences in functional network topography across the brain are not always associated with a clinical diagnosis but pertain to individual variation centered about a stable and common group level adult organization (Gratton et al., 2018; Seitzman et al., 2019).

Recent fMRI research has seen impressive leaps in the characterization of individual-specific large-scale functional brain networks using high signal-to-noise ratio precision functional mapping data (PFM) in adults (Gordon, Laumann, Gilmore, et al., 2017; Greene et al., 2020; Laumann et al., 2015; Marek et al., 2018; Sylvester et al., 2020; Zheng et al., 2021). PFM is the precise and reliable characterization of brain function in an individual person, commonly achieved by the collection of hours of non-invasive fMRI data per person over multiple visits. PFM data provide highly accurate measurements of functional connectivity at the individual level, and has shown that individual adults have broadly similar brain network organization, but with distinct, reliable, individually unique features (Gordon, Laumann, Gilmore, et al., 2017). Further, an individual's functional connectivity that varies from the group average (termed "network variants") are not found to coincide with anatomical differences and are highly stable across time (Seitzman et al., 2019) and across rest and task states (Kraus et al., 2021) within an individual. These findings in the PFM adult literature suggest that individual variance of functional network organization represents stable characteristics of an individual, and therefore may provide valuable insights to individual differences in cognition and behavior.

From a child development standpoint, less is understood about the range of individual variation that may be observed during the normative trajectory towards adulthood. At younger ages, the large-scale organization of functional brain networks generally resembles the organization observed in the central tendencies of adult functional networks, even in neonates

(Sylvester et al., 2023). This observation of general network structure very early in life often (even implicitly) results in the assumption that during development, childhood functional network organization is moving toward the "adult-like" brain. However, it is difficult to test the nature of this developmental trajectory towards adulthood with attention to individual variation, given the inherent challenges large-scale data collection and the reduction of individual specificity observed in group data that primarily collects less data due to time and financial constraints. PFM analyses comparing childhood samples to adults can provide valuable insight to the refinement and specialization of functional brain networks as we mature, which in turn will deepen our understanding of how functional network refinement may support executive function and cognitive control ability in the developing brain. Understanding the degree of expected inter-individual variation is especially important in work aiming to use resting state functional connectivity (RSFC) analyses to characterize deviations of functional network organization in neurodevelopmental disorders.

The current work leverages a unique PFM dataset comprising 12 densely-sampled children to quantify and characterize inter-individual variability of resting state functional brain organization during childhood. We characterize the extent to which the topography and connectivity of functional networks varies across individuals and compare these metrics to an established adult PFM dataset (Gordon, Laumann, Gilmore, et al., 2017). We contrast inter-individual variation observed across age-groups and discuss how differences in individuals' functional network organization may offer insights to the interaction between individualized brain maturation and the development of cognitive, sensory, and motor functions.

2.3 Methods

2.3.1 Participant demographics

Thirteen children were recruited to participate in this study; one withdrew due to claustrophobia. Hence, the Child Precision Functional Mapping (cPFM) dataset reported here comprises 12 children, ages 8-12 years old (6 female, 6 male). Three children met diagnostic criteria for neurodevelopmental disorders, and a benign brain cyst was discovered as an incidental finding in one child. Detailed demographic and diagnostic information is reported in Table 2.1. Children were recruited from the Washington University community and from databases of previous participants who were willing to be contacted again for future studies. Parents or legal guardians provided informed consent, and all child participants provided assent. The Washington University School of Medicine Human Studies Committee and Institutional Review Board approved this study.

The Midnight Scan Club (MSC) dataset of ten healthy young adults was used as an adult comparison PFM dataset. Demographic information is detailed in Gordon et al. (2017).

2.3.2 Neuroimaging acquisition

All cPFM participants were scanned at Washington University School of Medicine on a Siemens Prisma 3T MRI scanner with a 64-channel head coil. Foam padding was applied around the head for participant comfort and to mitigate head motion during scans. Verbal feedback was given between scans to ensure participant comfort and to provide feedback on participant motion. Real-time motion analytic software – FIRMM (Dosenbach et al., 2017) - was used to track participant motion during scans.

Participant data were collected over 3 to 12 visits (M=7.5). At least one T1-weighted structural MPRAGE sequence (TR=2500ms, TE=2.9ms, FOV=256x256, voxel resolution=1x1x1mm) and one T2-weighted structural image with turbo spin echo sequence (TR=3200ms, TE=564ms, FOV=256x256, voxel resolution=1x1x1mm) were collected across visits and used for preprocessing. Up to three 10-minute echo-planar sequence functional resting state scans (TR=1100ms, TE=33ms, flip angle=84°, MB factor=4, 54 axial slices, voxel resolution=2.6x2.6x2.6mm) were collected per visit. During resting state scans, participants were instructed to view a white fixation cross on a black background, stay awake, and lie as still as possible.

The adult Midnight Scan Club (Gordon, Laumann, Gilmore, et al., 2017) dataset was downloaded from www.openneuro.org (doi:10.18112/openneuro.ds000224.v1.0.4) in unprocessed NIfTI (Neuroimaging Informatics Technology Initiative) format. fMRI data specifics can be obtained from previously published material (Laumann et al., 2016). The adult data used to test for scanner and MRI sequence influences (SIC01-03) can be downloaded from www.openneuro.org (doi:10.18112/openneuro.ds002766.v3.0.2). Preprocessed fMRI data used for the analyses included in this study were obtained from authors of the original study and full fMRI preprocessing specifics (which closely matched those listed below) can be found in the original published work (Newbold et al., 2020).

2.3.3 Resting state preprocessing

All MRI data were preprocessed in-house, using a public release of the DCAN-Labs abcd-hcp-pipeline (Sturgeon et al., 2021). Additional FMRIB Software Library (Smith et al., 2004), Freesurfer (Dale et al., 1999), and Connectome Workbench (Marcus et al., 2011)

commands and custom MATLAB(The MathWorks Inc., 2020) scripts were also used for preprocessing and data analysis. The DCAN-Labs abcd-hcp-pipeline follows the primary steps of the Human connectome minimal preprocessing pipeline (Glasser et al., 2013), followed by additional resting state focused preprocessing steps, informed by best practices in the field (Caballero-Gaudes & Reynolds, 2017; Dipasquale et al., 2017; Hallquist et al., 2013; Lindquist et al., 2019; Power et al., 2012; Power et al., 2014).

The resting state focused preprocessing steps included: (1) de-meaning and de-trending of data; (2) general linear model "denoising" of signal related to white matter, cerebral spinal fluid, whole brain (global) signal, and six directions of motion plus their derivatives; (3) temporal band-pass filtering ($0.008Hz < f < 0.09Hz$); (4) respiratory motion filtering(Fair et al., 2020) (5) and motion censoring which excluded frames exceeding a framewise displacement (FD) of 0.2mm. Additionally, retained frames were required to be in clusters of at least 5 contiguous, below FD threshold frames. Registration steps and denoising are each done in a single pass to mitigate the reintroduction of noise (Lindquist et al., 2019).

All resting state data were then mapped to an MNI-transformed midthickness 32k fs_LR surface mesh (Van Essen et al., 2012) and spatial smoothing was applied via geodesic Gaussian smoothing (6mm FWHM, 2.55 sigma) to create the final CIFTI dense timeseries file used for analyses.

2.3.4 Reliability curves

Within-subject RSFC reliability curves were calculated to visualize the reliability of scan data across multiple visits and identify the quantity of RSFC data needed for within-participant reliability to gain little value from additional data collection. Reliability curves were calculated

for all cPFM participants with greater than 1 hour and 30 minutes of data using the following method. For each individual, resting state timeseries were extracted using 333 previously defined cortical parcels (Gordon et al., 2016). First, we created a baseline or "true" RSFC correlation matrix using 1 hour of data, pseudo-randomly sampled across all scan visits of that individual. This ensured that data from all scan visits were represented in each correlation matrix. A "test" correlation matrix was then created from pseudo-randomly sampling the remaining RSFC data, again, distributed across all scan visits, in 5-minute increments and the "true" and "test" matrices were correlated. The data used to create the "test" correlation matrices was increased until all remaining data was used. This process was completed 1K times and averaged per-participant.

2.3.5 Reliability curves

Individual-specific functional network organizations were identified using the Infomap community detection method (Rosvall & Bergstrom, 2008), similar to the methodologies presented in previous studies (Power et al., 2011; Gordon, Laumann, Gilmore, et al., 2017). In short, we computed pairwise Pearson r correlations among the BOLD time series across all cortical vertices, generating a correlation matrix of dimensions 59,412 x 59,412. Subsequently, this matrix was thresholded across a range of densities spanning from 0.1% to 5%. For each threshold, community assignments were found using the Infomap algorithm. To attribute putative network identities to each community at each threshold, we utilized a template matching procedure. The Jaccard index was used to calculate the spatial overlap of each community was a set of independent networks (Supplementary Figure 2.1) derived from a cohort of 7,316 (3,649 F) children in the Adolescent Brain Cognitive Development (ABCD) (Casey et al., 2018) study (See Supplementary Table 2.1 for full ABCD 7,316 group demographics). An assignment was

given to the best matching network if the Jaccard index was at least 0.1 (less than 0.1 overlap was not given an assignment to prevent poorly fitting matches). To consolidate assignments across sparsity thresholds, a consensus network assignment was derived for by retaining the network identity of a vertex at the sparsest threshold where it was successfully assigned to a known group network.

2.3.6 Probabilistic maps

We conducted a probabilistic/density map analysis identical to the approach taken by Dworetsky et al (Dworetsky et al., 2021). For each cortical vertex, we tallied the incidences of each network assignment across both age groups. cPFM11 and cPFM13 were removed from this analysis due excessive motion and a brain lesion, respectively. Following this step, every network map underwent normalization by dividing it by the total number of individuals within the corresponding age group. As a result, we generated a distinctive probabilistic map for each network, offering insights into the likelihood of a specific network assignment occurring at any given vertex within the designated age group. The combined network map encompasses the frequencies linked to the most common network assignment for every vertex.

2.3.7 Cortical Variants

Cortical resting state functional connectivity variants (regions that show strong dissimilarity to the group average functional connectivity) were identified using methods previously applied to adult datasets (Kraus et al., 2021; Seitzman et al., 2019). First, each individual's connectivity matrix was compared to an age-appropriate RSFC group average. For the cPFM participants, the comparison group average connectivity matrix was created from 185

(83 F) children recruited through the Adolescent Brain Cognitive Development (ABCD) (Casey et al., 2018) collection, ages 9-10.8 years old (M=10.2yrs) and did not include any sibling or twin pairs (See Supplementary Table 2.1 for RSFC comparison group demographics). All participants included in this group average were required to have at least 5 minutes of resting state data post motion censoring at 0.2mm FD (M=13m 55s). Additionally, all retained frames were required to be within groups of at least 5 contiguous, below FD threshold frames. To best mitigate methodological differences, the ABCD participants selected for the group average were scanned at Washington University School of Medicine, and data were preprocessed with the same DCAN-Labs abcd-hcp-pipeline (Sturgeon et al., 2021) and smoothed with a matching smoothing kernel of 6mm FWHM.

For the adult comparison (MSC) participants, the WashU 120 (Gordon, Laumann, Adeyemo, et al., 2017) group average was used, matching methods in the previous adult work using MSC data. fMRI preprocessing, motion censoring, and spatial smoothing were the same as described above.

Functional connectivity variants for each participant were identified by correlating the functional connectivity of each surface vertex of a given individual with the functional connectivity of the matching vertex in the group average data. This procedure resulted in an individual-to-group average spatial correlation map for all 59,412 cortical surface vertices. Cortical regions with the lowest 10% of correlations that also consisted of at least 30 contiguous surface vertices were then binarized and labeled as a functional network variant. The binarized variant maps for all participants were then used for all subsequent variant analyses.

Spatial overlap of participant variant maps was quantified using the Dice similarity coefficient (Dice, 1945). The Dice similarity coefficient is a spatial overlap index, ranging from

0 which indicates no spatial overlap of two binary sets, to 1 indicating complete overlap of two binary sets. Binary variant maps for all participants created in the previous step were used to calculate inter-individual variant map dice coefficients across both age groups to quantify the age-related similarity of functional connectivity variants of children and adults.

2.3.8 Functional network similarity

We calculated pairwise correlations between whole-cortex resting state functional network organization at the vertex level, for each pair of participants in each age cohort. An RSFC matrix was constructed for each participant utilizing 59,412 cortical surface vertices. Subsequently, we determined the correlation between the upper triangular components of the RSFC matrix for each participant and those of all other participants. This analysis aimed to discern whether participants' average within-group similarity of RSFC differed between the child and adult cohorts.

To investigate which brain regions display higher similarity in children compared to adults, we created an average spatial correlation map for each age group. The functional connectivity of each cortical vertex of each participant was correlated with the connectivity at that vertex with every other individual in the age group This procedure resulted in an individual-to-individual spatial correlation map for all 59,412 cortical vertices for each pair of individuals in each age group. These maps were then averaged in each group to create within age-group similarity maps. This enabled us to identify cortical regions of the brain with large similarity within their respective age groups and how within-group similarity changed within the child and adult cohorts. To further investigate the latter, a difference map was created by taking child within-group similarity minus adult within-group similarity maps. An identical approach was

taken to create the between age-group similarity map, except individual-to-individual spatial correlation maps were created now from each child to each adult pair, and then the average of these maps was used to create the between-group similarity map.

The vertices were further categorized into 10 canonical functional networks: visual, auditory, somatomotor face, somatomotor face, somatomotor foot, default mode, cingulo-opercular, frontoparietal, salience, dorsal attention, and ventral attention based off individual-specific functional networks labels.

2.4 Results

2.4.1 Collection of precision functional mapping data is feasible in a child sample

The collection of PFM data in a pediatric sample can be challenging (Greene et al., 2018) due to children being less tolerant of longer or repeated scan visits and exhibiting greater head motion than adults (Dosenbach et al., 2017). Here, we demonstrate feasibility in obtaining high-quality (i.e., low motion) PFM data from 12 children and make available the Child Precision Functional Mapping (cPFM) dataset. These children ranged in age from 8.2 - 11.9 years (M=9.9yrs) and included six males and six females (gender identity was not collected), and three with a reported neurodevelopmental disorder diagnosis. One additional child was recruited and screened but withdrew from the study prior to scanning due to claustrophobia. Each participant completed 3 - 12 fMRI visits, each visit including collection of 2 structural MRI scans and up to three 10-min resting state fMRI scans. Strict motion censoring was applied as part of the pre-processing steps to mitigate artifactual effects of motion (Engelhardt et al., 2017; Meissner et al., 2020; Power et al., 2015; Satterthwaite et al., 2012), and each participant retained 1 - 5.5 hours (M=3hrs) of resting state fMRI data (64 - 95% of total data retained per participant, M = 77%,

Figure 2.1A). Thus, the cPFM dataset demonstrates feasibility of obtaining a minimum of 1 hour of low-motion, usable resting state fMRI data across at least 3 scan sessions in children. Table 2.1 reports additional scan and demographic information.

2.4.2 RSFC is highly reliable with PFM data

To quantify the amount of data required for reliable estimation of cortical functional connectivity, we conducted an iterative split-data reliability analysis (Gordon, Laumann, Gilmore, et al., 2017; Laumann et al., 2015). We extracted resting state timeseries from each of 333 previously defined parcels (Gordon et al., 2016) (pseudo-randomly sampled in increasing lengths) from the set of all preprocessed resting state data of a given participant. Parcel-wise RSFC matrices were then created, and reliability curves were generated using all parcel-wise RSFC matrices for each child participant. Figure 2.1B shows that reliability curves reached a correlation of .9 for the majority of participants when using 45-50 minutes of "test" data, measured against 1 hour of "true" data. cPFM reliability curves appear to be approaching asymptotic values, showing minimal but non-negligible increases in reliability with amounts of data greater than 90 minutes.

Table 2.1: cPFM participant demographic information

Participant Demographic Information									
Child Precision Functional Mapping Dataset									
ID	**Sessions**	**Total Time Collected**	**Time ≤ 0.2 FD**	**Age at First Scan**	**Sex**	**IQ**	**Race**	**Ethnicity**	**Diagnosis**
cPFM05	12	5:59:42	5:40:14	9.2	M	122	White	NH	None
cPFM07	6	2:49:52	1:49:42	10.62	M	97	White	NH	None
cPFM08	12	5:59:42	3:51:12	9.88	M	118	White	NH	None
cPFM10	4	1:59:54	1:31:12	10.12	M	122	White, Black	NH	None
cPFM11	3	1:29:56	1:01:36	9.17	M	114	White, Black	NH	None
cPFM12	8	3:55:15	3:02:07	9.8	F	134	White	NH	Graves Disease
cPFM13	10	4:59:45	4:24:19	9.66	F	126	White, Asian	NH	Brain cyst
cPFM14	5	2:41:38	1:52:37	8.24	M	110	White	NH	TS, ADHD
cPFM15	8	3:39:49	2:37:51	11.9	F	102	White	NH	TS
cPFM17	6	2:29:53	2:07:12	10.13	F	137	White	NH	None
cPFM18	9	3:51:23	3:05:43	10.58	F	114	White	NH	TS
cPFM19	7	3:48:06	3:09:18	9.44	F	109	White	NH	None

NH = Non-Hispanic, TS = Tourette syndrome

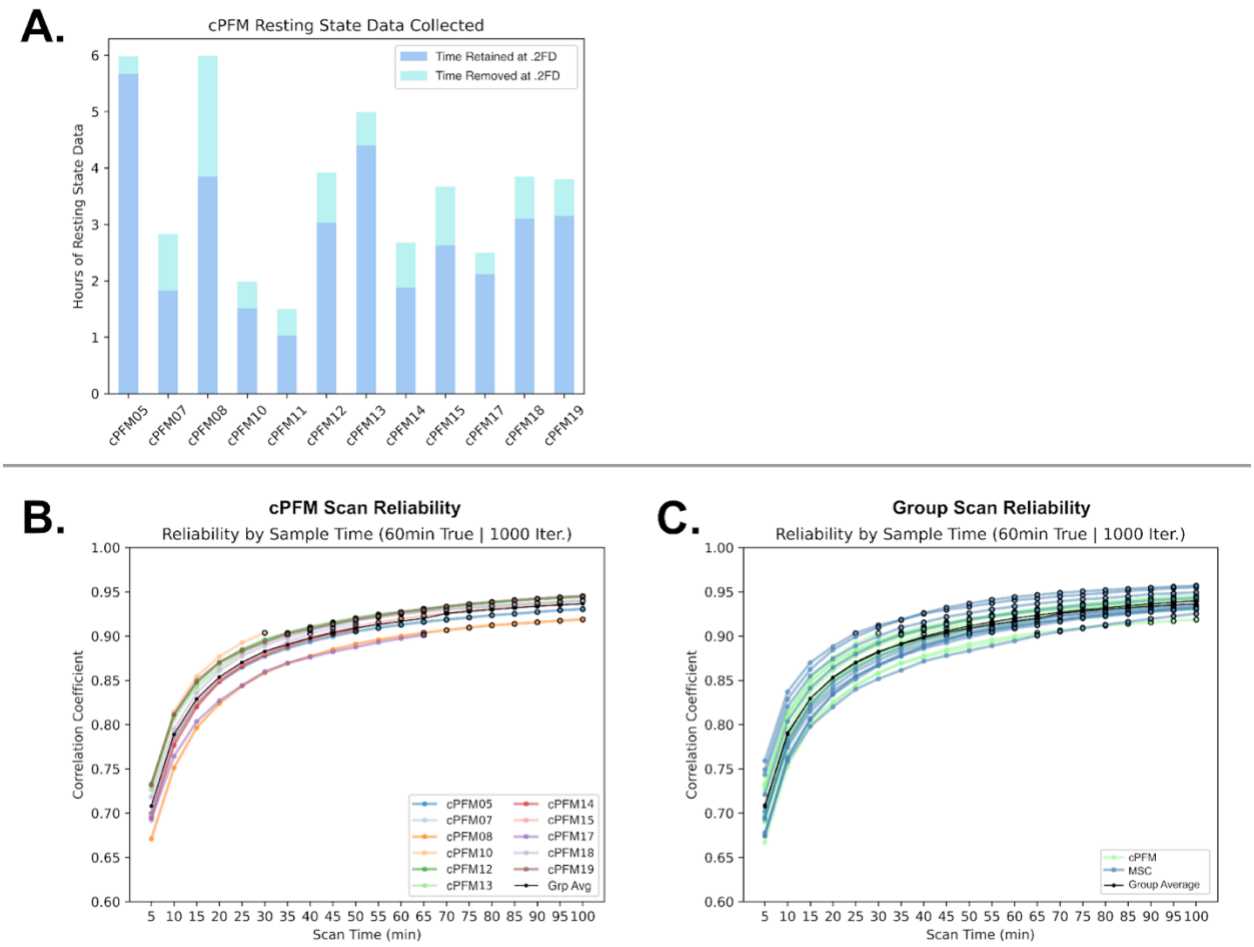

Figure 2.1 cPFM dataset summary and reliability. (A) Time resting state data retained and removed (motion scrubbed at .2FD) for each individual. (B) Reliability curves of RSFC data for each participant are compared in the cPFM dataset. (C) Reliability curves comparing the cPFM dataset to the MSC dataset

.

2.4.3 Individualized functional networks show broad similarities and individual features across children

Functional network topography for each child was identified using an information theory based community detection procedure as in prior studies (Gordon, Laumann, Gilmore, et al., 2017; Power et al., 2011). Networks were determined using a consensus approach across varying RSFC density thresholds, and then assigned a functional identity by applying a template matching process which finds the highest degree of spatial overlap between the community and a

predefined set of template functional networks (Supplementary Figure 2.1). Each participant exhibited individual-specific network organizations comprising 12 canonical functional networks: visual (VIS), somatomotor hand (SM Hand), somatomotor face (SM Face), somatomotor foot (SM Foot), auditory (AUD), default mode (DMN), cingulo-opercular (recently termed the action-mode network (Dosenbach et al., 2024) and referred to as CON/AMN hereafter), frontoparietal (FPN), dorsal attention (DAN), ventral attention (VAN, also referred to as the Language network), salience (SAL), and contextual association networks (CAN) (Figure 2.2; medial view found in Supplementary Figure 2.2). Qualitatively, all children shared broadly similar features of their functional network organization, with consistencies in the general topography of each network (between subject NMI = .44). At the same time, individual differences are apparent, with variability across individuals in specific features of each network. The reliability of each cortical network map was evaluated through a split-half procedure which found an average within-subject reliability to be .66 NMI.

To evaluate the consistency of functional network assignments among children, we generated density maps for each network which count the occurrences of that network at every cortical vertex across participants. As depicted in Figure 2.3, large consistency was evident for each network with the largest consistency occurring in somatomotor and medial vision regions. Echoing results from adult data (Dworetsky et al., 2021; Gordon, Laumann, Gilmore, et al., 2017), we identified canonical attributes in all children, such as DMN features in bilateral angular gyri, FPN in the lateral prefrontal cortex, and a distinct dorsal-ventral delineation between somatomotor foot, hand, and face regions. Further, core regions of each network had the largest consistency among the group, with regions on the edge of each network displaying the largest variability.

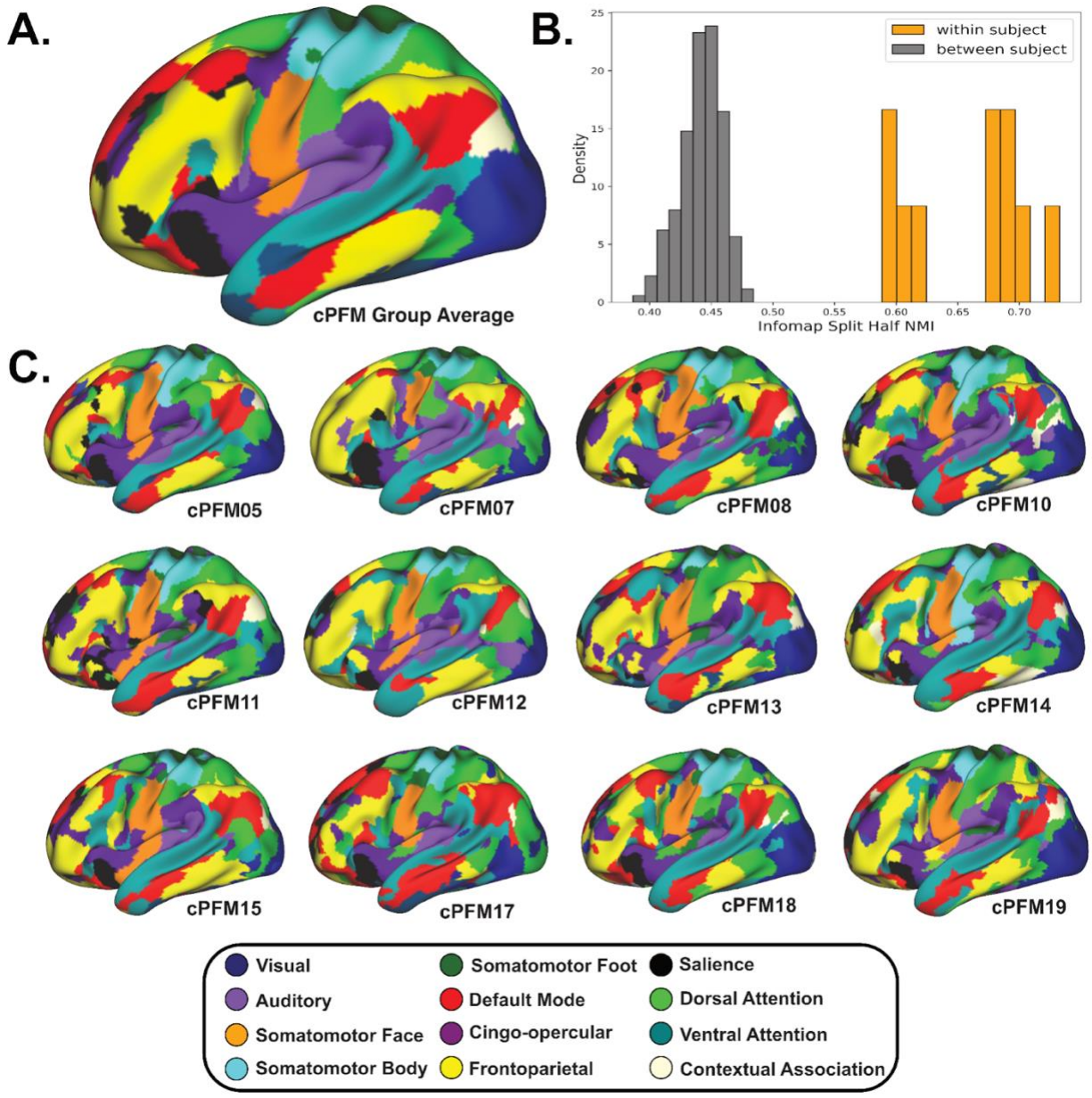

Figure 2.2: Childhood cortical functional networks (A) cPFM group average network organization. (B) Split half NMI of within subject and between subject analyses of cPFM participants. (C) Individual cPFM participant cortical network organization (left hemisphere, lateral surface).

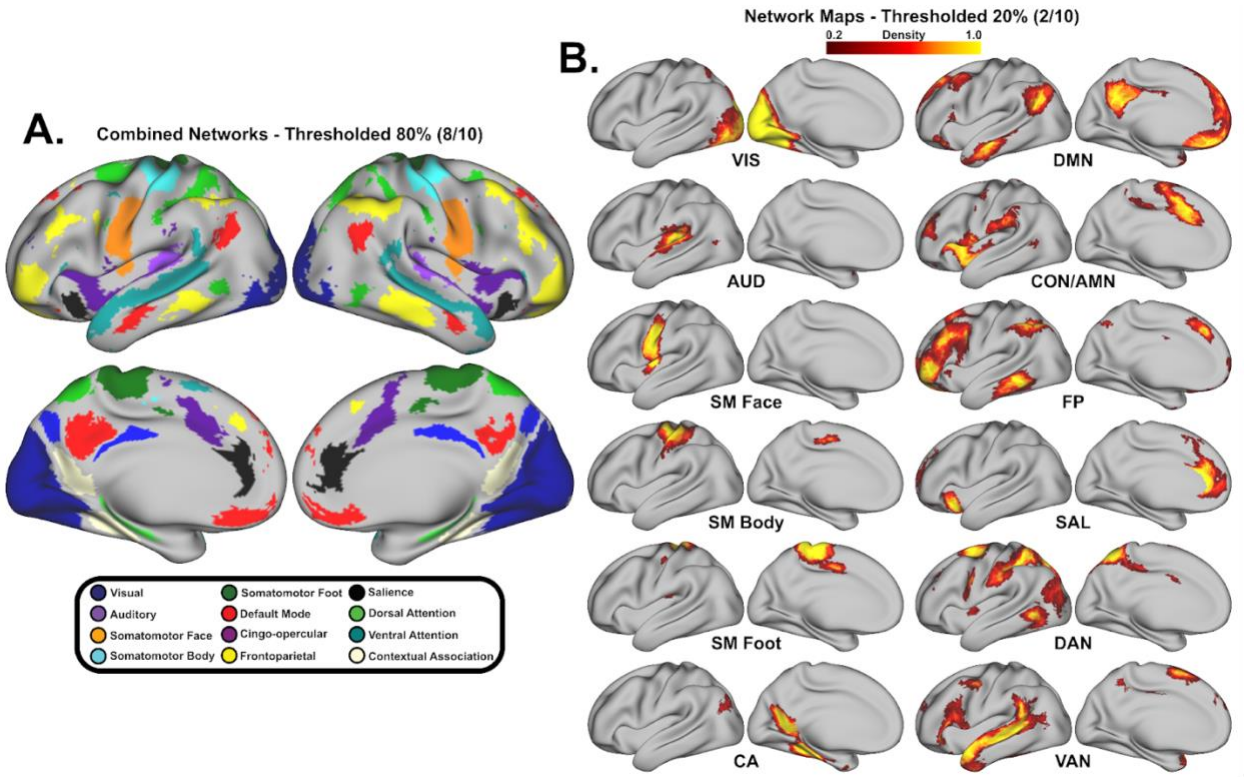

Figure 2.3: cPFM network density maps (A) cPFM combined networks where 80% of individuals have the same network assignment. (B) Density maps for individual networks with a threshold of 80% (8/10 cPFM participants) applied.

2.4.4 RSFC variant analysis identifies cortical regions of individual variability

To investigate individual variability in RSFC, cortical variants - regions of the brain with connectivity that is significantly different from a group average - were identified for each child. Following similar methods previously applied to adult PFM data (Seitzman et al., 2019), individual RSFC was calculated for all cortical vertices of each child and was then compared to a group average of 185 children's data selected from the ABCD study dataset (Supplementary Table 2.1). All children exhibited RSFC cortical variants, though variant count and locations differed across children (Figure 2.4) Across the cPFM group, RSFC variants were located primarily across the bi-lateral frontal cortex, the temporo–occipito–parietal junction, and along the cingulate gyrus (Figure 2.4A). Specifically, cortical variant peaks were most common across

the group in the left inferior precentral, inferior frontal, middle temporal, and posterior and middle cingulate, as well as the right middle and inferior frontal, middle temporal, and to a lesser extent, anterior cingulate brain regions. Additionally, split-half similarity analyses of functional variants were conducted within- and between-individuals. Individuals showed high similarity in their split-half data (quantified by the Dice coefficient; average split-half Dice = 0.74) with significantly lower similarity of split-half data to all other individuals.

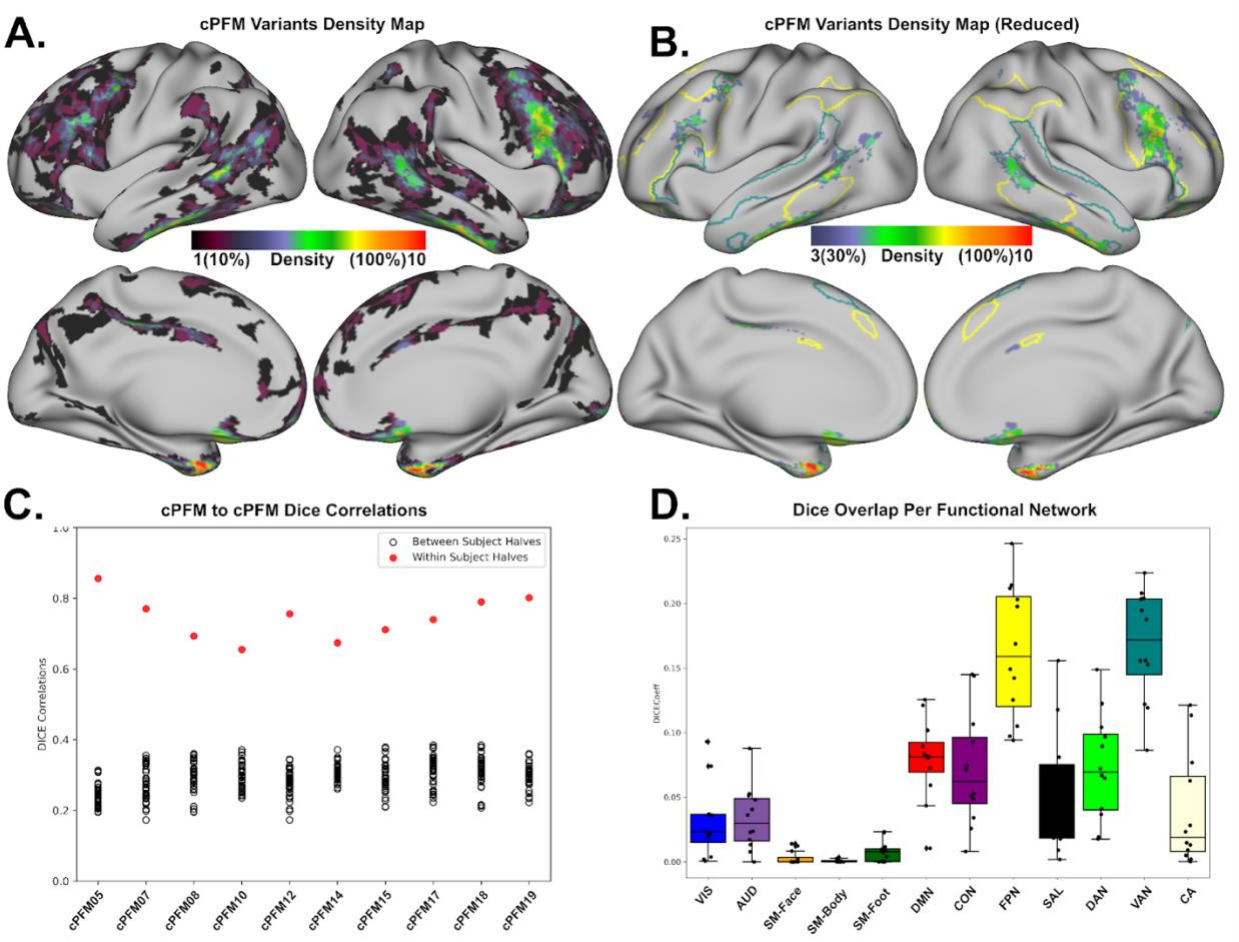

Figure 2.4: Cortical variants in childhood. (A) cPFM group variant density map. (B) cPFM group variant density map thresholded and overlaid with outlines of functional networks that overlapped most with variant locations (FPN in yellow, VAN in teal). (C) Split-half Dice coefficient within (red circles) and between (black circles) cPFM participants. (D) Bar plots depicting the variants overlap with each of the canonical RSFC functional networks

2.4.5 Inter-individual variability is lower in children compared to adults

Having established an understanding of the typical variability in individual-specific functional network organization among precision-mapped children, we next quantified differences between these children and a set of precision-mapped adults. Inter-individual functional network similarity was analyzed at the whole-cortex and regional levels. To assess

developmental differences, the child precision data (cPFM) was compared to adult precision data (MSC).

We computed the correlation of whole-cortex vertex-wise RSFC data between all pairs of participants in both age groups. As expected from the broad similarity and regions of consensus in functional network maps (Figure 2.3), inter-individual similarity was fairly high across the child (mean $z(r) = 0.61$; $sd = 0.05$) and adult groups (mean $z(r) = 0.52$; $sd = 0.03$) (Figure 2.5). Similarity within the child group was significantly higher than similarity in the adult group ($p < 0.001$, Figure 2.5B), suggesting inter-individual variability in network organization increases with age. To control for total scan time, as the MSC individuals have more data per person than the cPFM individuals, we conducted a control analysis sampling an identical amount of scan time and frame count from each participant and found similar results (Supplementary Figure 2.3). To control for the potential influence of MRI scanner and sequence differences, we ran the same analysis including three adult participants from an independent study (Newbold et al., 2020) that used the same scanner and sequences as the cPFM participants (Figure 2.5C). Despite having more scan time than the cPFM group on average, the children still had higher inter-individual similarity than these adults.

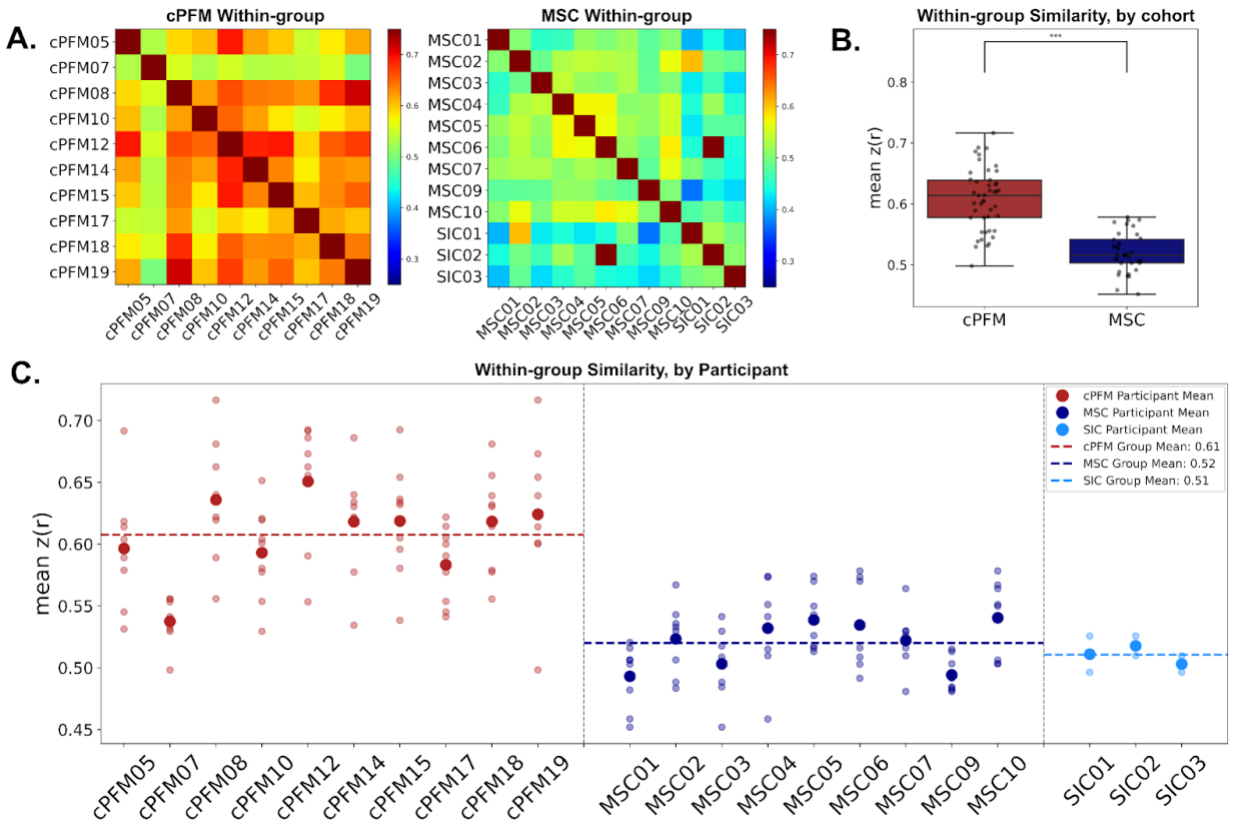

Figure 2.5: Functional network similarity across the child and adult PFM participants. (A-B) cPFM and MSC participant to participant similarity matrices comparing whole-cortex brain connectivity within each age group. (C) Within-group similarity values for each age cohort. (D) Participant level within-group similarity values, including SIC01, SIC02, SIC03 with equal scanning parameters to the cPFM group.

To investigate which cortical regions displayed increased similarity, we computed within-group similarity maps at the vertex level for each age group. In both cohorts, within-group similarity was largest in primary somatomotor and medial visual regions, the insula, precuneus, and posterior cingulate cortex (Figure 2.6A, B). By calculating the difference of these maps (child - adult), we found that the child cohort had larger within-group similarity values than the adult cohort across the somatomotor, superior parietal, temporal, and medial prefrontal cortex (Figure 2.6C). We further grouped vertex values by individual-specific functional network

identity at each vertex and found that childhood within-group similarity values were significantly larger in every functional network (Figure 2.6D) (FDR $p<0.05$).

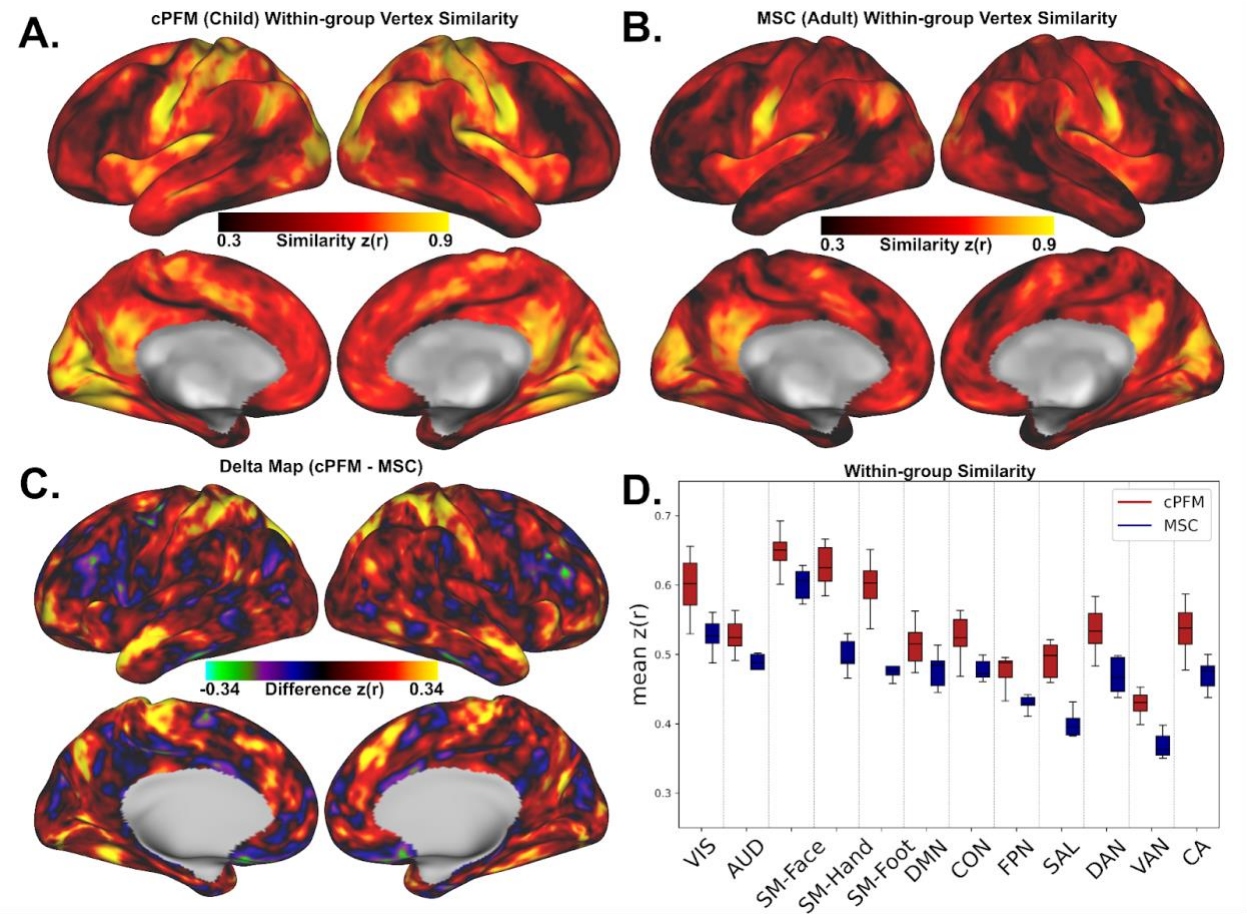

Figure 2.6: Within age-group similarity maps for children and adults. (A-B) Vertex-wise within-group similarity map for child and adult groups. (C) A difference map was created by taking child - adult maps. (D) Within-group similarity broken down by individual-specific network identity labels.

2.4.6 Age invariance is largest inside processing networks

Next, we calculated similarity values across all child to adult pairs. Age-invariance, or large between-group similarity, was substantial across the entire cortex (mean z(r) = .48; sd = .13), suggesting a pronounced population effect—an overarching functional organization that is

shared among both children and adults (Figure 2.7C). Like the regions with large within-group similarity, we found larger between-group similarity in primary somatomotor and visual regions, the insula, precuneus, and posterior cingulate cortex (Figure 2.7A). The individual-specific between-group similarity map for a representative child is shown in Figure 27B to highlight age-invariance in SMN, VIS, CON, AUD, and DMN regions.

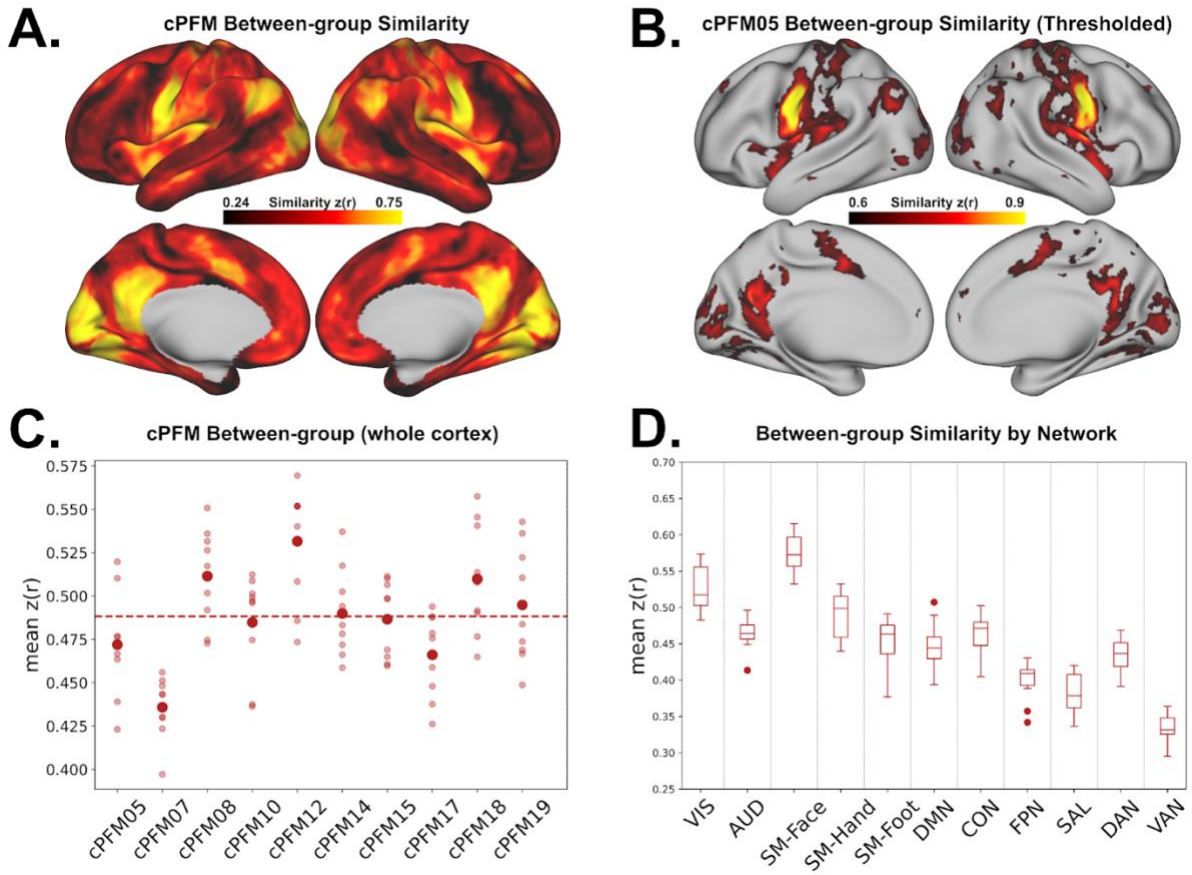

Figure 2.7: Between age-group similarity. (A) Between age-group similarity map created from averaging across all child-to-adult comparisons. (B) Individual-specific between group similarity map for a representative participant cPFM05. (C) Between-group similarity values for each child. (D) Between-group similarity broken down by individual-specific network identity.

2.5 Discussion

In the current study, we demonstrate the feasibility of collecting high-quality precision functional mapping resting state fMRI data in a pediatric sample. Although pediatric populations are generally considered more challenging than adults for fMRI data collection due to concerns of in-scanner motion and lower tolerance for repeated scanning (Dosenbach et al., 2017), we successfully collected an average of 3 hours of low-motion resting state fMRI data per child from 12 children across 3 to 12 scanning sessions each (Table 2.1). Despite an expected higher level of in-scanner motion for this age group, we retained approximately 75% of each participant's data after stringent motion correction (Figure 2.1A) and achieved reliable estimates of functional connectivity of a quantity and quality comparable to previous adult PFM datasets (Gordon, Laumann, Gilmore, et al., 2017). Additionally, this child PFM dataset of 12 children, aged 8 to 12 years old at their initial scan visit, will be made available as a public resource to continue to aid future work aiming to characterize brain development.

Precision functional mapping analyses conducted on the cPFM dataset revealed individually-specific features of functional brain network organization in childhood that were obscured in previous studies using common group-average approaches. While group-average analyses are important and necessary for identifying accurate brain-behavior associations (Marek et al., 2022), individual features of functional networks are necessarily obscured by group-average methods and the ability to measure inter-individual variation is reduced. Qualitatively, our cPFM dataset displayed functional network organization for each child that consisted of 12 canonical networks (Fig 2.2), each with common regions of consensus among the cores of these networks (Fig 2.3). Regions of inter-individual variability were, however, evident primarily along the edges of each network and in the association cortex (Fig 2.4A). Furthermore, specific

functional networks displayed larger variability than others, with the largest number of network variants in the frontoparietal network (FPN) and ventral-attention network (VAN) (Fig 2.4B, D).

These same methods, when applied to a set of precision mapped adults (Gordon, Laumann, Gilmore, et al., 2017), reveal comparable features of network consensus (Dworetsky et al., 2021) and variants (Seitzman et al., 2019). In fact, directly comparing the cPFM children to precision mapped adults (MSC) here, we find a large population, age-invariant, network organization is already in place with whole-cortex functional similarity between children and adults pairs being on average, $z(r)=0.48$ (Fig 2.7C). This supports previous work showing a stable group effect of functional brain networks (Gratton et al., 2018) and also supports the idea that an age-invariant organization is already in place in childhood and may even be present earlier as in neonates (Sylvester et al., 2023).

A major finding from this work is that inter-individual variability of functional network organization is larger in adults than in children (Fig 2.5C). This goes against the common assumption that the developmental trajectory of functional network organization begins in childhood with functional organization more variable and concludes in a stable 'adult-like' state. This assumption is perhaps justified as childhood is characterized by rapid and significant changes in cognitive development where children in the same 8- to 12-year-old range may have very different cognitive abilities (Tervo-clemmens et al., 2023). It is possible that inter-individual variability exists among 8- to 12-year-olds due to differences in developmental stages but that the effect is not the primary contributor to inter-individual variability. Instead, perhaps due to the accumulation of unique experiences, cognitive strategies, behaviors, or environmental factors, functional networks become more variable with age.

Evidence suggests that the core functional network organization is already in-place in neonates (Sylvester et al., 2023), supporting the idea of a large genetic component that is expressed in utero that establishes an individual's baseline network organization. Unique coactivations of brain regions and Hebbian-like processes may then selectively strengthen or weaken functional connectivity (Lewis et al, 2009) potentially causing inter-individual variability to increase during the lifetime. The refinement we see here occurs across every functional network (Figure 2.6D) suggesting maturation is a global process impacting the whole brain rather than being limited to a specific network or region. Indeed, age is associated with brain network integration and segregation across various sensory and control systems (Tooley et al., 2022), with RSFC - age relationships seemingly distributed randomly across the whole brain (Nielsen et al., 2018). Along with associations to age, RSFC-behavior relationships are significant across several functional networks (Marek et al., 2019; Cui et al., 2020; Tooley et al., 2022). It is thus suggested that neurodevelopmental changes are not limited to any specific attention or control system, but rather occur throughout the entire brain.

While the greater variability observed in the adult data may result from unique environmental, cognitive, or behavioral factors, other factors can potentially also influence this change in network organization. For example, age-related changes in vasculature (Bennett et al., 2024; Graff et al., 2021), myelination (Vandewouw et al., 2021), and cortical thinning (Petersen et al., 2022) may contribute to the observed increase in variance. Future longitudinal studies collecting these measures across multiple age ranges can help fill this gap and provide a more complete understanding of the factors leading to increased inter-individual variation in brain networks as we age. It is also possible that methodological or group factors may have some influence on the reported results. Although we made best efforts to check and control for

confounds between the child and adult datasets, inherent differences between the fMRI acquisition settings, reported and unreported individual behavioral diagnoses, and other common differences that arise from using multiple fMRI datasets for cross-sectional studies on development are some limitations of the current study. Differences in fMRI acquisition settings were addressed with the inclusion of the SIC adult comparison data (Figure 2.5), which matched the acquisition settings of the cPFM dataset and followed the results trend observed in the MSC adult data, suggesting that acquisition settings were perhaps an element, but not driving our main results. Further, 3 of the 12 children in the cPFM dataset had a neurobehavioral disorder diagnosis (Table 2.1) that were not matched in the adult data. Future PFM collections directly focusing on the influence of neurobehavioral disorders can help us to better understand how and to what extent these disorders may have influenced our main results. Lastly, the MSC and SIC adult datasets had longer post-processing and motion censored fMRI data times, in general, than the cPFM dataset. We addressed this by adjusting longer scan times to the cPFM average time in certain analyses. While the limitations of the current work should be addressed in the future, we suspect that the potential confounds of neurodevelopmental disorders or total scan time differences do not affect our results. Since the child group had more variable diagnostic phenotypes and less reliable data (less total scan time), we would reasonably expect both confounds to cause child functional brain networks to be more variable, rather than less variable, as we observe here.

Together, this study provides evidence of the feasibility of dense sampling and a PFM approach in a pediatric sample, a characterization of the inter-individual variability of functional brain networks during childhood (and compared to adult PFM data), and evidence for a trajectory of brain network refinement that begins more similar in childhood and becomes more

individually unique as we age. The results presented here and the release of this cPFM dataset for future work provide a foundation for understanding how brain networks are refined as we age and may inform how inter-individual differences in brain networks are involved in developmental disorders.

Acknowledgment

Chapter 2, in part, is currently being prepared for submission for publication of the material. Feigelis M, Demeter DV, Ali SA, Baim AR, Koithan E, Zreik S, Greene DJ. The dissertation author was the joint primary researcher and author of this material.

2.6 References

Bennett, H.C., Zhang, Q., Wu, Y., Manjila, S.B., Chon, U., Shin, D., Vanselow, D.J., Pi, H.-J., Drew, P.J., Kim, Y., 2024. Aging drives cerebrovascular network remodeling and functional changes in the mouse brain. Nat Commun 15, 6398. https://doi.org/10.1038/s41467-024-50559-8

Best, J.R., Miller, P.H., Naglieri, J.A., 2011. Relations between executive function and academic achievement from ages 5 to 17 in a large, representative national sample. Learning and Individual Differences 21, 327–336. https://doi.org/10.1016/j.lindif.2011.01.007

Blakemore, S.-J., 2012. Imaging brain development: The adolescent brain. NeuroImage 61, 397–406. https://doi.org/10.1016/j.neuroimage.2011.11.080

Caballero-Gaudes, C., Reynolds, R.C., 2017. Methods for cleaning the BOLD fMRI signal. NeuroImage 154, 128–149. https://doi.org/10.1016/j.neuroimage.2016.12.018

Casey, B.J., Cannonier, T., Conley, M.I., Cohen, A.O., Barch, D.M., Heitzeg, M.M., Soules, M.E., Teslovich, T., Dellarco, D.V., Garavan, H., Orr, C.A., Wager, T.D., Banich, M.T., Speer, N.K., Sutherland, M.T., Riedel, M.C., Dick, A.S., Bjork, J.M., Thomas, K.M., Chaarani, B., Mejia, M.H., Hagler, D.J., Daniela Cornejo, M., Sicat, C.S., Harms, M.P., Dosenbach, N.U.F., Rosenberg, M., Earl, E., Bartsch, H., Watts, R., Polimeni, J.R., Kuperman, J.M., Fair, D.A., Dale, A.M., 2018. The Adolescent Brain Cognitive Development (ABCD) study: Imaging acquisition across 21 sites. Developmental Cognitive Neuroscience 32, 43–54. https://doi.org/10.1016/j.dcn.2018.03.001

Cui, Z., Li, H., Xia, C.H., Larsen, B., Adebimpe, A., Baum, G.L., Cieslak, M., Gur, R.E., Gur, R.C., Moore, T.M., Oathes, D.J., Alexander-Bloch, A.F., Raznahan, A., Roalf, D.R., Shinohara, R.T., Wolf, D.H., Davatzikos, C., Bassett, D.S., Fair, D.A., Fan, Y., Satterthwaite, T.D., 2020. Individual Variation in Functional Topography of Association Networks in Youth. Neuron 106, 340-353.e8. https://doi.org/10.1016/j.neuron.2020.01.029

D. Sturgeon, Earl, E., Perrone, A., Kathy, 2021. DCAN-Labs/abcd-hcp-pipeline: Minor update to DCAN BOLD Processing and MRE version. https://doi.org/10.5281/ZENODO.4571051

Dale, A.M., Fischl, B., Sereno, M.I., 1999. Cortical Surface-Based Analysis. NeuroImage 9, 179–194. https://doi.org/10.1006/nimg.1998.0395

Dice, L.R., 1945. Measures of the Amount of Ecologic Association Between Species. Ecology 26, 297–302. https://doi.org/10.2307/1932409

Dipasquale, O., Sethi, A., Laganà, M.M., Baglio, F., Baselli, G., Kundu, P., Harrison, N.A., Cercignani, M., 2017. Comparing resting state fMRI de-noising approaches using multi- and single-echo acquisitions. PLoS ONE 12, e0173289. https://doi.org/10.1371/journal.pone.0173289

Dosenbach, N.U.F., Koller, J.M., Earl, E.A., Miranda-Dominguez, O., Klein, R.L., Van, A.N., Snyder, A.Z., Nagel, B.J., Nigg, J.T., Nguyen, A.L., Wesevich, V., Greene, D.J., Fair, D.A., 2017. Real-time motion analytics during brain MRI improve data quality and reduce costs. NeuroImage 161, 80–93. https://doi.org/10.1016/j.neuroimage.2017.08.025

Dosenbach, N.U.F., Raichle, M., Gordon, E.M., 2024. The brain's cingulo-opercular action-mode network. https://doi.org/10.31234/osf.io/2vt79

Dworetsky, A., Seitzman, B.A., Adeyemo, B., Neta, M., Coalson, R.S., Petersen, S.E., Gratton, C., 2021. Probabilistic mapping of human functional brain networks identifies regions of high group consensus. NeuroImage 237, 118164. https://doi.org/10.1016/j.neuroimage.2021.118164

Engelhardt, L.E., Roe, M.A., Juranek, J., DeMaster, D., Harden, K.P., Tucker-Drob, E.M., Church, J.A., 2017. Children's head motion during fMRI tasks is heritable and stable over time. Developmental Cognitive Neuroscience 25, 58–68. https://doi.org/10.1016/j.dcn.2017.01.011

Fair, D.A., Miranda-Dominguez, O., Snyder, A.Z., Perrone, A., Earl, E.A., Van, A.N., Koller, J.M., Feczko, E., Tisdall, M.D., Van Der Kouwe, A., Klein, R.L., Mirro, A.E., Hampton, J.M., Adeyemo, B., Laumann, T.O., Gratton, C., Greene, D.J., Schlaggar, B.L., Hagler, D.J., Watts, R., Garavan, H., Barch, D.M., Nigg, J.T., Petersen, S.E., Dale, A.M., Feldstein-Ewing, S.W., Nagel, B.J., Dosenbach, N.U.F., 2020. Correction of respiratory artifacts in MRI head motion estimates. NeuroImage 208, 116400. https://doi.org/10.1016/j.neuroimage.2019.116400

Giedd, J.N., Blumenthal, J., Jeffries, N.O., Castellanos, F.X., Liu, H., Zijdenbos, A., Paus, T., Evans, A.C., Rapoport, J.L., 1999. Brain development during childhood and adolescence: a longitudinal MRI study. Nat Neurosci 2, 861–863. https://doi.org/10.1038/13158

Glasser, M.F., Sotiropoulos, S.N., Wilson, J.A., Coalson, T.S., Fischl, B., Andersson, J.L., Xu, J., Jbabdi, S., Webster, M., Polimeni, J.R., Van Essen, D.C., Jenkinson, M., 2013. The minimal preprocessing pipelines for the Human Connectome Project. NeuroImage 80, 105–124. https://doi.org/10.1016/j.neuroimage.2013.04.127

Gordon, E.M., Laumann, T.O., Adeyemo, B., Gilmore, A.W., Nelson, S.M., Dosenbach, N.U.F., Petersen, S.E., 2017a. Individual-specific features of brain systems identified with resting state functional correlations. NeuroImage 146, 918–939. https://doi.org/10.1016/j.neuroimage.2016.08.032

Gordon, E.M., Laumann, T.O., Adeyemo, B., Huckins, J.F., Kelley, W.M., Petersen, S.E., 2016. Generation and Evaluation of a Cortical Area Parcellation from Resting-State Correlations. Cereb. Cortex 26, 288–303. https://doi.org/10.1093/cercor/bhu239

Gordon, E.M., Laumann, T.O., Gilmore, A.W., Newbold, D.J., Greene, D.J., Berg, J.J., Ortega, M., Hoyt-Drazen, C., Gratton, C., Sun, H., Hampton, J.M., Coalson, R.S., Nguyen, A.L., McDermott, K.B., Shimony, J.S., Snyder, A.Z., Schlaggar, B.L., Petersen, S.E., Nelson, S.M., Dosenbach, N.U.F., 2017b. Precision Functional Mapping of Individual Human Brains. Neuron 95, 791-807.e7. https://doi.org/10.1016/j.neuron.2017.07.011

Graff, B.J., Payne, S.J., El-Bouri, W.K., 2021. The Ageing Brain: Investigating the Role of Age in Changes to the Human Cerebral Microvasculature With an in silico Model. Front. Aging Neurosci. 13, 632521. https://doi.org/10.3389/fnagi.2021.632521

Gratton, C., Laumann, T.O., Nielsen, A.N., Greene, D.J., Gordon, E.M., Gilmore, A.W., Nelson, S.M., Coalson, R.S., Snyder, A.Z., Schlaggar, B.L., Dosenbach, N.U.F., Petersen, S.E., 2018. Functional Brain Networks Are Dominated by Stable Group and Individual Factors, Not Cognitive or Daily Variation. Neuron 98, 439-452.e5. https://doi.org/10.1016/j.neuron.2018.03.035

Grayson, D.S., Fair, D.A., 2017. Development of large-scale functional networks from birth to adulthood: A guide to the neuroimaging literature. NeuroImage 160, 15–31. https://doi.org/10.1016/j.neuroimage.2017.01.079

Greene, D.J., Koller, J.M., Hampton, J.M., Wesevich, V., Van, A.N., Nguyen, A.L., Hoyt, C.R., McIntyre, L., Earl, E.A., Klein, R.L., Shimony, J.S., Petersen, S.E., Schlaggar, B.L., Fair, D.A., Dosenbach, N.U.F., 2018. Behavioral interventions for reducing head motion during MRI scans in children. NeuroImage 171, 234–245. https://doi.org/10.1016/j.neuroimage.2018.01.023

Greene, D.J., Marek, S., Gordon, E.M., Siegel, J.S., Gratton, C., Laumann, T.O., Gilmore, A.W., Berg, J.J., Nguyen, A.L., Dierker, D., Van, A.N., Ortega, M., Newbold, D.J., Hampton, J.M., Nielsen, A.N., McDermott, K.B., Roland, J.L., Norris, S.A., Nelson, S.M., Snyder, A.Z., Schlaggar, B.L., Petersen, S.E., Dosenbach, N.U.F., 2020. Integrative and Network-Specific Connectivity of the Basal Ganglia and Thalamus Defined in Individuals. Neuron 105, 742-758.e6. https://doi.org/10.1016/j.neuron.2019.11.012

Hallquist, M.N., Hwang, K., Luna, B., 2013. The nuisance of nuisance regression: Spectral misspecification in a common approach to resting-state fMRI preprocessing reintroduces noise and obscures functional connectivity. NeuroImage 82, 208–225. https://doi.org/10.1016/j.neuroimage.2013.05.116

Houston, S.M., Herting, M.M., Sowell, E.R., 2013. The Neurobiology of Childhood Structural Brain Development: Conception Through Adulthood, in: Andersen, S.L., Pine, D.S. (Eds.), The Neurobiology of Childhood, Current Topics in Behavioral Neurosciences. Springer Berlin Heidelberg, Berlin, Heidelberg, pp. 3–17. https://doi.org/10.1007/978-3-662-45758-0_265

Keller, A.S., Pines, A.R., Shanmugan, S., Sydnor, V.J., Cui, Z., Bertolero, M.A., Barzilay, R., Alexander-Bloch, A.F., Byington, N., Chen, A., Conan, G.M., Davatzikos, C., Feczko, E., Hendrickson, T.J., Houghton, A., Larsen, B., Li, H., Miranda-Dominguez, O., Roalf, D.R., Perrone, A., Shetty, A., Shinohara, R.T., Fan, Y., Fair, D.A., Satterthwaite, T.D., 2023. Personalized functional brain network topography is associated with individual differences in youth cognition. Nat Commun 14, 8411. https://doi.org/10.1038/s41467-023-44087-0

Kraus, B.T., Perez, D., Ladwig, Z., Seitzman, B.A., Dworetsky, A., Petersen, S.E., Gratton, C., 2021. Network variants are similar between task and rest states. NeuroImage 229, 117743. https://doi.org/10.1016/j.neuroimage.2021.117743

Laumann, T.O., Gordon, E.M., Adeyemo, B., Snyder, A.Z., Joo, S.J., Chen, M.-Y., Gilmore, A.W., McDermott, K.B., Nelson, S.M., Dosenbach, N.U.F., Schlaggar, B.L., Mumford, J.A., Poldrack, R.A., Petersen, S.E., 2015. Functional System and Areal Organization of a Highly Sampled Individual Human Brain. Neuron 87, 657–670. https://doi.org/10.1016/j.neuron.2015.06.037

Laumann, T.O., Snyder, A.Z., Mitra, A., Gordon, E.M., Gratton, C., Adeyemo, B., Gilmore, A.W., Nelson, S.M., Berg, J.J., Greene, D.J., McCarthy, J.E., Tagliazucchi, E., Laufs, H., Schlaggar, B.L., Dosenbach, N.U.F., Petersen, S.E., 2016. On the Stability of BOLD fMRI Correlations. Cereb. Cortex cercor;bhw265v1. https://doi.org/10.1093/cercor/bhw265

Lewis, C.M., Baldassarre, A., Committeri, G., Romani, G.L., Corbetta, M., 2009. Learning sculpts the spontaneous activity of the resting human brain. Proc. Natl. Acad. Sci. U.S.A. 106, 17558–17563. https://doi.org/10.1073/pnas.0902455106

Lindquist, M.A., Geuter, S., Wager, T.D., Caffo, B.S., 2019. Modular preprocessing pipelines can reintroduce artifacts into fMRI data. Human Brain Mapping 40, 2358–2376. https://doi.org/10.1002/hbm.24528

Luna, B., Marek, S., Larsen, B., Tervo-Clemmens, B., Chahal, R., 2015. An Integrative Model of the Maturation of Cognitive Control. Annu. Rev. Neurosci. 38, 151–170. https://doi.org/10.1146/annurev-neuro-071714-034054

Luo, A.C., Sydnor, V.J., Pines, A., Larsen, B., Alexander-Bloch, A.F., Cieslak, M., Covitz, S., Chen, A.A., Esper, N.B., Feczko, E., Franco, A.R., Gur, R.E., Gur, R.C., Houghton, A., Hu, F., Keller, A.S., Kiar, G., Mehta, K., Salum, G.A., Tapera, T., Xu, T., Zhao, C., Salo, T., Fair, D.A., Shinohara, R.T., Milham, M.P., Satterthwaite, T.D., 2024. Functional connectivity development along the sensorimotor-association axis enhances the cortical hierarchy. Nat Commun 15, 3511. https://doi.org/10.1038/s41467-024-47748-w

Marcus, D.S., Harwell, J., Olsen, T., Hodge, M., Glasser, M.F., Prior, F., Jenkinson, M., Laumann, T., Curtiss, S.W., Van Essen, D.C., 2011. Informatics and Data Mining Tools and Strategies for the Human Connectome Project. Front. Neuroinform. 5. https://doi.org/10.3389/fninf.2011.00004

Marek, S., Siegel, J.S., Gordon, E.M., Raut, R.V., Gratton, C., Newbold, D.J., Ortega, M., Laumann, T.O., Adeyemo, B., Miller, D.B., Zheng, A., Lopez, K.C., Berg, J.J., Coalson, R.S., Nguyen, A.L., Dierker, D., Van, A.N., Hoyt, C.R., McDermott, K.B., Norris, S.A., Shimony, J.S., Snyder, A.Z., Nelson, S.M., Barch, D.M., Schlaggar, B.L., Raichle, M.E., Petersen, S.E., Greene, D.J., Dosenbach, N.U.F., 2018. Spatial and Temporal Organization of the Individual Human Cerebellum. Neuron 100, 977-993.e7. https://doi.org/10.1016/j.neuron.2018.10.010

Marek, S., Tervo-Clemmens, B., Calabro, F.J., Montez, D.F., Kay, B.P., Hatoum, A.S., Donohue, M.R., Foran, W., Miller, R.L., Hendrickson, T.J., Malone, S.M., Kandala, S., Feczko, E., Miranda-Dominguez, O., Graham, A.M., Earl, E.A., Perrone, A.J., Cordova, M., Doyle, O., Moore, L.A., Conan, G.M., Uriarte, J., Snider, K., Lynch, B.J., Wilgenbusch, J.C., Pengo, T., Tam, A., Chen, J., Newbold, D.J., Zheng, A., Seider, N.A., Van, A.N., Metoki, A., Chauvin, R.J., Laumann, T.O., Greene, D.J., Petersen, S.E., Garavan, H., Thompson, W.K., Nichols, T.E., Yeo, B.T.T., Barch, D.M., Luna, B., Fair, D.A., Dosenbach, N.U.F., 2022. Reproducible brain-wide association studies require thousands of individuals. Nature 603, 654–660. https://doi.org/10.1038/s41586-022-04492-9

Marek, S., Tervo-Clemmens, B., Nielsen, A.N., Wheelock, M.D., Miller, R.L., Laumann, T.O., Earl, E., Foran, W.W., Cordova, M., Doyle, O., Perrone, A., Miranda-Dominguez, O., Feczko, E., Sturgeon, D., Graham, A., Hermosillo, R., Snider, K., Galassi, A., Nagel, B.J., Ewing, S.W.F., Eggebrecht, A.T., Garavan, H., Dale, A.M., Greene, D.J., Barch, D.M., Fair, D.A., Luna, B., Dosenbach, N.U.F., 2019. Identifying reproducible individual differences in childhood functional brain networks: An ABCD study. Dev Cogn Neurosci 40, 100706. https://doi.org/10.1016/j.dcn.2019.100706

Meissner, T.W., Walbrin, J., Nordt, M., Koldewyn, K., Weigelt, S., 2020. Head motion during fMRI tasks is reduced in children and adults if participants take breaks. Developmental Cognitive Neuroscience 44, 100803. https://doi.org/10.1016/j.dcn.2020.100803

Mills, K.L., Goddings, A.-L., Herting, M.M., Meuwese, R., Blakemore, S.-J., Crone, E.A., Dahl, R.E., Güroğlu, B., Raznahan, A., Sowell, E.R., Tamnes, C.K., 2016. Structural brain development between childhood and adulthood: Convergence across four longitudinal samples. NeuroImage 141, 273–281. https://doi.org/10.1016/j.neuroimage.2016.07.044

Muetzel, R.L., Blanken, L.M.E., Thijssen, S., Van Der Lugt, A., Jaddoe, V.W.V., Verhulst, F.C., Tiemeier, H., White, T., 2016. Resting-state networks in 6-to-10 year old children. Human Brain Mapping 37, 4286–4300. https://doi.org/10.1002/hbm.23309

Newbold, D.J., Laumann, T.O., Hoyt, C.R., Hampton, J.M., Montez, D.F., Raut, R.V., Ortega, M., Mitra, A., Nielsen, A.N., Miller, D.B., Adeyemo, B., Nguyen, A.L., Scheidter, K.M., Tanenbaum, A.B., Van, A.N., Marek, S., Schlaggar, B.L., Carter, A.R., Greene, D.J., Gordon, E.M., Raichle, M.E., Petersen, S.E., Snyder, A.Z., Dosenbach, N.U.F., 2020. Plasticity and Spontaneous Activity Pulses in Disused Human Brain Circuits. Neuron 107, 580-589.e6. https://doi.org/10.1016/j.neuron.2020.05.007

Nielsen, A.N., Greene, D.J., Gratton, C., Dosenbach, N.U.F., Petersen, S.E., Schlaggar, B.L., 2019. Evaluating the Prediction of Brain Maturity From Functional Connectivity After Motion Artifact Denoising. Cereb Cortex 29, 2455–2469. https://doi.org/10.1093/cercor/bhy117

Paus, T., Keshavan, M., Giedd, J.N., 2008. Why do many psychiatric disorders emerge during adolescence? Nat Rev Neurosci 9, 947–957. https://doi.org/10.1038/nrn2513

Petersen, M., Nägele, F.L., Mayer, C., Schell, M., Rimmele, D.L., Petersen, E., Kühn, S., Gallinat, J., Hanning, U., Fiehler, J., Twerenbold, R., Gerloff, C., Thomalla, G., Cheng, B., 2022. Brain network architecture constrains age-related cortical thinning. NeuroImage 264, 119721. https://doi.org/10.1016/j.neuroimage.2022.119721

Power, J.D., Barnes, K.A., Snyder, A.Z., Schlaggar, B.L., Petersen, S.E., 2012. Spurious but systematic correlations in functional connectivity MRI networks arise from subject motion. NeuroImage 59, 2142–2154. https://doi.org/10.1016/j.neuroimage.2011.10.018

Power, J.D., Cohen, A.L., Nelson, S.M., Wig, G.S., Barnes, K.A., Church, J.A., Vogel, A.C., Laumann, T.O., Miezin, F.M., Schlaggar, B.L., Petersen, S.E., 2011. Functional Network Organization of the Human Brain. Neuron 72, 665–678. https://doi.org/10.1016/j.neuron.2011.09.006

Power, J.D., Mitra, A., Laumann, T.O., Snyder, A.Z., Schlaggar, B.L., Petersen, S.E., 2014. Methods to detect, characterize, and remove motion artifact in resting state fMRI. NeuroImage 84, 320–341. https://doi.org/10.1016/j.neuroimage.2013.08.048

Power, J.D., Schlaggar, B.L., Petersen, S.E., 2015. Recent progress and outstanding issues in motion correction in resting state fMRI. NeuroImage 105, 536–551. https://doi.org/10.1016/j.neuroimage.2014.10.044

Robson, D.A., Allen, M.S., Howard, S.J., 2020. Self-regulation in childhood as a predictor of future outcomes: A meta-analytic review. Psychological Bulletin 146, 324–354. https://doi.org/10.1037/bul0000227

Rosvall, M., Bergstrom, C.T., 2008. Maps of random walks on complex networks reveal community structure. Proc. Natl. Acad. Sci. U.S.A. 105, 1118–1123. https://doi.org/10.1073/pnas.0706851105

Satterthwaite, T.D., Wolf, D.H., Loughead, J., Ruparel, K., Elliott, M.A., Hakonarson, H., Gur, R.C., Gur, R.E., 2012. Impact of in-scanner head motion on multiple measures of functional connectivity: Relevance for studies of neurodevelopment in youth. NeuroImage 60, 623–632. https://doi.org/10.1016/j.neuroimage.2011.12.063

Seitzman, B.A., Gratton, C., Laumann, T.O., Gordon, E.M., Adeyemo, B., Dworetsky, A., Kraus, B.T., Gilmore, A.W., Berg, J.J., Ortega, M., Nguyen, A., Greene, D.J., McDermott, K.B., Nelson, S.M., Lessov-Schlaggar, C.N., Schlaggar, B.L., Dosenbach, N.U.F., Petersen, S.E., 2019. Trait-like variants in human functional brain networks. Proc. Natl. Acad. Sci. U.S.A. 116, 22851–22861. https://doi.org/10.1073/pnas.1902932116

Siegler, R.S., 2007. Cognitive variability. Developmental Science 10, 104–109. https://doi.org/10.1111/j.1467-7687.2007.00571.x

Smith, S.M., Jenkinson, M., Woolrich, M.W., Beckmann, C.F., Behrens, T.E.J., Johansen-Berg, H., Bannister, P.R., De Luca, M., Drobnjak, I., Flitney, D.E., Niazy, R.K., Saunders, J., Vickers, J., Zhang, Y., De Stefano, N., Brady, J.M., Matthews, P.M., 2004. Advances in functional and structural MR image analysis and implementation as FSL. NeuroImage 23, S208–S219. https://doi.org/10.1016/j.neuroimage.2004.07.051

Stiles, J., Jernigan, T.L., 2010. The Basics of Brain Development. Neuropsychol Rev 20, 327–348. https://doi.org/10.1007/s11065-010-9148-4

Sylvester, C.M., Kaplan, S., Myers, M.J., Gordon, E.M., Schwarzlose, R.F., Alexopoulos, D., Nielsen, A.N., Kenley, J.K., Meyer, D., Yu, Q., Graham, A.M., Fair, D.A., Warner, B.B., Barch, D.M., Rogers, C.E., Luby, J.L., Petersen, S.E., Smyser, C.D., 2023. Network-specific selectivity of functional connections in the neonatal brain. Cerebral Cortex 33, 2200–2214. https://doi.org/10.1093/cercor/bhac202

Sylvester, C.M., Yu, Q., Srivastava, A.B., Marek, S., Zheng, A., Alexopoulos, D., Smyser, C.D., Shimony, J.S., Ortega, M., Dierker, D.L., Patel, G.H., Nelson, S.M., Gilmore, A.W., McDermott, K.B., Berg, J.J., Drysdale, A.T., Perino, M.T., Snyder, A.Z., Raut, R.V., Laumann, T.O., Gordon, E.M., Barch, D.M., Rogers, C.E., Greene, D.J., Raichle, M.E., Dosenbach, N.U.F., 2020. Individual-specific functional connectivity of the amygdala: A substrate for precision psychiatry. Proc. Natl. Acad. Sci. U.S.A. 117, 3808–3818. https://doi.org/10.1073/pnas.1910842117

Tervo-Clemmens, B., Calabro, F.J., Parr, A.C., Fedor, J., Foran, W., Luna, B., 2023. A canonical trajectory of executive function maturation from adolescence to adulthood. Nat Commun 14, 6922. https://doi.org/10.1038/s41467-023-42540-8

Thomason, M.E., Dennis, E.L., Joshi, A.A., Joshi, S.H., Dinov, I.D., Chang, C., Henry, M.L., Johnson, R.F., Thompson, P.M., Toga, A.W., Glover, G.H., Van Horn, J.D., Gotlib, I.H., 2011. Resting-state fMRI can reliably map neural networks in children. NeuroImage 55, 165–175. https://doi.org/10.1016/j.neuroimage.2010.11.080

Tooley, U.A., Park, A.T., Leonard, J.A., Boroshok, A.L., McDermott, C.L., Tisdall, M.D., Bassett, D.S., Mackey, A.P., 2022. The Age of Reason: Functional Brain Network Development during Childhood. J Neurosci 42, 8237–8251. https://doi.org/10.1523/JNEUROSCI.0511-22.2022

Van Essen, D.C., Glasser, M.F., Dierker, D.L., Harwell, J., Coalson, T., 2012. Parcellations and Hemispheric Asymmetries of Human Cerebral Cortex Analyzed on Surface-Based Atlases. Cerebral Cortex 22, 2241–2262. https://doi.org/10.1093/cercor/bhr291

Vandewouw, M.M., Hunt, B.A.E., Ziolkowski, J., Taylor, M.J., 2021. The developing relations between networks of cortical myelin and neurophysiological connectivity. NeuroImage 237, 118142. https://doi.org/10.1016/j.neuroimage.2021.118142

Zheng, A., Montez, D.F., Marek, S., Gilmore, A.W., Newbold, D.J., Laumann, T.O., Kay, B.P., Seider, N.A., Van, A.N., Hampton, J.M., Alexopoulos, D., Schlaggar, B.L., Sylvester, C.M., Greene, D.J., Shimony, J.S., Nelson, S.M., Wig, G.S., Gratton, C., McDermott, K.B., Raichle, M.E., Gordon, E.M., Dosenbach, N.U.F., 2021. Parallel hippocampal-parietal circuits for self- and goal-oriented processing. Proc. Natl. Acad. Sci. U.S.A. 118, e2101743118. https://doi.org/10.1073/pnas.2101743118

Appendix

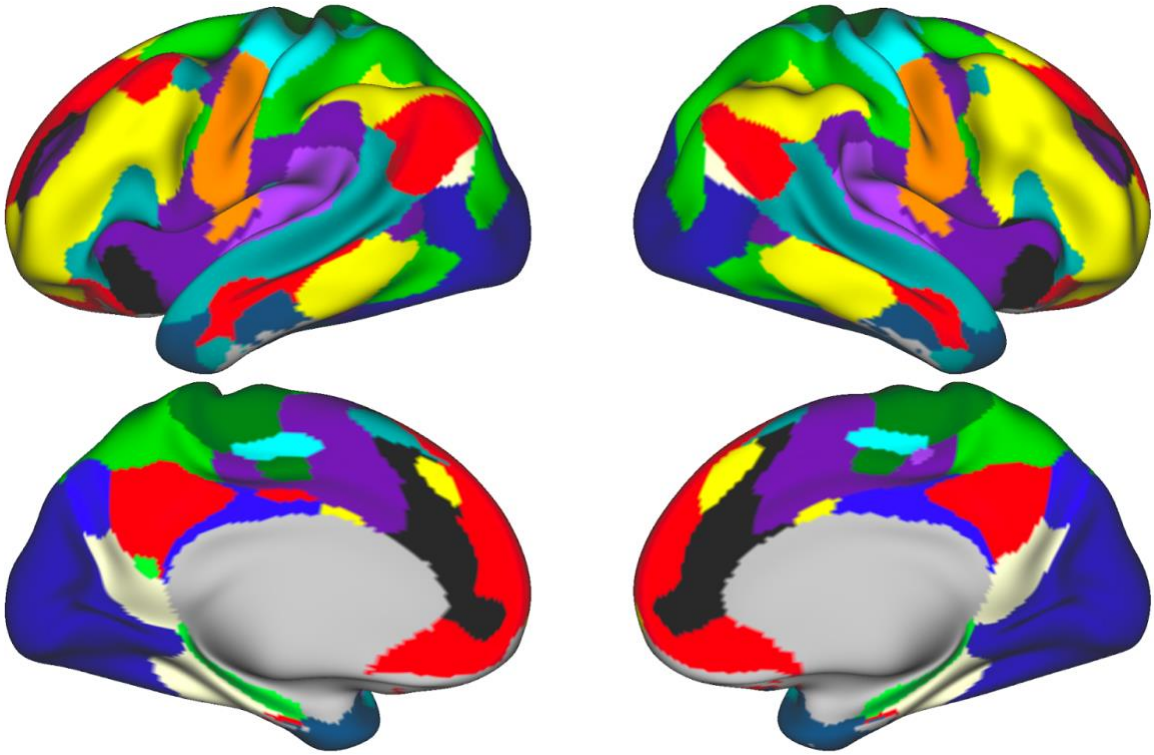

Supplementary Figure 2.1: ABCD 7,316 RSFC network template.

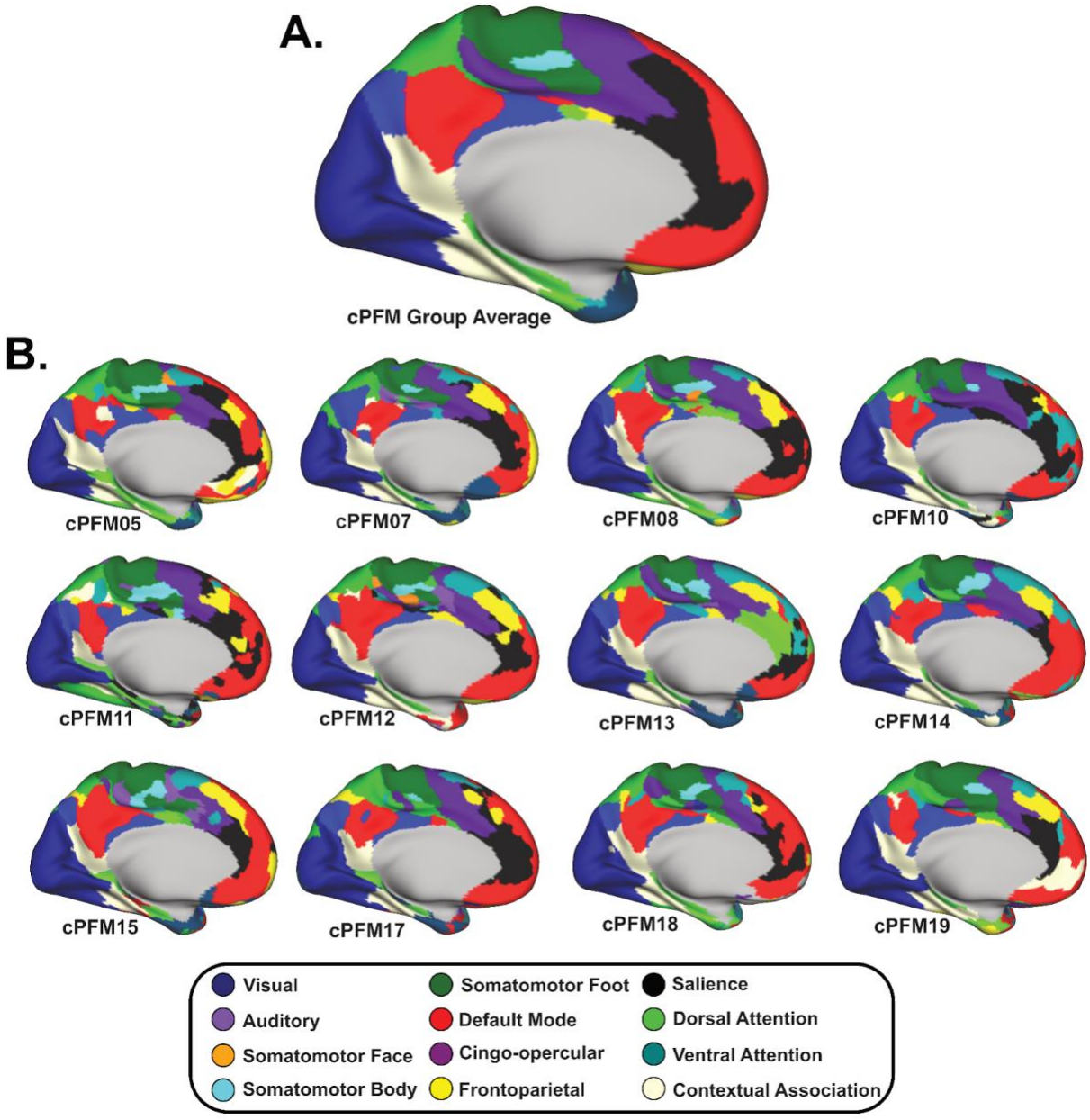

Supplementary Figure 2.2: cPFM cortical functional networks, medial view.

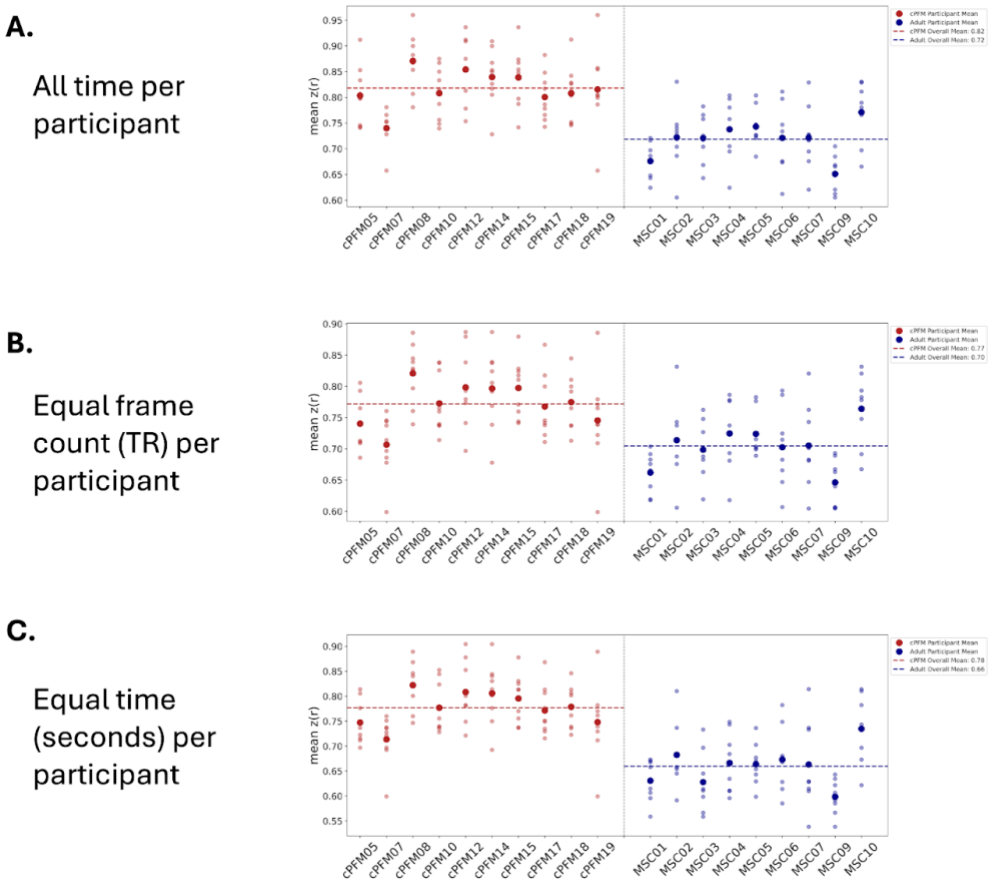

Supplementary Figure 2.3: cPFM functional network similarity controlling across age groups parcel-wise (A), then controlling for identical time (B) and frames (C).

Supplementary Table 2.1: RSFC comparison group demographics

Group RSFC Comparison Data Demographics	
ABCD 185 group	
Participants	102 Male (55%), 83 Female (45%)
Age Range (years)	9-10.9 years
Age (Mean)	10.2 years
Mean Scan Data	13 min 55 sec
Handedness	139 R (75%), 16 L (4%), 38 Ambi (21%)
Race and Ethnicity	
White	74 (40%)
Black	84 (45%)
Hispanic	5 (3%)
Asian	0
Other	22 (12%)
Not Reported	0
ABCD 7,316 group	
Participants	3,667 Male (50.1%), 3,649 Female (49.9%)
Age Range (years)	9-10.9 years
Age (Mean)	9.9 years
Mean Scan Data	15 min 13 sec
Handedness	5,891 R (81%), 501 L (7%), 917 Ambi (12%), 7 Unknown (<1%)
Race and Ethnicity	
White	4,137 (57%)
Black	918 (13%)
Hispanic	1,349 (18%)
Asian	145 (2%)
Other	759 (10%)
Not Reported	8 (<1%)

Chapter 3 Precision functional mapping of motor tics in individual children with Tourette syndrome

3.1 Abstract

In this study, we investigate the functional neuroanatomy of motor tics, one of the defining symptoms of Tourette syndrome. Using densely sampled resting-state functional magnetic resonance imaging (fMRI) data from three pediatric individuals with Tourette syndrome, during which they experienced naturally occurring motor tics, we used a precision functional mapping (PFM) approach to delineate each individual's large-scale functional brain networks and localize tic-related brain activity. Specifically, we investigate each individual's tic-related fMRI activations in the context of their individual-specific functional networks. We identify urge-related activity two seconds prior to tics that falls within the boundaries of each individual's cingulo-opercular action-mode network (CON/AMN) and somato-cognitive action network (SCAN). Activation within the somatomotor face network was associated with the urge in participants with a variety of facial tics, while the visual network and frontal/parietal eye fields were associated with eye movement tics. Regions of the CON/AMN displayed individual variability in their relationship to the urge across participants, particularly in the posterior cingulate and anterior insula. These findings highlight shared and individual-specific mechanisms underlying urge and tic symptoms in individuals with Tourette syndrome. Furthermore, they support the roles of action planning and control networks in Tourette syndrome and demonstrate PFM as a plausible method to localize individual-specific dysfunction.

3.2 Introduction

Tourette syndrome (TS) is a neurodevelopmental disorder that involves unwanted movements and vocalizations called tics. Common examples of tics include forceful blinking, head jerking, sniffing, and throat clearing (American Psychiatric Association, 2013). Chronic tics affect approximately 1–3% of the population, making them a significant public health concern (Cubo, 2012; Knight et al., 2012). In many individuals with Tourette syndrome, tics are preceded by an uncomfortable sensory or cognitive experience known as the premonitory urge (Leckman, Walker, and Cohen, 1993; Steinberg et al., 2010). This urge is described as a feeling of rising tension or pressure that is often, but not always, relieved after performing or releasing the tic. Although the sensation of the urge is involuntary, tics can be considered semi-voluntary actions because individuals may have the ability to suppress or replace them with a competing response.

The time preceding a tic, presumed to reflect the premonitory urge, has been associated with increased brain activity in the supplementary motor area (SMA), anterior cingulate cortex (ACC), parietal operculum, and insula (Bohlhalter et al., 2006; Neuner et al., 2014). In the context of large-scale functional brain networks, the SMA, ACC, operculum, and insula are highly functionally connected and comprise components of the cingulo-opercular action-mode network (CON/AMN, hereafter referred to as AMN) which is primarily involved in goal-directed action and processing arousal, error, pain, and discomfort (Dosenbach et al., 2007; Dosenbach et al., 2024). Electrical stimulation of the SMA, an important node of the AMN, has been shown to produce discomfort and an urge to move (Fried et al., 1991), similar in nature to the premonitory urge. Furthermore, both neurofeedback therapy and transcranial magnetic stimulation therapy targeting the SMA have successfully reduced tic severity in individuals with Tourette's (Sukhodolsky et al., 2020; Kahl et al., 2021). The SMA (and large-scale AMN) is functionally

connected to the newly characterized somato-cognitive action network (SCAN), which comprises three inter-effector regions that alternate with effector-specific areas within the primary motor cortex and are involved in whole-body action planning (Gordon et al., 2023). Connectivity to both the AMN and SCAN may be highly predictive of thalamic deep brain stimulation success in individuals with severe cases of Tourette's (Baldermann et al., 2024).

Still, the underlying cause of Tourette's remains unclear, with inconsistencies across neuroimaging studies regarding both structural and functional differences (see Greene et al., 2022). These inconsistencies may arise from standard methods that average data across groups to obtain group-level estimates of urge or tic activation maps, structural brain volumes, or resting-state connectivity. Such approaches typically require large sample sizes to achieve adequate power for detecting reliable group differences. However, underpowered studies are common due to the challenges associated with recruiting and scanning a large number of individuals with a neurodevelopmental disorder. Further complicating the issue is the known variability in both symptoms and functional brain organization across people. First, because symptoms vary across individuals (e.g., anatomical location of the tic, urge or tic severity), averaging across people will blur effects corresponding to any specific type of symptom (although a symptom-invariant effect may still be found).

Second, recent work has identified large individual differences in functional brain organization across people (Gordon, Laumann, Gilmore, et al., 2017); thus, even symptom-invariant effects could be difficult to accurately portray through group average approaches. For example, if tic symptoms activate slightly different anatomical regions across people–but all within the same functional network–averaging over people might blur the correspondence to the functional network, resulting in an averaged activation map that does not accurately represent

any single person. Variability in both clinical symptoms and functional brain organization has thus significantly challenged the basic and clinical utility of standard group-average neuroimaging techniques.

Precision functional mapping (PFM), which involves collecting large amounts of functional MRI data from each individual, has been used to precisely and reliably characterize functional brain organization at the individual level (Laumann et al., 2015; Gordon, Laumann, Gilmore, et al., 2017; Gratton et al., 2018; Marek et al., 2018; Greene et al., 2020; Sylvester et al., 2020). This approach has identified individual differences across the cortex and subcortex that were previously blurred by group-average analyses and can be useful, potentially necessary, for clinically relevant neurological and psychiatric biomarkers (Gratton et al., 2020; Kraus et al., 2023). Though PFM is a very recent approach for studying individual brain function, there is evidence of success in identifying state and trait markers for depression (Lynch et al., 2024). Tourette syndrome is unique among neuropsychiatric disorders in that we can directly observe the defining symptoms (tics) as they occur in the MRI scanner (through MRI-compatible video cameras). Precision fMRI may then be useful both to reliably characterize individual-specific functional organization in Tourette syndrome and to densely sample tic symptoms in the scanner in order to generate accurate activation maps at the individual level.

In this study, we investigate motor tics in individuals with Tourette syndrome using a precision fMRI approach designed to collect large amounts of data from each individual participant. A mixed resting-state and naturalistic event-based design was used to simultaneously record extensive resting-state data and naturally occurring tic events in the scanner. Brain activity linked to tic symptoms was modeled at the individual level and then referenced to each

individual's resting-state functional network space. Activation maps and functional networks were contrasted across individuals and related to tic symptoms.

3.3 Methods

3.3.1 Participants

Data were collected from three participants with Tourette syndrome (Table 3.1) who were recruited to participate in a larger PFM study on Tourette syndrome. All participants entered the study with a formal Tourette syndrome diagnosis. Psychiatric diagnoses and symptoms were further evaluated using the Kiddie Schedule for Affective Disorders and Schizophrenia (Kaufman et al., 1997) and the Yale Global Tic Severity Scale (YGTSS; Leckman et al., 1989). PT105 was additionally found to have attention-deficit/hyperactivity disorder and an anxiety disorder by a trained rater. The participants displayed a variety of facial tics impacting the eyes, nose, and mouth, with one participant (PT108) demonstrating almost exclusively tics related to eye movements. The participants were recruited from the San Diego community. The study was approved by the UC San Diego Institutional Review Board.

3.3.2 Neuroimaging acquisition

Participants were scanned at the University of California, San Diego on a Siemens Prisma 3T MRI scanner with a 64-channel head coil. Participant data were collected over 8 to 12 sessions. At least one T1-weighted structural MPRAGE sequence (TR=2500ms, TE=2.9ms, FOV=256x256, voxel resolution=1x1x1mm) and one T2-weighted structural image with turbo spin echo sequence (TR=3200ms, TE=564ms, FOV=256x256, voxel resolution=1x1x1mm) were collected in each visit and used for preprocessing. Up to five 6 minute multi-echo resting-state

fMRI runs, collected as a five-echo blood oxygen level dependent (BOLD) contrast sensitive gradient echo-planar sequence (TR=1761ms, multiband 6 acceleration, TE1: 14.20 ms, TE2: 38.93 ms, TE3: 63.66 ms, TE4: 88.39 ms, and TE5: 113.12 ms, flip angle=68°, resolution=2.0 mm isotropic), were collected per visit. During resting-state scans, participants were instructed to view a white fixation cross on a black background, stay awake, and tic freely in a natural state.

3.3.3 Behavioral data

An MR-compatible camera (MRC Systems) and microphone (Optoacoustics FOMRI III+) were attached to the head coil and positioned to capture the face. Audio and visual recordings were time-locked to the fMRI data. Video data was coded by M.F. for motor tics involving the eyebrows, eyes, nose, cheeks, mouth, and jaw to the nearest second.

3.3.4 Resting-state preprocessing

MRI data were preprocessed in-house using multi-echo processing toolkits Nordic (Moeller et al., 2020) and Tedana (DuPre et al., 2021) for multi-echo denoising and analysis, the DCAN-Labs abcd-hcp-pipeline (Sturgeon et al., 2021), as well as FMRIB Software Library, Freesurfer, Connectome Workbench commands, and custom MATLAB scripts. The DCAN-Labs abcd-hcp-pipeline follows the primary steps of the Human connectome minimal preprocessing pipeline (Glasser et al., 2013) and is then followed by additional resting-state focused preprocessing steps informed by best practices in the field (Power et al., 2012; Power et al., 2014; Hallquist, Hwang, and Luna, 2013). The resting-state steps included: (1) de-meaning and de-trending of data; (2) general linear model “denoising” of signal related to white matter, cerebral spinal fluid, whole brain (global) signal, and six directions of motion plus their

derivatives; (3) temporal band-pass filtering (0.008Hz < f < 0.09Hz); (4) respiratory motion filtering (Fair et al., 2020) (5) and motion censoring which excluded frames exceeding a framewise displacement (FD) of 0.2mm for PT102 and PT108, and 0.3mm for PT105. Visual inspection of FD traces were used to determine the floor for each individual. Additionally, retained frames were required to be in clusters of at least 5 contiguous below FD threshold frames. Registration steps and denoising are each done in a single pass to mitigate the reintroduction of noise (Lindquist et al., 2019). All resting-state data were then mapped to an MNI-transformed midthickness 32k fs_LR surface mesh (Van Essen et al., 2011).

3.3.5 Vertex-wise individual-specific network identification

Individual-specific functional network organizations were identified using the Infomap community detection method (Rosvall and Bergstrom, 2008), in similar fashion to the methodology presented by Gordon and colleagues (Gordon, Laumann, Gilmore, et al., 2017). First, we computed pairwise Pearson r correlations among the BOLD time series across all cortical vertices, generating a correlation matrix of dimensions 59,412 x 59,412. This matrix underwent thresholding across a range of densities spanning from 0.1% to 5%. For each threshold, community assignments were produced using the Infomap algorithm. Putative functional identities were given to each community through a template matching procedure. This involved comparing the subject's communities through Jaccard index (spatial overlap) with independent template networks (Gordon, Laumann, Adeyemo, et al., 2017). Briefly, for every threshold, each community was compared to each group network and then assignments were given to the best match, if the Jaccard index was at least 0.1 (lower overlap disregarded to prevent assignments to poorly fitting matches). To consolidate assignments across sparsity

thresholds, a consensus network assignment was derived by taking the network identity of a vertex at the sparsest threshold where it was successfully assigned.

3.3.6 Task fMRI

Analysis of tic events occurring naturally in the scanner was done using an event-based design in each participant separately. As some runs contained very few numbers of tic events (8 runs had 0 tic events, 20 runs had less than 2 tic events), runs were concatenated together before being analyzed. FSL (Jenkinson et al., 2012) FEAT first level analysis was used with default settings (5mm FWHM spatial smoothing, MCFLIRT motion correction, highpass filtering, gamma convolution with temporal filtering applied). Due to multicollinearity of regressors, we ran separate FSL models for the following conditions: urge event (2 seconds prior to a tic occurring, lasting 2 seconds), tic onset (lasting 1 second), and tic recovery (2 second after tic onset starts, lasting 2 seconds). Z-score activation maps were projected onto an individual's midthickness surface for visualization purposes.

3.3.7 Task-rest overlap

Binary masks were created from activation maps by thresholding at Z-statistics greater than 1.96. Binary masks were then overlaid on top of each individuals' resting-state network space. For each resting-state network, the amount of overlapping vertices between the activation mask and the resting-state was summed and then divided by the total size of the network.

3.4 Results

3.4.1 Data collection

Three children with TS (PT102, PT105, and PT108) underwent 8, 10, and 6 fMRI scanning sessions, respectively, spanning multiple weeks. During the resting-state fMRI scans, the participants were instructed to tic as needed while trying to remain as still as possible when not ticcing. In-scanner video positioned to capture the participants' faces was subsequently coded for facial motor tics. Two sessions were discarded for PT102 because one session had no tic events, and during another, the in-scanner microphone occluded the participant's nose from the view of the camera, a common tic location for her. Three sessions were discarded for PT105 due to excessive motion causing artifacts in the fMRI signal. Across the sessions used in this study, PT102 experienced 61 facial tics across the 6 fMRI sessions, PT105 experienced 117 tics across the 7 fMRI sessions, and PT108 experienced 70 tics across 6 fMRI sessions. Both PT102 and PT105 experienced a wide variety of simple facial tics across eyes, nose, and mouth areas, while PT108's tics were nearly all eye saccades and eye-rolling movements (Table 1). For resting-state analyses, data were preprocessed (see Methods) and underwent motion correction, resulting in 126 minutes of low-motion (<0.2 FD) resting-state scan time for PT102, 93 minutes of low-motion (<0.3 FD) resting-state scan time for PT105, and 104 minutes of low-motion (<0.2 FD) resting-state scan time for PT108.

Table 3.1: Participant demographic, clinical, and MRI information

Subject	Age	Sex	Dx	Types of tics	Mean YGTSS total tic score	# fMRI sessions used	Tic count during scan	Usable scan time
PT102	15	F	TS	Nasal flare, Mouth twitch, Rapid blinking, Nose scrunch, Jaw open and close, Head jerk	9	6	61	2h06m
PT105	10	F	TS, ADHD, Anxiety	Nasal flare, Mouth twitch, Rapid blinking, Nose scrunch, Eye jerk	23	7	117	1h33m
PT108	13	M	TS	Eye jerk, Eye roll, Face scrunch, Eyebrow raise	18	6	70	1h44m

Note: Dx = Diagnosis; TS = Tourette syndrome; ADHD = Attention-deficit/hyperactivity disorder; YGTSS = Yale Global Tic Severity Scale

3.4.2 Pre-tic urge activity

Analysis of tic events occurring naturally in the scanner was performed using an event-based design for each participant separately. Urge events were defined as the 2-second time window preceding tic onset as in previous studies (Bohlhalter et al., 2006; Neuner et al., 2014). Thresholded z-score maps for participants PT102, PT105, and PT108 are shown in Figure 3.1 (see Supplementary Figure 3.1 for unthresholded activation maps for each participant). All participants had urge-related activations in the anterior cingulate cortex, supplementary motor area, medial visual cortex, and M1/S1 regions resembling the somato-cognitive action network.

Participants with large amounts of mouth, nose, and eye blink tics (PT102, PT105) also displayed significant urge activations in M1/S1 face regions (Figure 3.1A, B). The participant with eye movement tics (saccades, rolls) displayed stronger activations in the medial visual cortex, as well as activations in the frontal and parietal eye fields (Figure 3.1C).

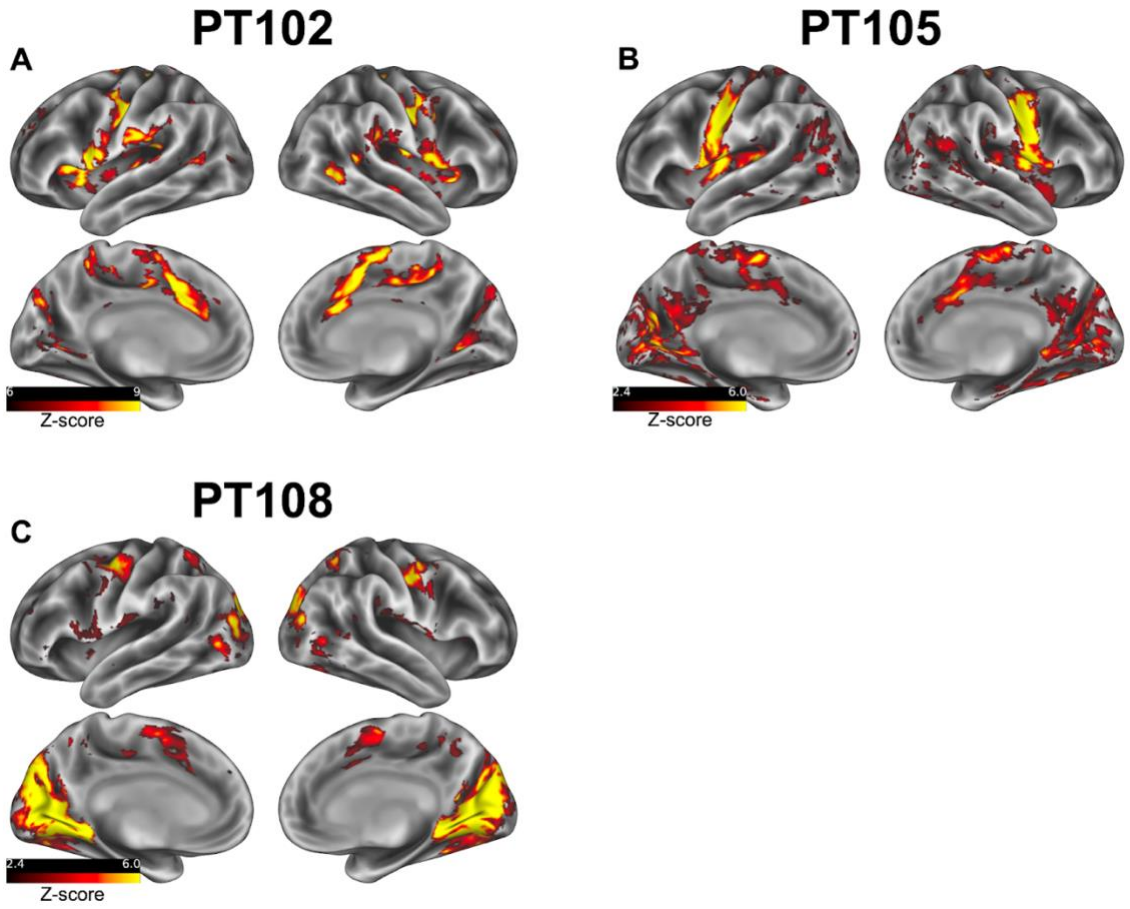

Figure 3.1: Urge activation maps. (A-C) Thresholded z-score maps of urge events two seconds prior to a tic for PT102, PT105, and PT108. Different thresholds were used to accommodate differences in observed effect sizes across the participants (PT102: $z \geq 6$; PT105: $z \geq 2.4$; PT108: $z \geq 2.4$). Unthresholded activation maps can be found in Supplementary Figure 3.1.

3.4.3 Individual-specific networks

Resting-state data were used to define individual-specific networks in each participant using the Infomap community detection algorithm. Each participant displayed a network

organization consisting of 12 canonical functional networks, including the default mode (DMN), somatomotor hand (SM-hand), somatomotor face (SM-face), somatomotor foot (SM-foot), action-mode (AMN), somato-cognitive action (SCAN), auditory (AUD), visual (VIS), salience (SAL), ventral attention (VAN / Language), dorsal attention (DAN), and frontoparietal networks (FPN) (Figure 3.2A, B, C). While individuals shared broad features of functional organization, each had unique network topography in regions commonly implicated in Tourette syndrome. For example, the shape and size of the AMN varied across individuals, particularly in the anterior cingulate and the supplementary motor area.

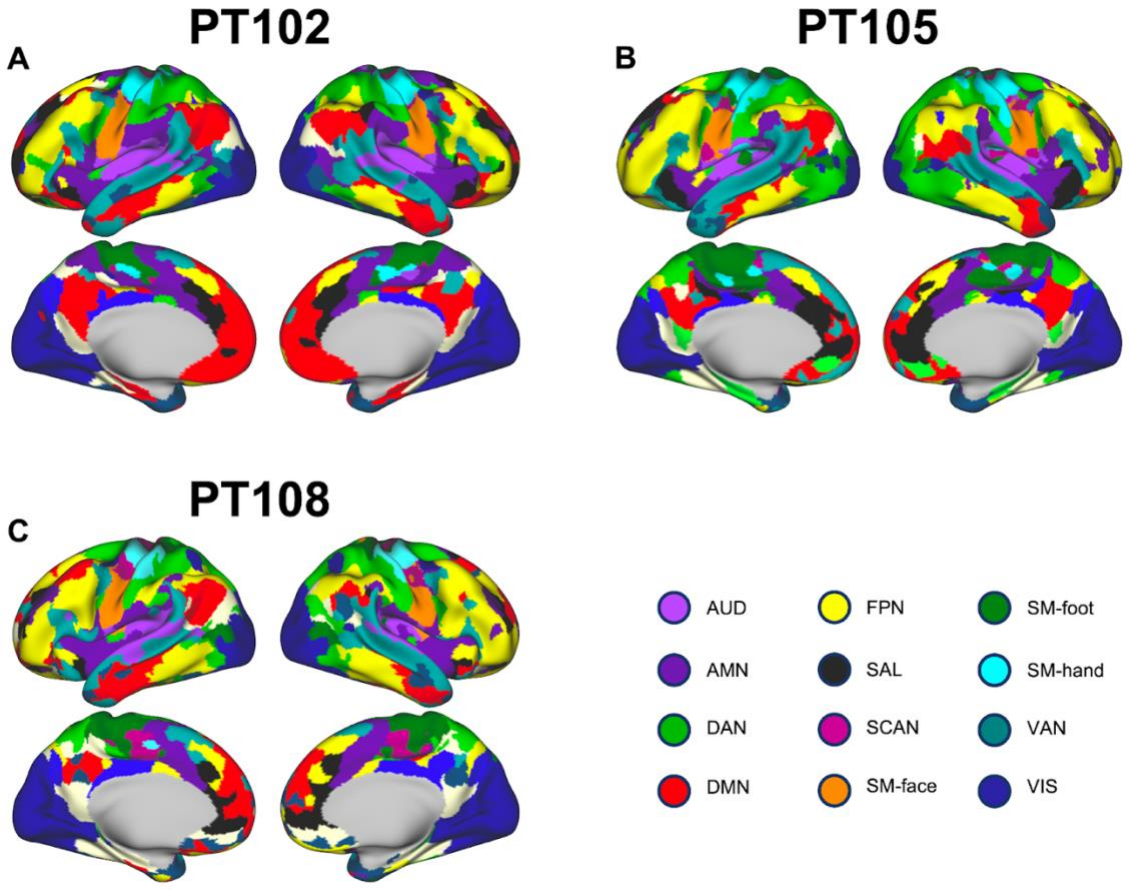

Figure 3.2: PT102, PT105, PT108 individual-specific functional networks. (A) PT102, (B) PT105, (C) PT108.

3.4.4 Urge activations overlap action related resting-state networks

Each individual's urge activation map was referenced to their individual-specific resting-state functional network organization. All participants showed a large overlap between significant urge activations and planning/control regions, including large parts of the AMN and SCAN (Figure 3.3). For participants with face tics, urge activations overlapped the SM-face network (Figure 3.3A, B), while for the participant with eye movement tics, overlap was greatest with the visual network (Figure 3.3C). There was variability in the amount of urge activation-network overlap across participants; for example, PT102's AMN nearly matched her cortical urge activations, while for PT105 and PT108, urge-AMN overlap was mostly confined to the ACC and SMA regions. To quantify overlap, we calculated the percentage of each network occupied by a significant urge activation for each participant (Figure 3.3H, I, J).

3.4.4 Cortical activity remains at onset, attenuates at offset

Additional models were run to identify significant activations during tic onset and offset windows (Figure 3.4; onset = 1 second window during tic action; offset = 2 second window succeeding the completion of tic onset). Cortical regions that were active during the urge were still active during tic onset in all participants. During the offset window, cortical activity attenuated relative to both urge and onset time periods in all participants. PT108 activation progression was a monotonically decreasing process, while PT102's activations increased during onset then decreased at offset. PT105 urge-onset maps were qualitatively similar, before experiencing an attenuation at offset.

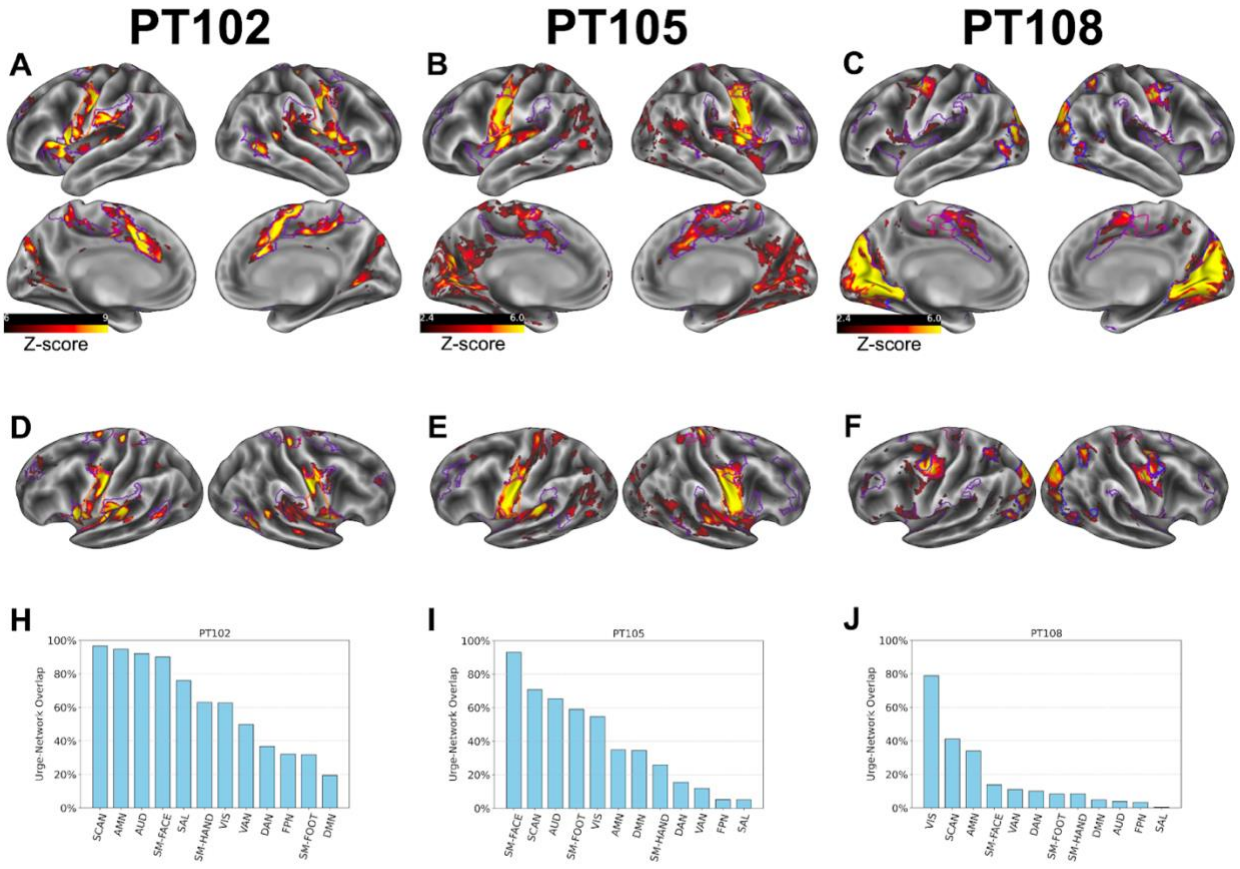

Figure 3.3: Network overlap with urge activation maps. Activation maps were referenced to each individual's functional network space for PT102 (A, D, H), PT105 (B, E, I), and PT108 (C, F, J). Lateral/medial views for each participant (A, B, C). Dorsal views for each participant to highlight superior SCAN nodes (D, E, F). PT108 threshold was dropped from z>2.4 to z>1.96 for the dorsal view. Bar plot depicting the percent of each functional network occupied by a significant urge activation (z > 1.96) (H, I, J). Action-mode network (purple), somatomotor face network (orange), somato-cognitive action network (burgundy), visual network (blue).

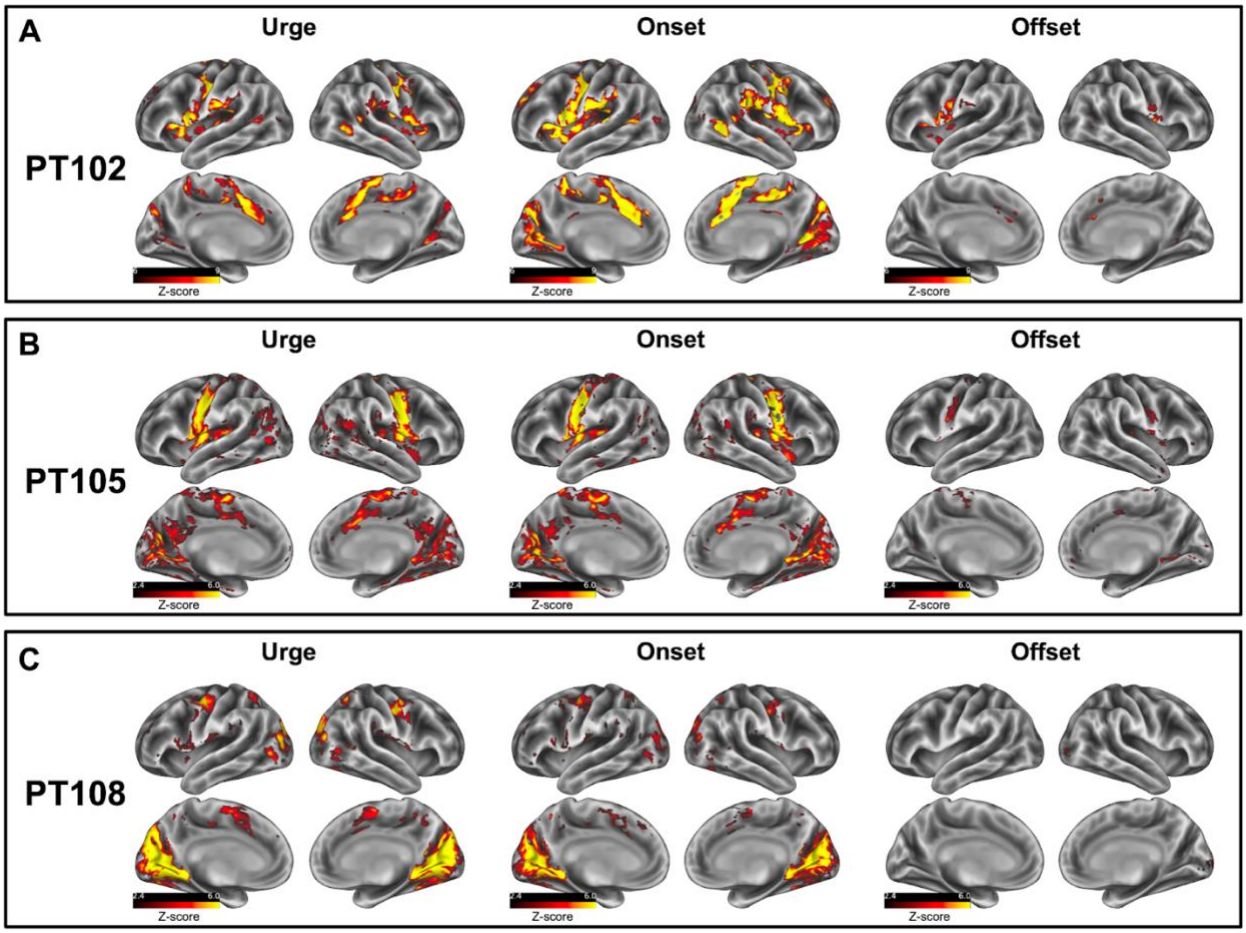

Figure 3.4: Urge, onset, offset, progression. Activation maps illustrating tic progression through the urge, onset, and offset windows for participants PT102 (A), PT105 (B), and PT108 (C). Unthresholded activation maps for all events are provided in Supplement Figure 3.1.

3.5 Discussion

In this study, we used precision functional mapping to investigate the neural correlates of motor tics in individuals with Tourette syndrome. By collecting large amounts of resting-state fMRI data and recording naturally occurring tic events during scan sessions, we were able to model tic symptoms at the individual level and reference them to each participant's individual-specific functional network organization.

Across all participants, the time preceding a tic was associated with significant activations of the supplementary motor area, anterior cingulate cortex, and parts of the insula. This time window is thought to reflect the premonitory urge. Thus, these results support previous research (Bohlhalter et al., 2006; Neuner et al., 2014) implicating these regions in the generation of the urge sensation. We further found that these regions fall within each individual's large-scale AMN. The AMN is named for its role in goal-directed action and has been implicated in processing arousal, pain, discomfort, and error detection (Dosenbach et al., 2007; Dosenbach et al., 2024). Experimental stimulation of the SMA, a key node of the AMN, causes a sense of discomfort and the urge to perform a complex movement (Fried et al., 1991) similar in nature to the premonitory urge and supporting the idea that the SMA activity may code for discomfort and urge sensations in Tourette syndrome. Going further, the SMA may be a plausible candidate for a transdiagnostic marker, coding for discomfort in the premonitory urge and in common comorbidities of Tourette syndrome including obsessive compulsive disorder (during obsessions) and attention-deficit/hyperactivity disorder.

Here, we also provide preliminary evidence for the involvement of the somato-cognitive action network (SCAN; Gordon et al., 2023) in the generation of the premonitory urge. The SCAN is a newly identified network consisting of inter-effector regions that interrupt the M1

foot, hand, and face representations, with strong functional connectivity to the AMN, and is thought to be involved in the transformation of action planning to axial body movements. Its activation alongside the AMN during the premonitory urge further implicates control and action planning networks in Tourette syndrome pathophysiology. In fact, AMN and SCAN connectivity with subcortical deep brain stimulation (DBS) targets may be highly predictive of thalamic DBS success (Baldermann et al., 2024).

While parts of all individuals' AMN were associated with the urge, there was individual variability in the strength and location of this association across participants. PT102 had strong activations across the entirety of her AMN, while PT105 and PT108 were more confined to the SMA and the operculum/insula. This heterogeneity of neural correlates may be a result of the heterogeneity of symptoms experienced by participants in the scanner or during their lifespan. PT102 and PT105 had a variety of tics impacting the eyebrows, eyes, nose, and mouth, while PT108 largely only had tics involving eye movements (saccades, eye rolls). PT102's face tics included large jaw movements. If larger actions correspond to larger urge-related activations, that might explain the more significant urge-related activations in PT102 compared to PT105 and PT108 who experienced smaller tic movements such as eye blinking and eye movements (although see Brandt et al., 2023 finding complex and simple tics do not differ in self-reported urge intensity). The variable urge activation patterns may also be due to age-related abilities in social cognition or self-referential processing. As the frequency of tics is affected by many environmental and social factors (Conelea and Woods, 2008), social and self-referential processes might increase urge activity in older individuals, such as PT102 (15 years old), who may learn strategies which cause a build-up of urge tension in an effort to avoid ticcing in public

social situations. It has also been suggested that a patient's individual ability to perceive interoceptive signals may correspond to urge severity (Ganos, 2016).

We further found that the anatomical location of the tic symptoms experienced by individuals impacted the corresponding tic activation map. The participants with variable facial tics (PT102, PT105) had significant activations in the SM-face area, while the participant with tics involving eye movements (PT108) had significant activations in the medial visual cortex and frontal/parietal eye fields. Animal studies support this idea of individual tic correlates by showing that stimulating different parts of the striatum leads to movement of different anatomical locations (Alexander and DeLong, 1985; Bronfeld et al., 2013). Characterizing individual-specific correlates, whether for similar or different tic locations, may have translational importance. For example, treatment strategies may depend on the location of the tic (eye vs. mouth) and the precise anatomical or functional localization of the urge in the individual. The precise characterization of individual activation patterns during the premonitory urge may offer a method of localization for brain stimulation therapies.

Lastly, by separately modeling urge, tic onset, and tic offset, we found that activation patterns during tic events returned to near baseline levels during offset, but not during onset. During onset, most regions active during the urge were still active, with regions such as M1/S1 being even more active in two of the participants. Two seconds after completing the tic, during the offset window, most regions were back near baseline for PT108 and were largely attenuated for PT102 and PT105 (Figure 3.4). This result conforms to self-reports of discomfort relief in Tourette's patients after tic completion (Leckman, Walker, and Cohen, 1993; Reese et al., 2014; Brandt et al., 2016). Tic release may not immediately offer a reward signal, but rather be associated with a slower relief signal after tic completion reflecting a "just-right" feeling.

While studying individuals offers the ability to map individual symptoms to individual functional organizations, work with larger sample sizes will be needed to better understand the results that are generalizable across individuals and those that are more individually specific. Future work should include additional subjects with variable tic symptoms, urge severity, and ages in order to test potential theories that could lead to the differential urge activation patterns we observe here. Furthermore, future work is needed to better track the temporal progression of the urge, from onset to offset signals. Here, we utilized fMRI data with a repetition time (TR) of 1.7 seconds, which, along with the multicollinearity of the timing events, made it difficult to precisely track signal propagation. As we localize cortical regions involved in tics here with fMRI, it is plausible that these regions could then be studied with magnetoencephalography, a functional neuroimaging method whose high temporal resolution may be used in conjunction with fMRI.

Here, we present preliminary results of highly sampled individuals with Tourette syndrome to demonstrate the feasibility and importance of individual-level analyses in studying the disorder. Our results suggest that individual differences in tic symptoms are associated with both shared and unique functional activation patterns across individuals. Specifically, we observed that regions of large-scale control networks—including the supplementary motor area, anterior cingulate cortex, and inter-effector SCAN nodes—were active in all participants during the premonitory urge. In contrast, other regions displayed more variable activation and may be related to tic type/location, and potentially participant characteristics such as age and symptom severity. An important next step will be to study larger samples of individuals with Tourette syndrome using PFM in order to identify reliable and generalizable differences associated with the disorder.

Acknowledgement

Chapter 3, in part, is currently being prepared for submission for publication of the material. Feigelis M, Baim AR, Zreik S, Demeter DV, Ali SA, Koithan E, Greene DJ. The dissertation author was the primary researcher and author of this material.

3.6 References

Alexander, G.E., DeLong, M.R., 1985. Microstimulation of the primate neostriatum. I. Physiological properties of striatal microexcitable zones. Journal of Neurophysiology 53, 1401–1416. https://doi.org/10.1152/jn.1985.53.6.1401

American Psychiatric Association, 2013. Diagnostic and Statistical Manual of Mental Disorders, Fifth Edition. ed. American Psychiatric Association. https://doi.org/10.1176/appi.books.9780890425596

Baldermann, J.C., Petry-Schmelzer, J.N., Schüller, T., Mahfoud, L., Brandt, G.A., Dembek, T.A., Van Der Linden, C., Krauss, J.K., Szejko, N., Müller-Vahl, K.R., Ganos, C., Al-Fatly, B., Heiden, P., Servello, D., Galbiati, T., Johnson, K., Butson, C.R., Okun, M.S., Andrade, P., Domschke, K., Fink, G.R., Fox, M., Horn, A., Kuhn, J., Visser-Vandewalle, V., Barbe, M.T., 2024. A Critical Role of Action-Related Functional Networks in Gilles de la Tourette Syndrome. https://doi.org/10.31219/osf.io/jxwmn

Bohlhalter, S., Goldfine, A., Matteson, S., Garraux, G., Hanakawa, T., Kansaku, K., Wurzman, R., Hallett, M., 2006. Neural correlates of tic generation in Tourette syndrome: an event-related functional MRI study. Brain 129, 2029–2037. https://doi.org/10.1093/brain/awl050

Brandt, V., Essing, J., Jakubovski, E., Müller-Vahl, K., 2023. Premonitory Urge and Tic Severity, Comorbidities, and Quality of Life in Chronic Tic Disorders. Movement Disord Clin Pract 10, 922–932. https://doi.org/10.1002/mdc3.13742

Brandt, V.C., Beck, C., Sajin, V., Baaske, M.K., Bäumer, T., Beste, C., Anders, S., Münchau, A., 2016. Temporal relationship between premonitory urges and tics in Gilles de la Tourette syndrome. Cortex 77, 24–37. https://doi.org/10.1016/j.cortex.2016.01.008

Bronfeld, M., Belelovsky, K., Bar-Gad, I., 2011. Spatial and temporal properties of tic-related neuronal activity in the cortico-basal ganglia loop. J Neurosci 31, 8713–8721. https://doi.org/10.1523/JNEUROSCI.0195-11.2011

Bronfeld, M., Yael, D., Belelovsky, K., Bar-Gad, I., 2013. Motor tics evoked by striatal disinhibition in the rat. Front. Syst. Neurosci. 7. https://doi.org/10.3389/fnsys.2013.00050

Conelea, C.A., Woods, D.W., 2008. The influence of contextual factors on tic expression in Tourette's syndrome: A review. Journal of Psychosomatic Research 65, 487–496. https://doi.org/10.1016/j.jpsychores.2008.04.010

Cubo, E., 2012. Review of prevalence studies of tic disorders: methodological caveats. Tremor Other Hyperkinet Mov (N Y) 2, tre-02-61-349-1. https://doi.org/10.7916/D8445K68

D. Sturgeon, Earl, E., Perrone, A., Kathy, 2021. DCAN-Labs/abcd-hcp-pipeline: Minor update to DCAN BOLD Processing and MRE version. https://doi.org/10.5281/ZENODO.4571051

Dosenbach, N.U.F., Fair, D.A., Miezin, F.M., Cohen, A.L., Wenger, K.K., Dosenbach, R.A.T., Fox, M.D., Snyder, A.Z., Vincent, J.L., Raichle, M.E., Schlaggar, B.L., Petersen, S.E., 2007. Distinct brain networks for adaptive and stable task control in humans. Proc Natl Acad Sci U S A 104, 11073–11078. https://doi.org/10.1073/pnas.0704320104

Dosenbach, N.U.F., Raichle, M., Gordon, E.M., 2024. The brain's cingulo-opercular action-mode network. https://doi.org/10.31234/osf.io/2vt79

DuPre, E., Salo, T., Ahmed, Z., Bandettini, P., Bottenhorn, K., Caballero-Gaudes, C., Dowdle, L., Gonzalez-Castillo, J., Heunis, S., Kundu, P., Laird, A., Markello, R., Markiewicz, C., Moia, S., Staden, I., Teves, J., Uruñuela, E., Vaziri-Pashkam, M., Whitaker, K., Handwerker, D., 2021. TE-dependent analysis of multi-echo fMRI with tedana. JOSS 6, 3669. https://doi.org/10.21105/joss.03669

Fair, D.A., Miranda-Dominguez, O., Snyder, A.Z., Perrone, A., Earl, E.A., Van, A.N., Koller, J.M., Feczko, E., Tisdall, M.D., Van Der Kouwe, A., Klein, R.L., Mirro, A.E., Hampton, J.M., Adeyemo, B., Laumann, T.O., Gratton, C., Greene, D.J., Schlaggar, B.L., Hagler, D.J., Watts, R., Garavan, H., Barch, D.M., Nigg, J.T., Petersen, S.E., Dale, A.M., Feldstein-Ewing, S.W., Nagel, B.J., Dosenbach, N.U.F., 2020. Correction of respiratory artifacts in MRI head motion estimates. NeuroImage 208, 116400. https://doi.org/10.1016/j.neuroimage.2019.116400

Fried, I., Katz, A., McCarthy, G., Sass, K.J., Williamson, P., Spencer, S.S., Spencer, D.D., 1991. Functional organization of human supplementary motor cortex studied by electrical stimulation. J Neurosci 11, 3656–3666. https://doi.org/10.1523/JNEUROSCI.11-11-03656.1991

Ganos, C., 2016. Tics and Tourette's: update on pathophysiology and tic control. Current Opinion in Neurology 29, 513–518. https://doi.org/10.1097/WCO.0000000000000356

Glasser, M.F., Sotiropoulos, S.N., Wilson, J.A., Coalson, T.S., Fischl, B., Andersson, J.L., Xu, J., Jbabdi, S., Webster, M., Polimeni, J.R., Van Essen, D.C., Jenkinson, M., 2013. The minimal preprocessing pipelines for the Human Connectome Project. NeuroImage 80, 105–124. https://doi.org/10.1016/j.neuroimage.2013.04.127

Gordon, E.M., Chauvin, R.J., Van, A.N., Rajesh, A., Nielsen, A., Newbold, D.J., Lynch, C.J., Seider, N.A., Krimmel, S.R., Scheidter, K.M., Monk, J., Miller, R.L., Metoki, A., Montez, D.F., Zheng, A., Elbau, I., Madison, T., Nishino, T., Myers, M.J., Kaplan, S., Badke D'Andrea, C.,

Demeter, D.V., Feigelis, M., Ramirez, J.S.B., Xu, T., Barch, D.M., Smyser, C.D., Rogers, C.E., Zimmermann, J., Botteron, K.N., Pruett, J.R., Willie, J.T., Brunner, P., Shimony, J.S., Kay, B.P., Marek, S., Norris, S.A., Gratton, C., Sylvester, C.M., Power, J.D., Liston, C., Greene, D.J., Roland, J.L., Petersen, S.E., Raichle, M.E., Laumann, T.O., Fair, D.A., Dosenbach, N.U.F., 2023. A somato-cognitive action network alternates with effector regions in motor cortex. Nature 617, 351–359. https://doi.org/10.1038/s41586-023-05964-2

Gordon, E.M., Laumann, T.O., Adeyemo, B., Gilmore, A.W., Nelson, S.M., Dosenbach, N.U.F., Petersen, S.E., 2017a. Individual-specific features of brain systems identified with resting state functional correlations. Neuroimage 146, 918–939. https://doi.org/10.1016/j.neuroimage.2016.08.032

Gordon, E.M., Laumann, T.O., Gilmore, A.W., Newbold, D.J., Greene, D.J., Berg, J.J., Ortega, M., Hoyt-Drazen, C., Gratton, C., Sun, H., Hampton, J.M., Coalson, R.S., Nguyen, A.L., McDermott, K.B., Shimony, J.S., Snyder, A.Z., Schlaggar, B.L., Petersen, S.E., Nelson, S.M., Dosenbach, N.U.F., 2017b. Precision Functional Mapping of Individual Human Brains. Neuron 95, 791-807.e7. https://doi.org/10.1016/j.neuron.2017.07.011

Gratton, C., Kraus, B.T., Greene, D.J., Gordon, E.M., Laumann, T.O., Nelson, S.M., Dosenbach, N.U.F., Petersen, S.E., 2020. Defining Individual-Specific Functional Neuroanatomy for Precision Psychiatry. Biological Psychiatry 88, 28–39. https://doi.org/10.1016/j.biopsych.2019.10.026

Gratton, C., Laumann, T.O., Nielsen, A.N., Greene, D.J., Gordon, E.M., Gilmore, A.W., Nelson, S.M., Coalson, R.S., Snyder, A.Z., Schlaggar, B.L., Dosenbach, N.U.F., Petersen, S.E., 2018. Functional Brain Networks Are Dominated by Stable Group and Individual Factors, Not Cognitive or Daily Variation. Neuron 98, 439-452.e5. https://doi.org/10.1016/j.neuron.2018.03.035

Greene, D.J., Kim, S., Black, K.J., Schlaggar, B.L., 2022. Neurobiology and Functional Anatomy of Tic Disorders, in: Tourette Syndrome. Oxford University Press, pp. 199–230. https://doi.org/10.1093/med/9780197543214.003.0014

Greene, D.J., Marek, S., Gordon, E.M., Siegel, J.S., Gratton, C., Laumann, T.O., Gilmore, A.W., Berg, J.J., Nguyen, A.L., Dierker, D., Van, A.N., Ortega, M., Newbold, D.J., Hampton, J.M., Nielsen, A.N., McDermott, K.B., Roland, J.L., Norris, S.A., Nelson, S.M., Snyder, A.Z., Schlaggar, B.L., Petersen, S.E., Dosenbach, N.U.F., 2020. Integrative and Network-Specific Connectivity of the Basal Ganglia and Thalamus Defined in Individuals. Neuron 105, 742-758.e6. https://doi.org/10.1016/j.neuron.2019.11.012

Hallquist, M.N., Hwang, K., Luna, B., 2013. The nuisance of nuisance regression: Spectral misspecification in a common approach to resting-state fMRI preprocessing reintroduces noise and obscures functional connectivity. NeuroImage 82, 208–225. https://doi.org/10.1016/j.neuroimage.2013.05.116

Jenkinson, M., Beckmann, C.F., Behrens, T.E.J., Woolrich, M.W., Smith, S.M., 2012. FSL. NeuroImage 62, 782–790. https://doi.org/10.1016/j.neuroimage.2011.09.015

Kahl, C.K., Kirton, A., Pringsheim, T., Croarkin, P.E., Zewdie, E., Swansburg, R., Wrightson, J., Langevin, L.M., Macmaster, F.P., 2021. Bilateral transcranial magnetic stimulation of the supplementary motor area in children with Tourette syndrome. Dev Med Child Neurol 63, 808–815. https://doi.org/10.1111/dmcn.14828

Kaufman, J., Birmaher, B., Brent, D., Rao, U., Flynn, C., Moreci, P., Williamson, D., Ryan, N., 1997. Schedule for Affective Disorders and Schizophrenia for School-Age Children-Present and Lifetime Version (K-SADS-PL): Initial Reliability and Validity Data. Journal of the American Academy of Child & Adolescent Psychiatry 36, 980–988. https://doi.org/10.1097/00004583-199707000-00021

Knight, T., Steeves, T., Day, L., Lowerison, M., Jette, N., Pringsheim, T., 2012. Prevalence of tic disorders: a systematic review and meta-analysis. Pediatr Neurol 47, 77–90. https://doi.org/10.1016/j.pediatrneurol.2012.05.002

Kraus, B., Zinbarg, R., Braga, R.M., Nusslock, R., Mittal, V.A., Gratton, C., 2023. Insights from personalized models of brain and behavior for identifying biomarkers in psychiatry. Neuroscience & Biobehavioral Reviews 152, 105259. https://doi.org/10.1016/j.neubiorev.2023.105259

Laumann, T.O., Gordon, E.M., Adeyemo, B., Snyder, A.Z., Joo, S.J., Chen, M.-Y., Gilmore, A.W., McDermott, K.B., Nelson, S.M., Dosenbach, N.U.F., Schlaggar, B.L., Mumford, J.A., Poldrack, R.A., Petersen, S.E., 2015. Functional System and Areal Organization of a Highly Sampled Individual Human Brain. Neuron 87, 657–670. https://doi.org/10.1016/j.neuron.2015.06.037

Leckman, J.F., Riddle, M.A., Hardin, M.T., Ort, S.I., Swartz, K.L., Stevenson, J., Cohen, D.J., 1989. The Yale Global Tic Severity Scale: initial testing of a clinician-rated scale of tic severity. J Am Acad Child Adolesc Psychiatry 28, 566–573. https://doi.org/10.1097/00004583-198907000-00015

Leckman, J.F., Walker, D.E., Cohen, D.J., 1993. Premonitory urges in Tourette's syndrome. Am J Psychiatry 150, 98–102. https://doi.org/10.1176/ajp.150.1.98

Lindquist, M.A., Geuter, S., Wager, T.D., Caffo, B.S., 2019. Modular preprocessing pipelines can reintroduce artifacts into fMRI data. Human Brain Mapping 40, 2358–2376. https://doi.org/10.1002/hbm.24528

Lynch, C.J., Elbau, I.G., Ng, T., Ayaz, A., Zhu, S., Wolk, D., Manfredi, N., Johnson, M., Chang, M., Chou, J., Summerville, I., Ho, C., Lueckel, M., Bukhari, H., Buchanan, D., Victoria, L.W., Solomonov, N., Goldwaser, E., Moia, S., Caballero-Gaudes, C., Downar, J., Vila-Rodriguez, F., Daskalakis, Z.J., Blumberger, D.M., Kay, K., Aloysi, A., Gordon, E.M., Bhati, M.T., Williams, N., Power, J.D., Zebley, B., Grosenick, L., Gunning, F.M., Liston, C., 2024. Frontostriatal

salience network expansion in individuals in depression. Nature 633, 624–633. https://doi.org/10.1038/s41586-024-07805-2

Marek, S., Siegel, J.S., Gordon, E.M., Raut, R.V., Gratton, C., Newbold, D.J., Ortega, M., Laumann, T.O., Adeyemo, B., Miller, D.B., Zheng, A., Lopez, K.C., Berg, J.J., Coalson, R.S., Nguyen, A.L., Dierker, D., Van, A.N., Hoyt, C.R., McDermott, K.B., Norris, S.A., Shimony, J.S., Snyder, A.Z., Nelson, S.M., Barch, D.M., Schlaggar, B.L., Raichle, M.E., Petersen, S.E., Greene, D.J., Dosenbach, N.U.F., 2018. Spatial and Temporal Organization of the Individual Human Cerebellum. Neuron 100, 977-993.e7. https://doi.org/10.1016/j.neuron.2018.10.010

McCairn, K.W., Bronfeld, M., Belelovsky, K., Bar-Gad, I., 2009. The neurophysiological correlates of motor tics following focal striatal disinhibition. Brain 132, 2125–2138. https://doi.org/10.1093/brain/awp142

Mink, J.W., 2006. Neurobiology of basal ganglia and Tourette syndrome: basal ganglia circuits and thalamocortical outputs. Adv Neurol 99, 89–98.
Moeller, S., Pisharady, P.K., Ramanna, S., Lenglet, C., Wu, X., Dowdle, L., Yacoub, E., Uğurbil, K., Akçakaya, M., 2021. NOise reduction with DIstribution Corrected (NORDIC) PCA in dMRI with complex-valued parameter-free locally low-rank processing. Neuroimage 226, 117539. https://doi.org/10.1016/j.neuroimage.2020.117539

Neuner, I., Werner, C.J., Arrubla, J., Stöcker, T., Ehlen, C., Wegener, H.P., Schneider, F., Shah, N.J., 2014. Imaging the where and when of tic generation and resting state networks in adult Tourette patients. Front Hum Neurosci 8, 362. https://doi.org/10.3389/fnhum.2014.00362

Power, J.D., Barnes, K.A., Snyder, A.Z., Schlaggar, B.L., Petersen, S.E., 2012. Spurious but systematic correlations in functional connectivity MRI networks arise from subject motion. NeuroImage 59, 2142–2154. https://doi.org/10.1016/j.neuroimage.2011.10.018

Power, J.D., Mitra, A., Laumann, T.O., Snyder, A.Z., Schlaggar, B.L., Petersen, S.E., 2014. Methods to detect, characterize, and remove motion artifact in resting state fMRI. NeuroImage 84, 320–341. https://doi.org/10.1016/j.neuroimage.2013.08.048

Reese, H.E., Scahill, L., Peterson, A.L., Crowe, K., Woods, D.W., Piacentini, J., Walkup, J.T., Wilhelm, S., 2014. The Premonitory Urge to Tic: Measurement, Characteristics, and Correlates in Older Adolescents and Adults. Behavior Therapy 45, 177–186. https://doi.org/10.1016/j.beth.2013.09.002

Rosvall, M., Bergstrom, C.T., 2008. Maps of random walks on complex networks reveal community structure. Proc. Natl. Acad. Sci. U.S.A. 105, 1118–1123. https://doi.org/10.1073/pnas.0706851105

Steinberg, T., Shmuel Baruch, S., Harush, A., Dar, R., Woods, D., Piacentini, J., Apter, A., 2010. Tic disorders and the premonitory urge. J Neural Transm 117, 277–284. https://doi.org/10.1007/s00702-009-0353-3

Sukhodolsky, D.G., Walsh, C., Koller, W.N., Eilbott, J., Rance, M., Fulbright, R.K., Zhao, Z., Bloch, M.H., King, R., Leckman, J.F., Scheinost, D., Pittman, B., Hampson, M., 2020. Randomized, Sham-Controlled Trial of Real-Time Functional Magnetic Resonance Imaging Neurofeedback for Tics in Adolescents With Tourette Syndrome. Biol Psychiatry 87, 1063–1070. https://doi.org/10.1016/j.biopsych.2019.07.035

Sylvester, C.M., Yu, Q., Srivastava, A.B., Marek, S., Zheng, A., Alexopoulos, D., Smyser, C.D., Shimony, J.S., Ortega, M., Dierker, D.L., Patel, G.H., Nelson, S.M., Gilmore, A.W., McDermott, K.B., Berg, J.J., Drysdale, A.T., Perino, M.T., Snyder, A.Z., Raut, R.V., Laumann, T.O., Gordon, E.M., Barch, D.M., Rogers, C.E., Greene, D.J., Raichle, M.E., Dosenbach, N.U.F., 2020. Individual-specific functional connectivity of the amygdala: A substrate for precision psychiatry. Proc. Natl. Acad. Sci. U.S.A. 117, 3808–3818. https://doi.org/10.1073/pnas.1910842117

Van Essen, D.C., Glasser, M.F., Dierker, D.L., Harwell, J., Coalson, T., 2012. Parcellations and Hemispheric Asymmetries of Human Cerebral Cortex Analyzed on Surface-Based Atlases. Cerebral Cortex 22, 2241–2262. https://doi.org/10.1093/cercor/bhr291

Appendix

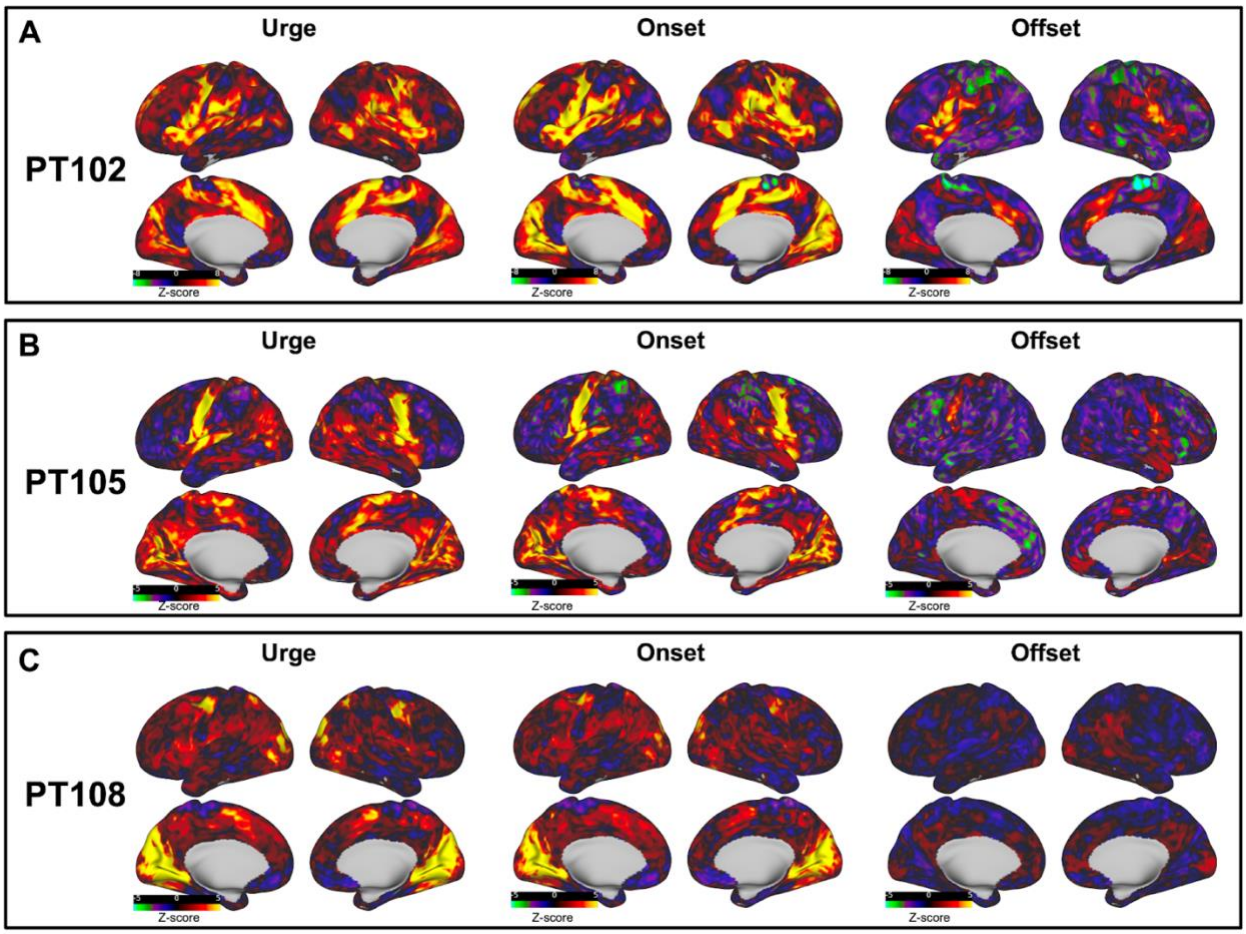

Supplementary Figure 3.1: Unthresholded activation maps for urge, onset, and offset windows. (A) PT102, (B) PT105, (C) PT108.